



An Insight into the Proofreading Functions of Multisubunit DNA-Dependent RNA Polymerases and Their Catalytic Mechanism

Peramachi Palanivelu^{1*#}

¹Department of Molecular Microbiology, School of Biotechnology, Madurai Kamaraj University, Madurai – 625 021, India.

Author's contribution

The sole author designed, analysed, interpreted and prepared the manuscript.

Article Information

DOI: 10.9734/IJBCRR/2021/v30i730278

Editor(s):

(1) Dr. Chunying Li, Georgia State University, USA.

Reviewers:

(1) Ioana Stanciu, University of Bucharest, Romania.

(2) Kruti Dave, Ganpat University, India.

(3) F. Solano, University of Murcia, Spain.

Complete Peer review History: <http://www.sdiarticle4.com/review-history/75573>

Original Research Article

Received 25 August 2021

Accepted 03 November 2021

Published 09 November 2021

ABSTRACT

Aim: To analyze the active sites of the proofreading (PR) functions in the multisubunit DNA-dependent RNA polymerases (MSU RNAPs) from prokaryotes, chloroplasts and eukaryotes, and propose a plausible unified catalytic mechanism for these enzymes.

Study Design: Data collected on these enzymes from bioinformatics, biochemical, site-directed mutagenesis (SDM), X-ray crystallography and cryo-electron microscopy (cryo-EM) were used for the analyses.

Methodology: The protein sequence data of MSU RNAPs from prokaryotes, prokaryotic-types (plant chloroplasts) and eukaryotes were obtained from PUBMED and SWISS-PROT databases. The advanced version of Clustal Omega was used for protein sequence analysis. Along with the conserved motifs identified by the bioinformatics analysis, the data already available from biochemical and SDM experiments, and X-ray crystallographic and cryo-EM data on these enzymes are also used to confirm the possible amino acids involved in the active site of the PR function in these MSU RNAPs

Results: All the seven types of MSU RNAPs (I-VII) reported from prokaryotes to eukaryotes were analyzed by the multiple sequence alignment (MSA) software, Clustal Omega, to find out

[#]Senior Professor & Head (Retd.);

*Corresponding author: E-mail: ppmkupp@gmail.com;

conservations among them. The MSA analysis showed many conserved amino acid motifs including small and large peptide regions from the MSU RNAPs of prokaryotes, eukaryotes and plant chloroplasts. Interestingly, the catalytic amino acid and template-binding pairs are highly conserved in all these polymerases, with a few exceptions. Most of them use a basic amino acid (R/K/H) for initiating catalysis and an -YG/FG- pair for template-binding. Some odd type of catalytic amino acids and template-binding pairs are observed in human pathogens, parasites and organisms which cannot ferment sugars. In all the MSU RNAPs, the proposed polymerase catalytic region also possessed three invariant Cs and an invariant H within it. The invariant Cs is shown to bind a zinc atom and proposed to involve in the PR function by excising any misincorporated nucleotide during the transcription process. In the plant-specific MSU RNAPs IV and V, which involve in transcriptional gene silencing in plants, the catalytic and template-binding pairs do not follow the regular distance conservations as observed with other five of the MSU RNAPs. Their polymerase/PR active site regions are similar to RNAP III rather than to RNAP II, as all three make only low molecular weight RNAs.

Conclusions: All the known MSU RNAPs possess three invariant Cs and an invariant H embedded within the polymerase active site itself. The three invariant Cs are shown to bind a zinc atom and the invariant H could act as the proton acceptor from a metal-bound water molecule, for initiating excision of the mismatches by a Zn-mediated hydrolysis. Thus, the PR function in MSU RNAPs is integrated within the polymerase active site itself, which is in sharp contrast to the PR functions reported in DNA-dependent DNA polymerases and RNA-dependent RNA polymerases. Therefore, all the seven MSU RNAPs from prokaryotes and eukaryotes are proposed to follow a unified mechanism to excise the mismatches during transcription. The discovery of intrinsic self-correcting RNA transcription mechanism fulfils the missing link in molecular evolution.

Keywords: *Multisubunit RNA polymerases; E. coli; chloroplasts; S. cerevisiae; plant-specific RNA polymerases; Arabidopsis thaliana; human pathogens; zinc-binding site; proofreading active site; catalytic mechanism.*

1. INTRODUCTION

MSU RNAPs (EC 2.7.7.6) are key enzymes involved in gene expression in both prokaryotes and eukaryotes and play a crucial role in the flow of genetic information from DNA to proteins through the intermediate transcription process. Therefore, they are one of the essential enzymes found in all living cells and play an important role in copying DNA sequences into RNA molecules. The transcription process forms the first step and a key control point in gene expression and regulation in all organisms. The number and subunit compositions of these MSU RNAPs are varied in different organisms. For example, both eubacteria and archaeobacteria contain a single type of MSU RNAP, whereas eukaryotes contain at least five distinct types of MSU RNAPs, viz. RNAP I to RNAP V [1]. Whereas the eubacterial enzymes are composed of 5 different subunits, the eukaryotic enzymes are made up of 12-17 different subunits. Despite such major differences in their compositions, there are striking similarities among the transcriptional mechanisms by these MSU RNAPs across the three major domains of life [1 and references therein]. For example, the amino acid sequences, overall 3D structures and functions

of these MSU RNAPs are more or less universally conserved in all organisms like eubacteria, archaeobacteria, plants, insects and animals, with small, but significant differences in their active sites, catalytic amino acids, template-binding pairs and zinc-binding sites. Errors in eukaryotic transcription process can potentially lead to aberrant gene products, which could eventually lead to various diseases in humans, including cancer. For example, one major class of transcription error, known as transcriptional slippages, are implicated in the development of a wide variety of diseases, like colon cancer, non-familial Alzheimer's, Down's syndrome, etc. [2]. Recently, the *in vitro* transcribed mRNAs have come into focus as a potential new class of drugs known as 'mRNA therapeutics' to deliver genetic information through mRNAs to correct the malfunction(s) [3,4] and also potential vaccines against cancer and viral infections, e.g., SARS-CoV-2 [5,6]. In fact, many anti-cancer drugs act by inhibiting the transcription step itself. Therefore, understanding the catalytic mechanism and regulation of these MSU RNAPs will be useful in designing novel mRNA-based drugs for many diseases.

1.1 Proofreading Functions in MSU RNAPs

As transcription is the first and crucial step in gene expression, the mechanism of transcription is highly conserved in all organisms. It is accomplished mainly by the MSU RNAPs both in prokaryotes and eukaryotes. As the RNAPs are the key enzymes in creating an equivalent copy of RNA from the DNA sequence, they maintain a very high fidelity during the transcription process. Generally, the MSU RNAPs misincorporates only one wrong nucleotide per ~100,000 bases. Such mismatched nucleotides during transcription usually lead to conformational changes at the polymerase active site resulting in stalling of the RNAP. Fidelity of DNA replications by DNA polymerases (DNAPs) is regulated by a well established PR mechanism. However, existence of a similar mechanism for RNA synthesis is not well understood [7,8]. The polymerization and PR active sites of replicative DNA polymerases are located either on different domains on the same polypeptide or in a different subunit associated with the replicase [1,9]. However, such distinct PR domain(s) or subunit(s) are not demonstrated in MSU RNAPs. Therefore, it has been proposed that in MSU RNAPs, the transcriptional fidelity could be achieved by a different mechanism, (i.e.), it could be achieved in two steps. In the first step, it could discriminate deoxynucleoside triphosphates (dNTPs) from nucleoside triphosphates (NTPs) and allow only the NTPs at the polymerization site. In the second step, they could also employ a PR function to repair any mismatch. The second step in these MSU RNAPs has been proposed to be possibly achieved by a PR site integrated within the polymerase active site itself. Thus, any mismatch could be repaired by an intrinsic PR mechanism and hence, there may not be any separate domains or subunits to perform the function as in the replicative polymerases [10,11]. Interestingly, huge volume of genomic and protein sequence data that are available for most of the prokaryotic and eukaryotic MSU RNAPs could be effectively utilized to analyze the structure-function relationships and catalytic mechanism of these key enzymes. Therefore, in this communication, the PR function in these MSU RNAPs is analyzed in detail and reported.

2. MATERIALS AND METHODS

The protein sequence data of MSU RNAPs from prokaryotes, eukaryotes and plant chloroplasts were obtained from PUBMED and SWISS-PROT

databases. The advanced version of Clustal Omega was used for protein sequence analysis. The data already available from bioinformatics methods, biochemical and SDM experiments and X-ray crystallographic and cryo-EM analysis on these enzymes were also used to confirm the possible amino acids involved in the PR exonuclease active site of these MSU RNAPs.

3. RESULTS AND DISCUSSION

3.1 Analysis of PR Active Site in the MSU RNAPs from Prokaryotes

The MSA of the elongation subunits β' of the MSU RNAPs from prokaryotes is shown in Fig. 1. The most well studied among them is the RNAP of *E. coli*. The *E. coli* RNAP is a MSU enzyme with a molecular mass of ~410 kDA. The core enzyme consists of four different subunits and organized into $\alpha_2\beta\beta'\omega$ in bacteria. In addition to the core enzyme, the RNAP also requires an additional subunit, viz. the sigma factor (σ) which essentially involves in promoter recognitions [8]. In bacteria, the β subunit involves in the initiation of RNA synthesis and the β' subunit is responsible for further elongation and completion of the RNA transcription cycle. Thus, the β and β' subunits are complementary to each other in the RNA synthesis. In fact, the β subunit involves in synthesis of short primers for initiation of RNA synthesis, and the β' is responsible for further extension of the primers and production of the complete RNA chains, ready for translation. Therefore, it is important for the elongation β' subunit to harbour both the polymerization and the PR active sites for an error-free transcription process. The β' elongation subunits from various bacterial sources were analyzed by MSA and the results are shown in Fig. 1. (The *E. coli* β' subunit, the template-binding and catalytic pairs are highlighted in yellow; the Mg^{2+} binding site is highlighted in light green and the possible Zn^{2+} binding motif $-Cx_6CxxC-$ is highlighted in orange).

3.1.1 Identifications of Mg^{2+} - and Zn^{2+} -Binding Sites in the MSU RNAPs from prokaryotes

The MSA shows a highly conserved Cs with the Zn^{2+} -binding pattern $-Cx_6Cx_2C-$ within the polymerase active site region (Fig. 1). The presence of a Zn^{2+} binding site is further confirmed by X-ray crystallographic analysis of the bacterial (*E. coli* and *T. thermophilus*) MSU RNAPs [9] and references therein. Zhang et al

[12] found that the MSU RNAP from *T. aquaticus* showed an unusual Zn²⁺-binding motif in the β' elongation subunit of the enzyme. They reported that the three C residues are arranged in a sequence (¹⁹⁴CX₆CX₂C), similar to a typical Zn-binding motif. The fourth C participating in the Zn²⁺ chelation is C¹¹³, (i.e.,) 82 residues away. An absolute conservation of the four C residues

in all β' subunits from prokaryotes further support this finding (C⁸⁸⁸, C⁸⁹⁵ and C⁸⁹⁸ - numbering from *E. coli* β'). Moreover, the complete conservation of the zinc binding motif in the active sites of the elongation subunits in the bacterial MSU RNAPs by MSA analysis further confirms this finding (Fig.1). This finding was further corroborated by

CLUSTAL O (1.2.4) MSA of the elongation subunits, β' of bacterial MSU RNAPs (Only the Mg²⁺-binding and polymerization regions are shown here).

AEG34223.1	LHRLGIQAFQPVLVVEGQSIQLHPLVCEAF	NADFDGQ	QMAVHVPL	SSFAQAEARIQMLSAH	767		
sp Q9KWU6 RPOC_THEAQ	LHRLGIQAFQPVLVVEGQSIQLHPLVCEAF	NADFDGQ	QMAVHVPL	SSFAQAEARIQMLSAH	767		
ASR51305.1	LHRLGIQAFEPVLIIEGKAIQLHPLVCAAY	NADFDGQ	QMAVHVPL	SLEAQLAEARLMMSTN	489		
OXR47930.1	LHRLGIQAFEPVLIIEGKAIQLHPLVCAAY	NADFDGQ	QMAVHVPL	SLEAQLAEARLMLASN	488		
sp A7MQQ8 RPOC_CROS8	LHRLGIQAFEPVLIIEGKAIQLHPLVCAAY	NADFDGQ	QMAVHVPL	FLEAQLAEARLMMSTN	488		
sp Q32AG0 RPOC_SHIDS	LHRLGIQAFEPVLIIEGKAIQLHPLVCAAY	NADFDGQ	QMAVHVPL	FLEAQLAEARLMMSTN	488		
sp Q0SY12 RPOC_SHIF8	LHRLGIQAFEPVLIIEGKAIQLHPLVCAAY	NADFDGQ	QMAVHVPL	FLEAQLAEARLMMSTN	488		
sp B2TWH4 RPOC_SHIB3	LHRLGIQAFEPVLIIEGKAIQLHPLVCAAY	NADFDGQ	QMAVHVPL	FLEAQLAEARLMMSTN	488		
sp P0A8T7 RPOC_ECOLI	LHRLGIQAFEPVLIIEGKAIQLHPLVCAAY	NADFDGQ	QMAVHVPL	FLEAQLAEARLMMSTN	488		
sp Q3YUZ6 RPOC_SHISS	LHRLGIQAFEPVLIIEGKAIQLHPLVCAAY	NADFDGQ	QMAVHVPL	FLEAQLAEARLMMSTN	488		
sp B1XBZ0 RPOC_ECODH	LHRLGIQAFEPVLIIEGKAIQLHPLVCAAY	NADFDGQ	QMAVHVPL	FLEAQLAEARLMMSTN	488		
sp A8A787 RPOC_ECOHS	LHRLGIQAFEPVLIIEGKAIQLHPLVCAAY	NADFDGQ	QMAVHVPL	FLEAQLAEARLMMSTN	488		
BAE77332.1	LHRLGIQAFEPVLIIEGKAIQLHPLVCAAY	NADFDGQ	QMAVHVPL	FLEAQLAEARLMMSTN	488		
tr A0A237JUP3 A0A237JUP3_SHISO	LHRLGIQAFEPVLIIEGKAIQLHPLVCAAY	NADFDGQ	QMAVHVPL	FLEAQLAEARLMMSTN	488		
tr A0A0F1RBF2 A0A0F1RBF2_ENTAS	LHRLGIQAFEPVLIIEGKAIQLHPLVCAAY	NADFDGQ	QMAVHVPL	FLEAQLAEARLMMSTN	488		
tr A0A1B3EWG0 A0A1B3EWG0_ENTCL	LHRLGIQAFEPVLIIEGKAIQLHPLVCAAY	NADFDGQ	QMAVHVPL	FLEAQLAEARLMMSTN	488		
tr A0A0FOX62 A0A0FOX62_9ENTR	LHRLGIQAFEPVLIIEGKAIQLHPLVCAAY	NADFDGQ	QMAVHVPL	FLEAQLAEARLMMSTN	488		
sp Q5PK92 RPOC_SALPA	LHRLGIQAFEPVLIIEGKAIQLHPLVCAAY	NADFDGQ	QMAVHVPL	FLEAQLAEARLMMSTN	488		
sp A9MHE9 RPOC_SALAR	LHRLGIQAFEPVLIIEGKAIQLHPLVCAAY	NADFDGQ	QMAVHVPL	FLEAQLAEARLMMSTN	488		
tr A0A232XM43 A0A232XM43_SALMU	LHRLGIQAFEPVLIIEGKAIQLHPLVCAAY	NADFDGQ	QMAVHVPL	FLEAQLAEARLMMSTN	488		
tr B5RFK0 B5RFK0_SALG2	LHRLGIQAFEPVLIIEGKAIQLHPLVCAAY	NADFDGQ	QMAVHVPL	FLEAQLAEARLMMSTN	488		
sp P0A2R5 RPOC_SALTI	LHRLGIQAFEPVLIIEGKAIQLHPLVCAAY	NADFDGQ	QMAVHVPL	FLEAQLAEARLMMSTN	488		
sp Q57H68 RPOC_SALCH	LHRLGIQAFEPVLIIEGKAIQLHPLVCAAY	NADFDGQ	QMAVHVPL	FLEAQLAEARLMMSTN	488		
sp P0A2R4 RPOC_SALTY	LHRLGIQAFEPVLIIEGKAIQLHPLVCAAY	NADFDGQ	QMAVHVPL	FLEAQLAEARLMMSTN	488		
sp A6TGP1 RPOC_KLEP7	LHRLGIQAFEPVLIIEGKAIQLHPLVCAAY	NADFDGQ	QMAVHVPL	FLEAQLAEARLMMSTN	488		
tr A0A0J2K6S7 A0A0J2K6S7_9ENTR	LHRLGIQAFEPVLIIEGKAIQLHPLVCAAY	NADFDGQ	QMAVHVPL	FLEAQLAEARLMMSTN	488		
tr A0A0G3RZQ0 A0A0G3RZQ0_KLEOX	LHRLGIQAFEPVLIIEGKAIQLHPLVCAAY	NADFDGQ	QMAVHVPL	FLEAQLAEARLMMSTN	488		
tr A0A212HDS5 A0A212HDS5_9ENTR	LHRLGIQAFEPVLIIEGKAIQLHPLVCAAY	NADFDGQ	QMAVHVPL	FLEAQLAEARLMMSTN	488		
tr A0A1R0FP41 A0A1R0FP41_CITBR	LHRLGIQAFEPVLIIEGKAIQLHPLVCAAY	NADFDGQ	QMAVHVPL	FLEAQLAEARLMMSTN	488		
tr A0A078LHA5 A0A078LHA5_CITKO	LHRLGIQAFEPVLIIEGKAIQLHPLVCAAY	NADFDGQ	QMAVHVPL	FLEAQLAEARLMMSTN	488		
sp A8AKT8 RPOC_CITK8	LHRLGIQAFEPVLIIEGKAIQLHPLVCAAY	NADFDGQ	QMAVHVPL	FLEAQLAEARLMMSTN	488		
	*****:***:***:*****	*****	*****	*****	*****		
AEG34223.1	HLLIKAAEAGEIQEVPVRSPLTQ	OTRYGV	QKCYG	DLSMARPVSI	GEAVGIVAAQSIGE	1231	
sp Q9KWU6 RPOC_THEAQ	HFLIKAAEAGEVREVPVRSPLTQ	OTRYGV	QKCYG	DLSMARPVSI	GEAVGVVAEESIGE	1231	
ASR51305.1	ENANIATIEALGQAARISPLI	GEATMGV	GKCYG	DLARGTFVNI	GEAVGVIAAQSIGE	920	
OXR47930.1	EDLVEMIDSLGVDEVKIRTP	LETTRRGIC	AHCYGR	DLGRSLVNR	GEAVGVIAAQSIGE	925	
WP_093971861.1	EDLVEMIDSLGVDEVKIRTP	LETTRRGIC	AHCYGR	DLGRSLVNR	GEAVGVIAAQSIGE	925	
sp A7MQQ8 RPOC_CROS8	EQWCDLLEANSVDVAVKVR	SVVSD	DTDFGV	AHCYGR	DLARGHI	INKGEAIGVIAAQSIGE	925
sp Q32AG0 RPOC_SHIDS	EQWCDLLEANSVDVAVKVR	SVVSD	DTDFGV	AHCYGR	DLARGHI	INKGEAIGVIAAQSIGE	925
sp Q0SY12 RPOC_SHIF8	EQWCDLLEANSVDVAVKVR	SVVSD	DTDFGV	AHCYGR	DLARGHI	INKGEAIGVIAAQSIGE	925
sp B2TWH4 RPOC_SHIB3	EQWCDLLEANSVDVAVKVR	SVVSD	DTDFGV	AHCYGR	DLARGHI	INKGEAIGVIAAQSIGE	925
sp P0A8T7 RPOC_ECOLI	EQWCDLLEANSVDVAVKVR	SVVSD	DTDFGV	AHCYGR	DLARGHI	INKGEAIGVIAAQSIGE	925
sp Q3YUZ6 RPOC_SHISS	EQWCDLLEANSVDVAVKVR	SVVSD	DTDFGV	AHCYGR	DLARGHI	INKGEAIGVIAAQSIGE	925
sp B1XBZ0 RPOC_ECODH	EQWCDLLEANSVDVAVKVR	SVVSD	DTDFGV	AHCYGR	DLARGHI	INKGEAIGVIAAQSIGE	925
sp A8A787 RPOC_ECOHS	EQWCDLLEANSVDVAVKVR	SVVSD	DTDFGV	AHCYGR	DLARGHI	INKGEAIGVIAAQSIGE	925
tr A0A237JUP3 A0A237JUP3_SHISO	EQWCDLLEANSVDVAVKVR	SVVSD	DTDFGV	AHCYGR	DLARGHI	INKGEAIGVIAAQSIGE	925
tr A0A0F1RBF2 A0A0F1RBF2_ENTAS	EHWCDDLEANSVDSVKVR	SVVSD	DTDFGV	AHCYGR	DLARGHI	INKGEAIGVIAAQSIGE	925
tr A0A1B3EWG0 A0A1B3EWG0_ENTCL	EQWCDLLEANSVDSVKVR	SVVSD	DTDFGV	AHCYGR	DLARGHI	INKGEAIGVIAAQSIGE	925
tr A0A0FOX62 A0A0FOX62_9ENTR	EQWCDLLEANSVDSVKVR	SVVSD	DTDFGV	AHCYGR	DLARGHI	INKGEAIGVIAAQSIGE	925
sp Q5PK92 RPOC_SALPA	EQWCDLLEANSVDSVKVR	SVVSD	DTDFGV	AHCYGR	DLARGHI	INKGEAIGVIAAQSIGE	925
sp A9MHE9 RPOC_SALAR	EQWCDLLEANSVDSVKVR	SVVSD	DTDFGV	AHCYGR	DLARGHI	INKGEAIGVIAAQSIGE	925
tr A0A232XM43 A0A232XM43_SALMU	EQWCDLLEANSVDSVKVR	SVVSD	DTDFGV	AHCYGR	DLARGHI	INKGEAIGVIAAQSIGE	925
tr B5RFK0 B5RFK0_SALG2	EQWCDLLEANSVDSVKVR	SVVSD	DTDFGV	AHCYGR	DLARGHI	INKGEAIGVIAAQSIGE	925
sp P0A2R5 RPOC_SALTI	EQWCDLLEANSVDSVKVR	SVVSD	DTDFGV	AHCYGR	DLARGHI	INKGEAIGVIAAQSIGE	925
sp Q57H68 RPOC_SALCH	EQWCDLLEANSVDSVKVR	SVVSD	DTDFGV	AHCYGR	DLARGHI	INKGEAIGVIAAQSIGE	925
sp P0A2R4 RPOC_SALTY	EQWCDLLEANSVDSVKVR	SVVSD	DTDFGV	AHCYGR	DLARGHI	INKGEAIGVIAAQSIGE	925
sp A6TGP1 RPOC_KLEP7	EHWCDDLEANSVDSVKVR	SVVSD	DTDFGV	AHCYGR	DLARGHI	INKGEAIGVIAAQSIGE	925
tr A0A0J2K6S7 A0A0J2K6S7_9ENTR	EQWCDLLEANSVDSVKVR	SVVSD	DTDFGV	AHCYGR	DLARGHI	INKGEAIGVIAAQSIGE	925
tr A0A0G3RZQ0 A0A0G3RZQ0_KLEOX	EHWCDDLEANSVDSVKVR	SVVSD	DTDFGV	AHCYGR	DLARGHI	INKGEAIGVIAAQSIGE	925
tr A0A212HDS5 A0A212HDS5_9ENTR	EQWCDLLEANSVDSVKVR	SVVSD	DTDFGV	AHCYGR	DLARGHI	INKGEAIGVIAAQSIGE	925
tr A0A1R0FP41 A0A1R0FP41_CITBR	EQWCDLLEANSVDSVKVR	SVVSD	DTDFGV	AHCYGR	DLARGHI	INKGEAIGVIAAQSIGE	925
tr A0A078LHA5 A0A078LHA5_CITKO	EQWCDLLEANSVDSVKVR	SVVSD	DTDFGV	AHCYGR	DLARGHI	INKGEAIGVIAAQSIGE	925
sp A8AKT8 RPOC_CITK8	EQWCDLLEANSVDSVKVR	SVVSD	DTDFGV	AHCYGR	DLARGHI	INKGEAIGVIAAQSIGE	925
	. : : . * : * : * * * * . . .	***:***:***:*****					

```
// end of the prokaryotic β' elongation subunits
AEG34223.1      AARRG-----VKREQPGKQA-      1524
ASR51305.1      APVAAEFPEA--VDTDAE-----      1403
OXR47930.1      VTVESAFEADSVDNNEVQDGNEE-     1416
WP_093971861.1  VTVESAFEADSVDNNEVQDGNEE-     1416
sp|A7MQQ8|RPOC_CROS8      ASLA-----ELL-NA-GLGGNDNE      1407
sp|Q32AG0|RPOC_SHIDS      ASLA-----ELL-NA-GLGGSDNE      1407
sp|Q0SY12|RPOC_SHIF8      ASLA-----ELL-NA-GLGGSDNE      1407
sp|B2TWH4|RPOC_SHIB3      ASLA-----ELL-NA-GLGGSDNE      1407
sp|P0A8T7|RPOC_ECOLI      ASLA-----ELL-NA-GLGGSDNE      1407
BAE77332.1      ASLA-----ELL-NA-GLGGSDNE      1407
sp|A8A787|RPOC_ECOHS      ASLA-----ELL-NA-GLGGSDNE      1407
sp|Q3YUZ6|RPOC_SHISS      ASLA-----ELL-NA-GLGGSDNE      1407
sp|B1XBZ0|RPOC_ECODH      ASLA-----ELL-NA-GLGGSDNE      1407
tr|A0A237JUP3|A0A237JUP3_SHISO  ASLA-----ELL-NA-GLGGSDNE      1407
tr|A0A0F1RBF2|A0A0F1RBF2_ENTAS  ASLA-----ELL-NA-GLGGSDNE      1407
tr|A0A1B3EWG0|A0A1B3EWG0_ENTCL  ASLA-----ELL-NA-GLGGSDNE      1407
tr|A0A0F0XM62|A0A0F0XM62_9ENTR  ASLA-----ELL-NA-GLGGSDNE      1407
sp|Q5PK92|RPOC_SALPA      ASLA-----ELL-NA-GLGGSDNE      1407
sp|A9MHE9|RPOC_SALAR      ASLA-----ELL-NA-GLGGSDNE      1407
tr|A0A232XM43|A0A232XM43_SALMU  ASLA-----EPL-NA-GLGGSDNE      1407
tr|B5RFK0|B5RFK0_SALG2      ASLA-----ELL-NA-GLGGSDNE      1407
sp|P0A2R5|RPOC_SALTI      ASLA-----ELL-NA-GLGGSDNE      1407
sp|Q57H68|RPOC_SALCH      ASLA-----ELL-NA-GLGGSDNE      1407
sp|P0A2R4|RPOC_SALTY      ASLA-----ELL-NA-GLGGSDNE      1407
sp|A6TGP1|RPOC_KLEP7      ANLA-----ELL-NA-GLGGSDNE      1407
tr|A0A0J2K6S7|A0A0J2K6S7_9ENTR  ANLA-----ELL-NA-GLGGSDNE      1407
tr|A0A0G3RZQ0|A0A0G3RZQ0_KLEOX  ANLA-----ELL-NA-GLGGSDNE      1407
tr|A0A212HDS5|A0A212HDS5_9ENTR  ASLA-----ELL-NA-GLGGSDNE      1407
tr|A0A1R0FP41|A0A1R0FP41_CITBR  ASLA-----ELL-NA-GLGGSDNE      1407
tr|A0A078LHA5|A0A078LHA5_CITKO  ASLA-----ELL-NA-GLGGSDNE      1407
sp|A8AKT8|RPOC_CITK8      ASLA-----ELL-NA-GLGGSDNE      1407
```

Fig. 1. MSA of the β' elongation subunits of the MSU RNAPs from different bacteria

AEG34223.1 <i>Thermus thermophilus</i>	Q9KWU6 RPOC_THEAQ <i>Thermus aquaticus</i>
ASR51305.1 <i>Blastomonas fulva</i>	OXR47930.1 <i>Pusillimonas</i> sp.
WP_093971861.1 <i>Pusillimonas</i> sp. T2	A7MQQ8 RPOC_CROS8 <i>Cronobacter sakazakii</i>
Q32AG0 RPOC_SHIDS <i>Shigella dysenteriae</i> ,	Q0SY12 RPOC_SHIF8 <i>Shigella flexneri</i> serotype 5b
B2TWH4 RPOC_SHIB3 <i>Shigella boydii</i> ,	P0A8T7 RPOC_ECOLI <i>Escherichia coli</i> (strain K12)
A8A787 RPOC_ECOHS <i>Escherichia coli</i> O9:H4	Q3YUZ6 RPOC_SHISS <i>Shigella sonnei</i>
B1XBZ0 RPOC_ECODH <i>Escherichia coli</i> (K12)	A0A237JUP3_SHISO <i>Shigella sonnei</i>
A0A0F1RBF2_ENTAS <i>Enterobacter asburiae</i>	A0A1B3EWG0_ENTCL <i>Enterobacter cloacae</i>
A0A0F0XM62_9ENTR <i>Enterobacter kobei</i>	Q5PK92 RPOC_SALPA <i>Salmonella paratyphi</i> A
A9MHE9 RPOC_SALAR <i>Salmonella arizonae</i>	A0A232XM43_SALMU <i>Salmonella muenchen</i>
B5RFK0_SALG2 <i>Salmonella gallinarum</i>	P0A2R5 RPOC_SALTI <i>Salmonella typhi</i>
Q57H68 RPOC_SALCH <i>Salmonella choleraesuis</i>	P0A2R4 RPOC_SALTY <i>Salmonella typhimurium</i> (LT2)
A6TGP1 RPOC_KLEP7 <i>Klebsiella pneumoniae</i>	A0A0J2K6S7_9ENTR <i>Klebsiella michiganensis</i>
A0A0G3RZQ0_KLEOX <i>Klebsiella oxytoca</i>	A0A212HDS5_9ENTR <i>Citrobacter</i> sp. 86
A0A1R0FP41_CITBR <i>Citrobacter braakii</i>	A0A078LHA5_CITKO <i>Citrobacter koseri</i>
A8AKT8 RPOC_CITK8 <i>Citrobacter koseri</i> (K8)	

an SDM experiment where the first two Cs modification (marked in dark blue) lead to the loss of the enzyme activity [13]. It is interesting to note that similar intrinsic zinc binding PR site is not observed in the initiation subunits β, as they make only small primers for RNA elongation (-⁵³⁹TRER⁶AGFEVRDVPHTHYGR⁵⁵⁷- numbering from *E. coli* β subunit) [8].

In addition to the Zn²⁺-binding motif, X-ray crystallographic analysis of the *T. aquaticus* RNAP also showed a Mg²⁺-binding site. The Mg²⁺ was chelated at an absolutely conserved – NADFDGD- motif in the β' subunits and that

apply to all other prokaryotic RNAPs (e.g., –⁴⁸⁸NADFDGD- (numbering from *E. coli* β' subunit) [14]. The Mg²⁺-binding site (site A) was further confirmed by SDM experiments. Substitution of the invariant Ds by A (D→A) gave rise to a dominant lethal phenotype and showed no detectable enzyme activity [13]. Sydow and Cramer have suggested that a mismatch during transcription could cause loss of the catalytic metal ion A (Mg²⁺) which might give way for the metal ion B (Zn²⁺) to perform the PR activity [11]. These results strengthen the bifunctional, “tunable” mode of active site in MSU RNAPs [10].

3.1.2 Proposed mechanism for the PR and polymerization reactions in bacterial MSU RNAPs

As suggested elsewhere, the PR function is found to be integrated into the polymerase active site itself in MSU RNAPs. Thus, the polymerization is achieved using the metal ion Mg^{2+} and the PR function is achieved by the second metal ion Zn^{2+} . Modeling of the substrate NTP bound to the *T. thermophilus* RNAP active site suggests that N⁴⁵⁸ (numbering from *E. coli* RNA polymerase) within a highly conserved sequence motif -⁴⁵⁸NADFDGD⁴⁶⁴- that includes the catalytic Asp triad (D⁴⁶⁰, D⁴⁶² and D⁴⁶⁴) which could mediate specific recognition of the O2 ribose atom and NTP selection [15,12] Both the catalytic metal ions are coordinated by a set of completely conserved amino acids in all the MSU RNAPs. Fig. 2A shows the proposed active amino acids of the PR exonuclease in the MSU RNAP from *E. coli*.

During a mismatch the polymerase pauses, giving way for the PR exonuclease active site, embedded within the polymerases active site itself, to excise the wrongly inserted nucleotide. The RNAP PR exonuclease unlike the PR exonucleases of DNAPs and RNA-dependent RNAPs, backtracks one nucleotide from the mismatch and make a cut on the penultimate base removing a dinucleotide [16] (Fig. 2B).

3.2 Analysis of PR Active Site in the MSU RNAPs from Plant Chloroplasts

MSU RNAP from plant chloroplasts is also a well characterized one. It belongs to prokaryotic-type and is very similar to eubacterial MSU RNAP discussed elsewhere. The MSU RNAP from plant chloroplasts is encoded by the plastids and hence, also known as plastid-encoded

polymerase (PEP). The MSU enzyme from chloroplasts is structurally similar to their eubacterial counterparts, except having an additional subunit, β'' and hence the chloroplast enzyme's subunit composition is α , β , β' , β'' and ω . [9]. (Chloroplasts also possess another RNAP which is encoded by the nucleus (NEP) and imported into the chloroplasts. It is structurally unrelated to PEP and belongs to the single subunit (SSU) RNAP types and is very similar to the SSU RNAPs of bacteriophages T3, T7, SP6, etc. in structure and function). In chloroplast MSU RNAPs, the β is involved in the initiation of transcription like in prokaryotes and both the β' and β'' subunits involve in the elongation process. Whereas the Mg^{2+} -binding site is found in the β' subunit, the polymerization active site is found in the β'' subunit. MSAs show the Mg^{2+} -binding site from β' subunits and the polymerization active site from β'' subunits of the RNAPs of chloroplasts from various plant species (Figs. 3a, 3b).

Figure 3a shows the Mg^{2+} -binding site in the β' subunits from various plant sources. It shows a completely conserved Mg^{2+} -binding site (-NADFDGD-) with three invariant Ds as in the prokaryotic types, suggesting its possible prokaryotic origin. The maize enzyme is highlighted in yellow and the Mg^{2+} -binding site is in light green.

Figure 3b shows the polymerization active site region from the β'' subunits of the MSU RNAPs of chloroplasts from various plant sources. The template-binding and catalytic pairs are highlighted in yellow and the Zn^{2+} -binding Cys residues are highlighted in orange. It shows very similar polymerization active site with the zinc-binding motif (-CX₆CX₂C-) like the prokaryotic type with similar template-binding and catalytic pairs, suggesting its possible origin.

-883RSVVS⁸⁸⁸C⁸⁸⁸DTDFGV⁸⁹⁵C⁸⁹⁵AHC⁸⁹⁸YGR⁹⁰¹- RNAP active site (*E. coli*)

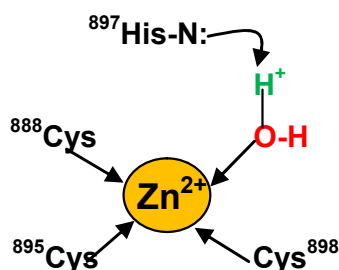


Fig. 2A. Proposed active site in prokaryotic MSU RNAPs (numbering from *E. coli* β' subunit)

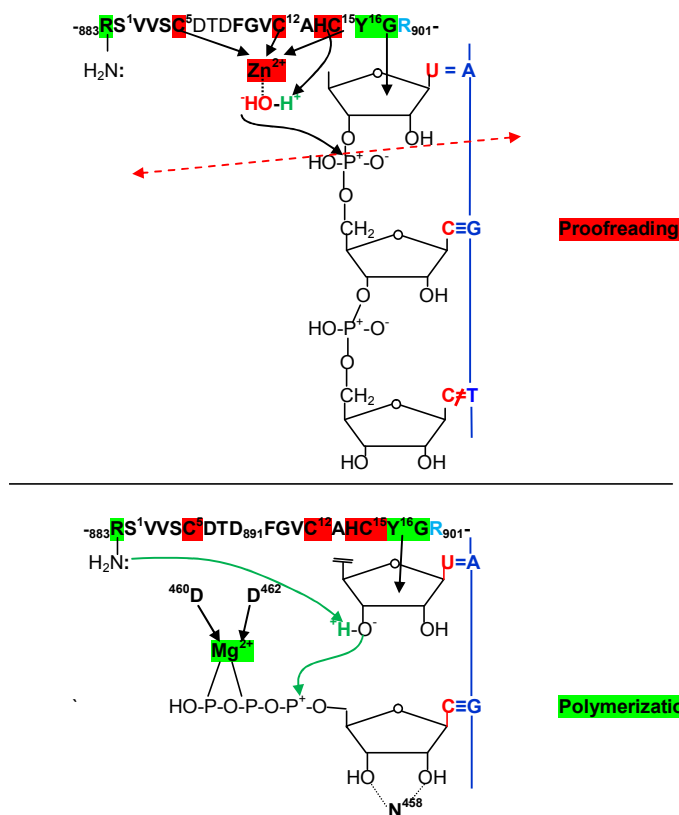


Fig. 2B. A simplified, schematic diagramme showing the proposed reactions of the PR and polymerization active sites in the mismatch repair and polymerization processes in bacterial MSU RNAPs (numbering from *E. coli* β' subunit).

CLUSTAL O (1.2.4) MSA of the elongation subunits β' of MSU RNAPs from plant chloroplasts (Only the Mg^{2+} -binding region of the β' subunits is shown here)

SP P0C506 RPOC1_ORYSJ	RAPTLHRLGIQAFQPTLVEGRTICLHPLVCKGF	NADFDGQ	QMAVHI	PLSLEAQAEARLLM	513
SP A7M957 RPOC1_CUSRE	RAPTLHRLGIQAFQPLVEGHVLC	NADFDGQ	QMAVHV	PLSLEAQAEARLLM	520
SP B1X3M9 RPOC1_PAUCH	RAPTLHRLGIQAFEPKLVDGRAIQ	NADFDGQ	QMAVHV	PLSIEAQTEARLLM	504
SP Q1XDN6 RPOC1_PYRYE	RAPTLHRLGIQAFEPILVEGRAIK	NADFDGQ	QMAVHV	PLSLEAQAEARLLM	496
SP P42080 RPOC1_CYAPA	RAPTLHRLSIQAFEPILVEGRAIQ	NADFDGQ	QMAVHV	PLSLEAQTEARLLM	495
SP Q4G3A6 RPOC1_EMIHU	RAPTLHRLGIQSFEPILVSGRAIK	NADFDGQ	QMAVHI	PLSLEAQSEARLLM	484
SP O19897 RPOC1_CYACA	RAPTLHRLGIQAFDFVLVDGRAIK	NADFDGQ	QMAVHI	PLSIEAQTEARLLM	492
SP P51251 RPOC1_PORPU	RAPTLHRLGIQAFEPILVEGRAIK	NADFDGQ	QMAVHV	PLSLEAQAEARLLM	496
SP Q6B8R7 RPOC1_GRATL	RAPTLHRLGIQAFEPILVEGRAIK	NADFDGQ	QMAVHV	PLSLEAQAEARLLM	496
SP P56763 RPOC1_ARATH	RAPTLHRLGIQSFQPI	NADFDGQ	QMAVHV	PLSLEAQAEARLLM	513
SP P16024 RPOC1_MAIZE	RAPTLHRLGIQAFQPTLVEGRTICLHPLVCKGF	NADFDGQ	QMAVHPL	SLEAQAEARLLM	513
SP Q85FM8 RPOC1_ADICA	RAPTLHRLGIQAFQPLLEIGRAIK	NADFDGQ	QMAVHV	PLSVEAQTEARLLM	513
SP Q85CL6 RPOC1_ANTFO	RAPTLHRLGIQAFEPILVEGRAIK	NADFDGQ	QMAVHI	PLSLEAQVEARLLM	513
SP P42079 RPOC1_SYNE7	RAPTLHRLGIQAFEPILVEGRAIQ	NADFDGQ	QMAVHV	PLSIEAQAEARMLM	490
SP P11705 RPOC1_SPIOL	RAPTLHRLGIQAFQPI	NADFDGQ	QMAVHV	PLSLEAQAEARLLM	513
SP P14563 RPOC1_NOSCO	RAPTLHRLGIQSFEPILVEGRAIQ	NADFDGQ	QMAVHV	PLSLESQAEARLLM	487
SP Q2MIA9 RPOC1_SOLLC	RAPTLHRLGIQAFQPLVEGRAIQ	NADFDGQ	QMAVHV	PLSLEAQVEARLLM	513
SP Q6ENI3 RPOC1_ORYNI	RAPTLHRLGIQAFQPTLVEGRTICLHPLVCKGF	NADFDGQ	QMAVHI	PLSLEAQAEARLLM	513
SP P46819 RPOC1_SINAL	RAPTLHRLGIQSFQPI	NADFDGQ	QMAVHV	PLSLEAQAEARLLM	521
SP P58131 RPOC1_EUGLO	RAPTLHRLNIQAFQPKLTIGKSIK	NADFDGQ	QMGVHI	PLSLKAQAEARNIL	64
SP O78484 RPOC1_GUIITH	RAPTLHRLGIQAFEPILVEGRAIK	NADFDGQ	QMAVHI	PLSLEAQAEARMLM	490
SP Q2VEI5 RPOC1_SOLTU	RAPTLHRLGIQAFQPLVEGRAIK	NADFDGQ	QDFKVI	PLSLEAQVEARLLM	519
SP A6MVX3 RPOC1_RHDSA	RAPTLHRLGIQAFEPILVEGRAIK	NADFDGQ	QMAVHI	PLSLEAQAEARLLM	490
	***** .**.*.*	* * .:	*****	.*.*****	::**.*.* *


```
//End of the β' elongation subunits
SP|P56764|RPOC2_ARATH AALRGRIDWLKGLKENVVLGGVIPAAGTGFNFKGLVHCSRQHTNIILEKKTKNLALFEGDMR 1354
SP|Q85FM9|RPOC2_ADICA AALRGRIDWLKGLKENVVLGDSVPGTGSPEIYQQLNI-NKE-----KESRLASGGSK 1378
SP|Q6L3A5|RPOC2_SACHY AALRGRIDWLKGLKENVVLGGIIPVGTGF-QKFVHRSPQDKNLYFE--IQKKNLFASEMR 1500
SP|P0C509|RPOC2_ORYSJ AALRGRIDWLKGLKENVVLGGIIPVGTGF-QKFVHRYPQKNLYFE--IQKKNLFASEMR 1481
SP|Q85C71|RPOC2_ANTFO AALRGRIDWLKGLKENVIFGGVISAAGTGCQEVV-WQVILEKRRKETYSKRKKNLFSGRVR 1408
SP|P16025|RPOC2_MAIZE AALRGRIDWLKGLKENVVLGGIIPVGTGF-QKFVHRSPQDKNLYLE--IQKKNLFASEMR 1493
SP|B1X3M8|RPOC2_PAUCH AAIEGKTDYLRGLKENVILGRLIPAGTGFSGFEE-----ELRS-----EAGHPH 1277
SP|P48120|RPOC2_CYAPA AAVEGKIDQLRGLKENVILGNLIPAGTGFSAFYND-----NAVF-----QONEDIE 1236
SP|P11704|RPOC2_SPIOL AALRGRIDWLKGLKENVVLGGMIPVGTGF-KGFVHSSQHKDIPK--TKKQNLFEEMGM 1344
SP|B1VKH5|RPOC2_CRYJA SALQGRIDWLKGLKENVILGGMIPVGTGFNR-LVKRSKMN-----SRTSQKSLFINKVE 1145
SP|Q01923|RPOC2_SORBI AALRGRIDWLKGLKENVVLGGIIPVGTGF-QKFVHRSPQDKNLYFE--IKKKNLFASEMR 1486
SP|Q6ENI2|RPOC2_ORYNI AALRGRIDWLKGLKENVVLGGIIPVGTGF-QKFVHRYPQDKNLYFE--IQKKNLFASEMR 1481
TR|E5KU86|E5KU86_CORLA AALRGRIDWLKGLKENVVLGGMIPVGTGF-KGLAPRSRQHNNIPL--TKKKNFFEGEMR 1348
SP|A8W3B4|RPOC2_CUSEX AALGGRIDWLKGLKENVVLGGVIPAAGTGF-RGLVDPSPKQYKTIPLK----TNLFEGGMR 1360
SP|Q1KVX8|RPOC2_TETOB ASISRKDDFLKGLKENIILVGNLMPSTGTYMVL---RKNL----- 2552
SP|Q0ZJ30|RPOC2_VITVI AALWGRIDWLKGLKENVVLGGMIPVGTGF-KGLVHRSRQHNNIPL--TKKKNLFFEREMR 1362
SP|P60290|RPOC2_PHYPA AALRGRIDWLKGLKENVILGGIIPVGTGFCCEVL-WQITLEKQKNILLKKNKSKLPHNKVK 1309
SP|P60289|RPOC2_AMBTC AALRSRIDWLKGLKENVVLGGMIPVGTGF-KGFVHHSREHNNISLE--IKKKNLFDGKMR 1349
SP|Q2MIB0|RPOC2_SOLLC AALRGRIDWLKGLKENVVLGGVIPAAGTGF-KGLVHPSKQHNNIPL--TKKTNLFEGEMR 1360
::: * : :*****:.* : ***
```

Fig. 3b. MSA of β' subunits MSU RNAPs from chloroplasts

P56764 RPOC2_ARATH	<i>Arabidopsis thaliana</i>	Q85FM9 RPOC2_ADICA	<i>Adiantum capillus-veneris</i>
Q6L3A5 RPOC2_SACHY	<i>Saccharum hybrid</i>	P0C509 RPOC2_ORYSJ	<i>Oryza sativa subsp. japonica</i>
Q85C71 RPOC2_ANTFO	<i>Anthoceros formosae</i>	P16025 RPOC2_MAIZE	<i>Zea mays</i>
B1X3M8 RPOC2_PAUCH	<i>Paulinella chromatophora</i>	P48120 RPOC2_CYAPA	<i>Cyanophora paradoxa</i>
P11704 RPOC2_SPIOL	<i>Spinacia oleracea</i>	B1VKH5 RPOC2_CRYJA	<i>Cryptomeria japonica</i>
Q01923 RPOC2_SORBI	<i>Sorghum bicolor</i>	Q6ENI2 RPOC2_ORYNI	<i>Oryza nivara</i>
E5KU86 E5KU86_CORLA	<i>Corynocarpus laevigatus</i>	A8W3B4 RPOC2_CUSEX	<i>Cuscuta exaltata</i>
Q1KVX8 RPOC2_TETOB	<i>Tetradesmus obliquus</i>	Q0ZJ30 RPOC2_VITVI	<i>Vitis vinifera</i>
P60290 RPOC2_PHYPA	<i>Physcomitrella patens</i>	P60289 RPOC2_AMBTC	<i>Amborella trichopoda</i>
Q2MIB0 RPOC2_SOLLC	<i>Solanum lycopersicum</i>		

4. PR FUNCTION IN THE MSU RNAPS FROM EUKARYOTES

Unlike in the prokaryotes where a single RNAP transcribes all the cellular RNAs like mRNAs, rRNAs, tRNAs, in eukaryotes at least 3 distinct RNAPs, viz. RNAP I, RNAP II and RNAP III transcribe the three major RNA species. All the three polymerases are MSU RNAPs and catalyze DNA-dependent RNA synthesis and are localized in the nucleus. RNAP I synthesizes the rRNAs, whereas the RNAP II and RNAP III synthesize mRNAs and tRNAs, respectively. In addition to the three major polymerases, two more MSU RNAPs, viz. the RNAP IV and V are reported from plant sources and they mainly involve in synthesizing small interfering RNAs (siRNAs) for gene silencing in plants [17]. Table 1 shows the composition of the major eukaryotic MSU RNAPs, their compositions and functions in the cell. The initiation and elongation subunits are distinct in all three RNAPs. The unique subunits and common subunits for all the three RNAPs are shown in red and green, respectively. The largest subunit, also known as the elongation subunit with a molecular mass of ~160 kDa (which is functionally equivalent to prokaryotic β') is named; RPA1; RPB1; RPC1 and the second-largest subunit, also known as the initiation subunit with a molecular mass of

~150 kDa (which is functionally equivalent to prokaryotic β); is named RPA2; RPB2; RPC2 from RNAP I, RNAP II and RNAP III, respectively.

4.1 PR Function in the Eukaryotic MSU RNAP I

The RNAP I is localized in the nucleolus sub-compartment of the nucleus and involve in the transcription of precursor rRNAs (pre-rRNA). In yeast, RNAP I activity accounts for up to 60% of all nuclear transcription, and the product, the rRNA accounts for up to 80% of the total cellular RNAs [20]. The common cellular rRNAs like 5.8S, 18S, 28S rRNAs are derived from the 45S pre-rRNA by the pre-rRNA processing. These 3 rRNAs together with the 5S rRNA synthesized by the RNAP III, comprise the enzymatic and structural components of the ribosomes. The transcription of the rRNA genes leads to the synthesis of the several millions copies of ribosomes needed in actively growing cells. Therefore, their synthesis is the first step in ribosome biogenesis and regulation of cell growth. In fact, in the rapidly growing cancer cells, high levels of rRNA synthesis are always maintained. Thus, the up- and down-regulations of rRNA transcription play an important role in oncogenesis.

Table 1. Subunit compositions and functions of the three major eukaryotic polymerases

Subunit structure	RNAP I	RNAP II	RNAP III*
Unique core subunits ($\alpha_2\beta\beta'$ -like)	A190 A135 AC40 AC19 A12.2	Rpb1 (β')** Rpb2 (β) Rpb3 (α) Rpb11 Rpb9	C160 C128 AC40 AC19 C11
Common subunits	Rpb5 Rpb6 Rpb8 Rpb10 Rpb12	Rpb5 Rpb6 (ω) Rpb8 Rpb10 Rpb12	Rpb5 Rpb6 Rpb8 Rpb10 Rpb12
Stalk sub-complex (A14+A43)	A14 A43	Rpb4 Rpb7	C17 C25
TFIIF- like sub-complex (A49+A34.5)	A49 A34.5	TFIIF- α TFIIF- β	C37 C53
Total No. of subunits	14	12	17
Products	pre-rRNAs (45S RNA→28S, 5.8S & 18S)	pre-mRNAs, 5 snRNAs [^] , SnoRNAs & microRNAs	pre-tRNAs, 5S, 7S RNAs [§] & U6-snRNA
Sensitivity to α -Amanitin	Nil	High (1 μ g/ml)	Moderate (10 μ g/ml)
Sensitivity to Actinomycin-D#	0.05 μ g/ml	0.5 μ g/ml	5.0 μ g/ml

Adapted from [18,19]

Current subunit nomenclatures of the RNAPs I, II and III are, RPA1-A14; RPB1-B12; RPC1-C17

*Pol III also possesses a trimeric sub-complex made up of C82-C34-C31.

**The largest subunit of RNAP II (Rpb1) possesses a unique CarboxyTerminal Domain (CTD)

[^]U1-U5 of ~200 bases, involves in the formation of spliceosomes

[§]7S RNA from the signal recognition particle (SRP), which is involved in the transport of proteins into the endoplasmic reticulum.

The RNAP I has a molecular mass of ~600 kDa and made up of 14 subunits [21]. The subunits Rpb5, Rpb6, Rpb8, Rpb10, and Rpb12 are identical in all three polymerases. The two large RNAP I subunits, viz. A190 and A135 are similar in function to the RNAP II subunits Rpb1 (= prokaryotic β') and Rpb2 (= prokaryotic β), respectively [20] and references therein] (Table 1).

The RNAP I from yeast is extensively studied by both cryo-EM and X-ray crystallography [18]. The cryo-EM structure of the complete 14-subunit core enzyme from yeast at 12Å exhibited that the RNAP I showed a strong intrinsic 3'-RNA cleavage activity as compared to RNAP II and RNAP III, which apparently enables rRNA PR activity and end trimming. Furthermore, incubation of the backtracked complex with Mg²⁺ ions led to efficient shortening of the RNA from the 3'-end. An RNAP I variant, lacking residues 79–125 of A12.2 subunit = Rpb9 was totally inactive in RNA cleavage, but bound to the nucleic-acid scaffold and retained elongation

activity, suggesting the C-terminal domain in the involvement of other subunits in RNA I PR function. Interestingly, the conserved polymerase active site of RNAP I was capable of RNA cleavage in the absence of cleavage stimulatory factors. Thus, the intrinsic RNA cleavage activity apparently enables rRNA 3' trimming and PR activities to prevent any possible errors in rRNAs [18]. The crystal structure of RNAP I from the yeast, *S. cerevisiae*, at 2.8Å resolution with all its 14 subunits was studied by Engel et al [20]. The yeast RNAP I structure reveals the 10-subunit RNAP I core and the sub-complexes A49–A34.5 and A14–A43 on opposite sides. Thus, a composite active site of RNAP I and RNAP III enables efficient PR and termination.

Figure 4 shows the MSA analysis of the elongation subunits of RNAP I from different yeasts. The *S. cerevisiae* sequence, template-binding and the catalytic pairs are highlighted in yellow and the 3 invariant Cs (proposed Zn²⁺-binding site) are highlighted in orange. Though the catalytic pair is almost completely conserved

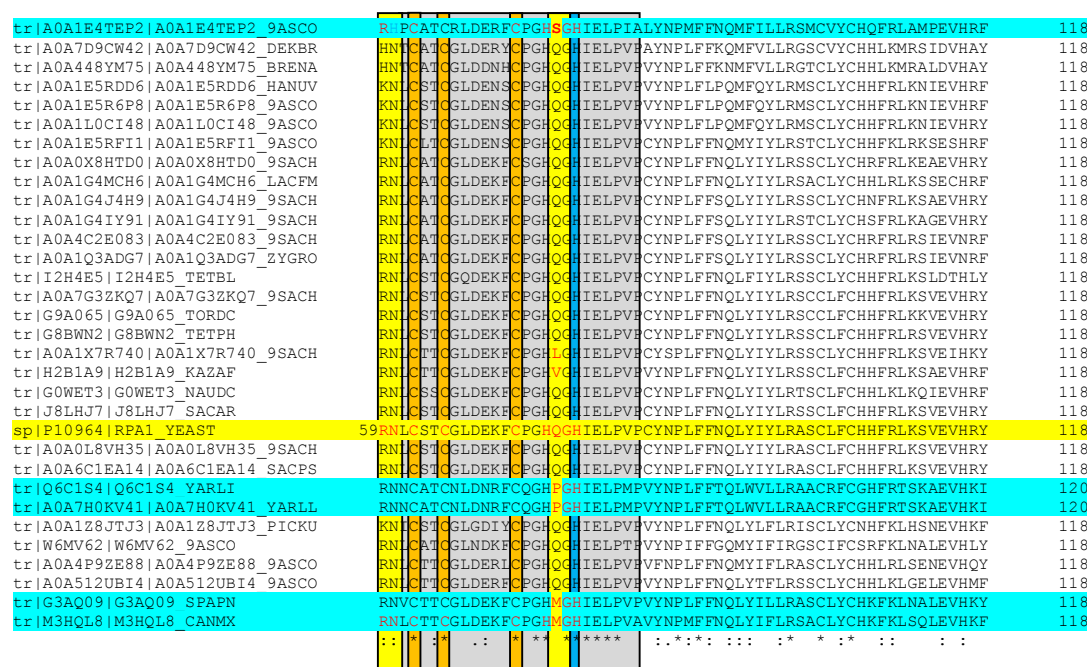
in all, the template-binding pairs are markedly different as compared to other MSU RNAPs discussed above. Most of them use -QG- (with a few exceptions) instead of the regular -YG/FG-pair. Human pathogens and yeasts, which could not ferment sugars showed altogether different sets of template-binding pairs are discussed in Table 2. However, the Mg²⁺-binding site with three Ds is completely conserved in all (highlighted in light green). The human pathogens and yeasts, which could not ferment sugars are highlighted in light blue. All the template-binding pairs are followed by an invariant H (Fig. 4).

Figure 5 shows the MSA analysis of the elongation subunits of RNAP I from higher fungi. The catalytic pair is completely conserved in all but with a basic amino acid H, instead of the usual R/K, which is followed by an invariant hydrophobic amino acid (V/I). The higher fungal group also uses an uncommon template-binding pairs, e.g., most of them use a -TG- pair instead of the regular -YG/FG- pair and some of them use -PG- or -NG- pairs showing a great diversity in the template-binding pairs among the higher fungi. It is interesting to note that the higher fungi that use the unusual template-binding pairs like -NG-/PG- are having something in common,

(i.e.), most of them are pathogenic, e.g., *Talaromyces marneffeii*, *Ajellomyces capsulatus*, and *Blastomyces dermatitidis* are human pathogens [22] The *Talaromyces cellulolyticus* is a cellulolytic fungus (Table 2). However, the Mg²⁺-binding motif is completely conserved in all of them (Fig. 5).

Figure 6 shows the MSA of the elongation subunits of RNAP I from various plant sources. Only polymerization and metal-binding regions are shown. *Arabidopsis thaliana* and *Arachis hypogaea* sequences are used as the standards and highlighted in yellow; the Mg²⁺-binding site is highlighted in light green; the Zn²⁺-binding site is highlighted in orange. The plant system uses the catalytic amino acid R/K as in most of RNAPs, but the template-binding pair is different from the yeast and higher fungi; most of them use an uncommon type of template-binding pair, viz. a -CG- pair and only six of them use a regular -FG- pair (marked in red). Interestingly, all the six of them belong to the family Fabaceae (Leguminosae). However, all of the plant RNAP I template-binding pairs are followed by an invariant H, as in yeast and higher fungi. The Mg²⁺-binding 3 invariant Ds are completely conserved in all (Fig. 6).

CLUSTAL O (1.2.4) MSA of the elongation subunits A1 of RNAP I from yeasts (Only the polymerization active site and Mg²⁺ binding sites are shown here)



tr I2H4E5 I2H4E5_TETBL	NNVGTGSFDILAKASNNN-----	1659
tr A0A7G3ZKQ7 A0A7G3ZKQ7_9SACH	SNVGTGSFDVLRVFNNGR-----	1669
tr G9A065 G9A065_TORDC	SNVGTGSFDLLTKIPNSGV-----	1665
tr G8BWN2 G8BWN2_TETPH	NNVGTGAFDVLAKASHAN-----	1648
tr A0A1X7R740 A0A1X7R740_9SACH	NGGVTGSFDVLAKVPARA-----	1664
tr H2B1A9 H2B1A9_KAZAF	NNVGTGSFDVLAKVPNAA-----	1662
tr GOWET3 GOWET3_NAUDC	NNVGTGSFDILAKVNAV-----	1669
tr J8LHJ7 J8LHJ7_SACAR	NNVGTGSFDVLAKVPNAA-----	1667
sp P10964 RPA1_YEAST	NNVGTGSFDVLAKVPNAA-----	1664
tr A0A0L8VH35 A0A0L8VH35_9SACH	NNVGTGSFDVLAKVPNAA-----	1664
tr A0A6C1EA14 A0A6C1EA14_SACPS	NNVGTGSFDVLAKVPNAA-----	1664
tr Q6C1S4 Q6C1S4_YARLI	SGVGTGSFDVKAPIIEEPFEE----	1628
tr A0A7H0KV41 A0A7H0KV41_YARLL	SGVGTGSFDVKAPIIEEPFEE----	1628
tr A0A1Z8JTJ3 A0A1Z8JTJ3_PICKU	NFAGTGSFDLMAKMPDA-----	1600
tr W6MV62 W6MV62_9ASCO	SNVGTGKFDVMARMPPTAA----	1609
tr A0A4P9ZE88 A0A4P9ZE88_9ASCO	NGMGVTGSFDMTRLFISAQDGVMY	1656
tr A0A512UBI4 A0A512UBI4_9ASCO	NGVGTGSFDMKMKDHSPEAV---	1664
tr G3AQ09 G3AQ09_SPAPN	SNVGTGSFDVFAQIPKGN-----	1639
tr M3HQL8 M3HQL8_CANMX	SKVGTGSFDIFAQMPKI-----	1653

Fig. 4. MSA of the elongation subunits A1 of RNAPs I from different yeasts

A0A1E4TEP2_9ASCO <i>Tortispora caseinolytica</i>	A0A7D9CW42_DEKBR <i>Dekkera bruxellensis</i>
A0A448YM75_BRENA <i>Brettanomyces naardenensis</i>	A0A1E5RDD6_HANUV <i>Hanseniaspora uvarum</i>
A0A1E5R6P8_9ASCO <i>Hanseniaspora opuntiae</i>	A0A1L0CI48_9ASCO <i>Hanseniaspora guilliermondii</i>
A0A1E5RF11_9ASCO <i>Hanseniaspora osmophila</i>	A0A0X8HTD0_9SACH <i>Eremothecium sincaudum</i>
A0A1G4MCH6_LACFM <i>Lachancea fermentati</i>	A0A1G4J4H9_9SACH <i>Lachancea nothofagi</i>
A0A1G4IY91_9SACH <i>Lachancea</i> sp.	A0A4C2E083_9SACH <i>Zygosaccharomyces mellis</i>
A0A1Q3ADG7_ZYGRO <i>Zygosaccharomyces rouxii</i>	I2H4E5_TETBL <i>Tetrapisispora blattae</i>
A0A7G3ZKQ7_9SACH <i>Torulaspora globosa</i>	G9A065_TORDC <i>Torulaspora delbrueckii</i>
G8BWN2_TETPH <i>Tetrapisispora phaffii</i>	A0A1X7R740_9SACH <i>Kazachstania saulgeensis</i>
H2B1A9_KAZAF <i>Kazachstania africana</i>	GOWET3_NAUDC <i>Naumovozyma dairenensis</i>
J8LHJ7_SACAR <i>Saccharomyces arboricola</i>	P10964 RPA1_YEAST <i>Saccharomyces cerevisiae</i>
A0A0L8VH35_9SACH <i>Saccharomyces boulardii</i>	A0A6C1EA14_SACPS <i>Saccharomyces pastorianus</i>
Q6C1S4_YARLI <i>Yarrowia lipolytica</i>	A0A7H0KV41_YARLL <i>Yarrowia lipolytica</i>
A0A1Z8JTJ3_PICKU <i>Pichia kudriavzevii</i>	W6MV62_9ASCO <i>Kuraishia capsulate</i>
A0A4P9ZE88_9ASCO <i>Metschnikowia bicuspidate</i>	A0A512UBI4_9ASCO <i>Metschnikowia</i> sp.
G3AQ09_SPAPN <i>Spathaspora passalidarum</i>	M3HQL8_CANMX <i>Candida albicans maltose</i>

CLUSTAL O (1.2.4) MSA of the elongation subunits A1 of RNAP I from higher fungi

tr B6QC93 B6QC93_TALMQ	MASFARFVASELASVDFSVYSEDIKIKISVKRIFNTPSLDSLHNPIPHSLYDPALGAWGD	60
tr A0A478EDC7 A0A478EDC7_9EURO	MSSFARFVASELASVDFSVYSEDIKIKISVKRIFNTPSLDSLHNPIPHSLYDPALGAWGD	60
tr W6QED6 W6QED6_PENRF	MATFARFVASTINGVDNFVYSEEEIKALSVKRIHNTPTLDSFNNPVPGGQLDPAMGAWGD	60
tr A0A167Y3R7 A0A167Y3R7_PENCH	MATFARFVASTINGVDNFVYSEEEIKALSVKRIHNTPTLDSFNNPVPGGQLDPAMGAWGD	60
tr K9G5R8 K9G5R8_PEND1	MATFARFVASTINGVDNFVYSEEEIKALSVKRIHNTPTLDSFNNPVPGGQLDPAMGAWGD	60
tr A0A0A2I945 A0A0A2I945_PENEN	MATFARFVASTINGVDNFVYSEEEIKALSVKRIHNTPTLDSFNNPVPGGQLDPAMGAWGD	60
tr CONL49 CONL49_AJECG	MASFTRPISSSIEGVDFRVLNSNEEIKTISVKLIYNTPTLDSLNNPVPGGLYDPALGAWGD	60
tr T5BX79 T5BX79_AJEDE	MASFTRPISSSIEGVDFRVLNSNEEIKTISVKLIYNTPTLDSLNNPVPGGLYDPALGAWGD	60
tr A0A318ZLE2 A0A318ZLE2_9EURO	MATFARFVASTIAGIDFGVYDDEDIKALSVKRIQNTPALDSFNNPVPGGLYDPALGAWGD	60
tr A0A1L9RJK4 A0A1L9RJK4_ASPWE	MATFARFVASSIGGVDFGVYSDEDIKISVKRIHNTPTLDSFNNPVPGGLYDPALGAWGD	60
tr A1D226 A1D226_NEOFI	MATFARFVASSISGIEFGVYSDEDIKISVKRIHNTPTLDSFNNPVPGGLYDPALGAWGD	60
tr A0A229XZP5 A0A229XZP5_ASPFM	MATFARFVASSISGIEFGVYSDEDIKISVKRIHNTPTLDSFNNPVPGGLYDPALGAWGD	60
tr Q4WS60 Q4WS60_ASPFU	MATFARFVASSISGIEFGVYSDEDIKISVKRIHNTPTLDSFNNPVPGGLYDPALGAWGD	60
tr A0A0J5Q544 A0A0J5Q544_ASPFM	MATFARFVASSISGIEFGVYSDEDIKISVKRIHNTPTLDSFNNPVPGGLYDPALGAWGD	60
tr A0A3R7HU02 A0A3R7HU02_9EURO	MATFARFVASSISGIEFGVYSDEDIKISVKRIHNTPTLDSFNNPVPGGLYDPALGAWGD	60
tr A0A397GCI6 A0A397GCI6_9EURO	MATFARFVASSISGIEFGVYSDEDIKISVKRIHNTPTLDSFNNPVPGGLYDPALGAWGD	60
:::***: : : * * : : : * : *** * **::*:***: * * **::**::*		
tr B6QC93 B6QC93_TALMQ	HVCTTRQNSWFTCTGHPGHIELPVPVYVNTFFDQVYRLLRAKCDYCHRLRMPRIEINAF	120
tr A0A478EDC7 A0A478EDC7_9EURO	HVCTTRQNSWFTCTGHPGHIELPVPVYVNTFFDQVYRLLRAKCDYCHRFRIARIEIHAYT	120
tr W6QED6 W6QED6_PENRF	HVCTTRQNSWFTCTGHPGHIELPVPVYVNTFFDHIIFRLLRAQCVCYCLRLQMGRRQVNYI	120
tr A0A167Y3R7 A0A167Y3R7_PENCH	HVCTTRQNSWFTCTGHPGHIELPVPVYVNTFFDHIIFRLLRAQCVCYCLRLQMGRRQVNYI	120
tr K9G5R8 K9G5R8_PEND1	HVCTTRQNSWFTCTGHPGHIELPVPVYVNTFFDHIIFRLLRAQCVCYCLRLQMGRRQVNYI	120
tr A0A0A2I945 A0A0A2I945_PENEN	HVCTTRQNSWFTCTGHPGHIELPVPVYVNTFFDHIIFRLLRAQCVCYCLRLQMGRRQVNYI	120
tr CONL49 CONL49_AJECG	HVCTTRQNSWFTCTGHPGHIELPVPVYVNTFFDQVYRLLRAKCDYCHRFRRMSRADIKSYT	120
tr T5BX79 T5BX79_AJEDE	HVCTTRQNSWFTCTGHPGHIELPVPVYVNTFFDQVYRLLRAKCDYCHRFRRMSRADIKSYT	120
tr A0A318ZLE2 A0A318ZLE2_9EURO	HVCTTRQNSWFTCTGHPGHIELPVPVYVNTFFDQVYRLLRAKCDYCHRFRRMSRADIKSYT	120
tr A0A1L9RJK4 A0A1L9RJK4_ASPWE	HVCTTRQNSWFTCTGHPGHIELPVPVYVNTFFDQVYRLLRAKCDYCHRFRRMSRADIKSYT	120
tr A1D226 A1D226_NEOFI	HVCTTRQNSWFTCTGHPGHIELPVPVYVNTFFDQVYRLLRAKCDYCHRFRRMSRADIKSYT	120
tr A0A229XZP5 A0A229XZP5_ASPFM	HVCTTRQNSWFTCTGHPGHIELPVPVYVNTFFDQVYRLLRAKCDYCHRFRRMSRADIKSYT	120
tr Q4WS60 Q4WS60_ASPFU	HVCTTRQNSWFTCTGHPGHIELPVPVYVNTFFDQVYRLLRAKCDYCHRFRRMSRADIKSYT	120
tr A0A0J5Q544 A0A0J5Q544_ASPFM	HVCTTRQNSWFTCTGHPGHIELPVPVYVNTFFDQVYRLLRAKCDYCHRFRRMSRADIKSYT	120
tr A0A3R7HU02 A0A3R7HU02_9EURO	HVCTTRQNSWFTCTGHPGHIELPVPVYVNTFFDQVYRLLRAKCDYCHRFRRMSRADIKSYT	120
tr A0A397GCI6 A0A397GCI6_9EURO	HVCTTRQNSWFTCTGHPGHIELPVPVYVNTFFDQVYRLLRAKCDYCHRFRRMSRADIKSYT	120
:::***: : : * * : : : * : *** * **::*:***: * * **::**::*		

tr A0A314XYK8 A0A314XYK8_PRUYE	S-TY	NADFDGSEMN-----	-----	FTSGDPIRALI	-----	594
tr A0A251N7U5 A0A251N7U5_PRUPE	S-TYNADFDGDE	EMNVHFFQDEISRSEAYNI	VNANNQYVKPTSGDPIRALI	-----	-----	619
sp Q9SVY0 NRPA1_ARATH	S-TYNADFDGDE	EMNVHFFQDEISRSEAYNI	VNANNQYARFNSNGEPLRALI	-----	-----	645
tr V4NE24 V4NE24_EUTSA	S-TYNADFDGDE	EMNVHFFQDEISRSEAYNI	VNANNQYSRFNSNGDPLRALI	QVVHPSYFFK	-----	638
tr A0A3P6GLX8 A0A3P6GLX8_BRAOL	S-TYNADFDGDE	EMNVHFFQDEISRSEAYNI	VNANNQYARFNSNGDPLRALI	-----	-----	619
tr A0A6J0P6B6 A0A6J0P6B6_RAPSA	S-TYNADFDGDE	EMNVHFFQDEISRSEAYNI	VNANNQYARFNSNGDPLRALI	-----	-----	630
tr A0A6P4CDY4 A0A6P4CDY4_ARADU	S-TYNADFDGDE	EMNVHFFQDEISRSEAYNI	VNANNQYVKPTSGDPIRALI	-----	-----	619
tr A0A445AID5 A0A445AID5_ARAHY	S-TYNADFDGDE	EMNVHFFQDEISRSEAYNI	VNANNQYVKPTSGDPIRALI	-----	-----	619
tr A0A6A5MQU4 A0A6A5MQU4_LUPAL	S-TYNADFDGDE	EMNVHFFQDEISRSEAYNI	VNANNQYVKPTSGDPIRALI	-----	-----	643
tr A0A1S2Z239 A0A1S2Z239_CICAR	S-TYNADFDGDE	EMNVHFFQDEISRSEAYNI	VNANNQYVKPTSGDPIRALI	-----	-----	621
tr A0A371FKI2 A0A371FKI2_MUCPR	S-TYNADFDGDE	EMNVHFFQDEISRSEAYNI	VNANNQYVKPTSGDPIRALI	-----	-----	629
tr I1L9X1 I1L9X1_SOYBN	S-TYNADFDGDE	EMNVHFFQDEISRSEAYNI	VNANNQYVKPTSGDPIRALI	-----	-----	630
tr A0A061EW90 A0A061EW90_THECC	S-TYNADFDGDE	EMNVHFFQDEISRSEAYNI	VNANNQYVRFNSNGEPIRALI	-----	-----	648
tr A0A6J1A455 A0A6J1A455_9ROSI	S-TYNADFDGDE	EMNVHFFQDEISRSEAYNI	VNANNQYVRFNSNGEPIRALI	-----	-----	648
tr A0A6P5YS23 A0A6P5YS23_DURZI	S-TYNADFDGDE	EMNVHFFQDEISRSEAYNI	VNANNQYVRFNSNGEPIRALI	-----	-----	648
tr A0A5J5WM67 A0A5J5WM67_GOSBA	S-TYNADFDGDE	EMNVHFFQDEISRSEAYNI	VNANNQYVRFNSNGEPLRALI	-----	-----	647
tr A0A5D3A8H9 A0A5D3A8H9_GOSMU	S-TYNADFDGDE	EMNVHFFQDEISRSEAYNI	VNANNQYVRFNSNGEPLRALI	-----	-----	647
tr A0A5D2D2X8 A0A5D2D2X8_GOSDA	S-TYNADFDGDE	EMNVHFFQDEISRSEAYNI	VNANNQYVRFNSNGEPLRALI	-----	-----	647
tr A0A0D2QHR9 A0A0D2QHR9_GOSRA	S-TYNADFDGDE	EMNVHFFQDEISRSEAYNI	VNANNQYVRFNSNGEPLRALI	-----	-----	647
tr A0A7J7BY57 A0A7J7BY57_TRIWF	S-TYNADFDGDE	EMNVHFFQDEVSRSEAYNI	VNANNQYIRPSSGDP	IRSLI	-----	651
tr A0A5C7IM32 A0A5C7IM32_9ROSI	S-TYNADFDGDE	EMNVHFFQDEVSRSEAYNI	VNANNQYVRFNSNGEPLRALI	-----	-----	653
tr B9SL65 B9SL65_RICCO	SITYNADFDGDE	EMNVHFFQDEVSRSEAYNI	VNANNQYVRFNSNGEPLRGLI	-----	-----	641
tr A0A2C9V7G8 A0A2C9V7G8_MANES	S-TYNADFDGDE	EMNVHFFQDEVSRSEAYNI	VNANNQYVRFNSNGEPLRALI	-----	-----	637
	*	*****	*****			**
						**

// End of A1 of RNAP I sequences	
tr A0A314XYK8 A0A314XYK8_PRUYE	ECTER 1628
tr A0A251N7U5 A0A251N7U5_PRUPE	ECTQR 1528
sp Q9SVY0 NRPA1_ARATH	----- 1670
tr V4NE24 V4NE24_EUTSA	----- 1697
tr A0A3P6GLX8 A0A3P6GLX8_BRAOL	----- 1640
tr A0A6J0P6B6 A0A6J0P6B6_RAPSA	----- 1650
tr A0A6P4CDY4 A0A6P4CDY4_ARADU	----- 1661
tr A0A445AID5 A0A445AID5_ARAHY	----- 1653
tr A0A6A5MQU4 A0A6A5MQU4_LUPAL	----- 1674
tr A0A1S2Z239 A0A1S2Z239_CICAR	----- 1650
tr A0A371FKI2 A0A371FKI2_MUCPR	----- 1630
tr I1L9X1 I1L9X1_SOYBN	----- 1651
tr A0A061EW90 A0A061EW90_THECC	----- 1665
tr A0A6J1A455 A0A6J1A455_9ROSI	----- 1690
tr A0A6P5YS23 A0A6P5YS23_DURZI	----- 1675
tr A0A5J5WM67 A0A5J5WM67_GOSBA	----- 1674
tr A0A5D3A8H9 A0A5D3A8H9_GOSMU	----- 1674
tr A0A5D2D2X8 A0A5D2D2X8_GOSDA	----- 1674
tr A0A0D2QHR9 A0A0D2QHR9_GOSRA	----- 1674
tr A0A7J7BY57 A0A7J7BY57_TRIWF	----- 1733
tr A0A5C7IM32 A0A5C7IM32_9ROSI	----- 1720
tr B9SL65 B9SL65_RICCO	----- 1686
tr A0A2C9V7G8 A0A2C9V7G8_MANES	----- 1707

Fig. 6. MSA of the elongation subunits A1 of RNAPs I from plant sources

A0A314XYK8_PRUYE	<i>Prunus yedoensis</i>	A0A251N7U5_PRUPE	<i>Prunus persica</i>
Q9SVY0 NRPA1_ARATH	<i>Arabidopsis thaliana</i>	V4NE24_EUTSA	<i>Eutrema salsugineum</i>
A0A3P6GLX8_BRAOL	<i>Brassica oleracea</i>	A0A6J0P6B6_RAPSA	<i>Raphanus sativus</i>
A0A6P4CDY4_ARADU	<i>Arachis duranensis</i>	A0A445AID5_ARAHY	<i>Arachis hypogaea</i>
A0A6A5MQU4_LUPAL	<i>Lupinus albus</i>	A0A1S2Z239_CICAR	<i>Cicer arietinum</i>
A0A371FKI2_MUCPR	<i>Mucuna pruriens</i>	I1L9X1_SOYBN	<i>Glycine max</i>
A0A061EW90_THECC	<i>Theobroma cacao</i>	A0A6J1A455_9ROSI	<i>Herrania umbstratica</i>
A0A6P5YS23_DURZI	<i>Durio zibethinus</i>	A0A5J5WM67_GOSBA	<i>Gossypium barbadense</i>
A0A5D3A8H9_GOSMU	<i>Gossypium mustelinum</i>	A0A5D2D2X8_GOSDA	<i>Gossypium darwinii</i>
A0A0D2QHR9_GOSRA	<i>Gossypium raimondii</i>	A0A7J7BY57_TRIWF	<i>Tripterygium wilfordii</i>
A0A5C7IM32_9ROSI	<i>Acer yangbiense</i>	B9SL65_RICCO	<i>Ricinus communis</i>
A0A2C9V7G8_MANES	<i>Manihot esculenta</i>		

Figure 7 shows the MSA analysis of the elongation subunits A1 of the RNAP I from various animal sources. The human sequence is highlighted in yellow. Remarkably, the N- and C-terminals are almost completely conserved in the elongation subunits of animal RNAPs I. The catalytic and the template-binding pairs are –

K/R/E- and -L/G- in all the sequences. The -L/G- pair is followed by an invariant H as found in yeasts, higher fungi and plant sources. The Mg²⁺-binding site is completely conserved in all as found in yeasts, higher fungi and plant sources.

CLUSTAL O (1.2.4) MSA of the elongation subunits A1 of RNAP I from animal sources

tr A0A452TQ80 A0A452TQ80_URISMA	MLGSKNMPWRRLLQGISFGMYSAEELKKLKLSVKSITNPRYLDLSLGNP	SVNGLYDLALG	PADS	60
tr S9X3I0 S9X3I0_CAMFR	MLGSKNMPWRRLLQGISFGMYSAEELKKLKLSVKSITNPRYLDLSLGNP	SVNGLYDLALG	PADS	60
tr A0A7J8FKW0 A0A7J8FKW0_ROUAE	MLGSKNMPWRRLLQGISFGMYSAEELKKLKLSVKSITNPRYLDLSLGNP	SVNGLYDLALG	PADS	60
tr A0A3Q2I2F1 A0A3Q2I2F1_HORSE	MLGSKNMPWRRLLQGISFGMYSAEELKKLKLSVKSITNPRYLDLSLGNP	SVNGLYDLALG	PADS	60
tr A0A3Q2HZF4 A0A3Q2HZF4_HORSE	MLGSKNMPWRRLLQGISFGMYSAEELKKLKLSVKSITNPRYLDLSLGNP	SVNGLYDLALG	PADS	60
tr A0A673UI45 A0A673UI45_SURSU	MLGSKTMPWRRLLQGISFGMYSAEELKKLKLSVKSITNPRYLDLSLGNP	SVNGLYDLALG	PADS	60
tr A0A6P4VUC2 A0A6P4VUC2_PANPR	MLGSKTMPWRRLLQGISFGMYSAEELKKLKLSVKSITNPRYLDLSLGNP	SVNGLYDLALG	PADS	60
tr A0A6P6I466 A0A6P6I466_PUMCO	MLGSKTMPWRRLLQGISFGMYSAEELKKLKLSVKSITNPRYLDLSLGNP	SVNGLYDLALG	PADS	60
tr A0A6I9ZYC2 A0A6I9ZYC2_ACIBJ	MLGSKTMPWRRLLQGISFGMYSAEELKKLKLSVKSITNPRYLDLSLGNP	SVNGLYDLALG	PADS	60
tr M3WAJ5 M3WAJ5_FELCA	MLGSKTMPWRRLLQGISFGMYSAEELKKLKLSVKSITNPRYLDLSLGNP	SVNGLYDLALG	PADS	60
tr J9P5G4 J9P5G4_CANLF	MLGSKNMPWRRLLQGISFGMYSAEELKKLKLSVKSITNPRYLDLSLGNP	SVNGLYDLALG	PADS	60
tr A0A5F4C883 A0A5F4C883_CANLF	MLGSKNMPWRRLLQGISFGMYSAEELKKLKLSVKSITNPRYLDLSLGNP	SVNGLYDLALG	PADS	60
tr A0A2U3X0D3 A0A2U3X0D3_ODORO	MLGSKNMPWRRLLQGISFGMYSAEELKKLKLSVKSITNPRYLDLSLGNP	SVNGLYDLALG	PADS	60
tr G1LGX3 G1LGX3_AILME	MLSSKNMPWRRLLQGISFGMYSAEELKKLKLSVKSITNPRYLDLSLGNP	SVNGLYDLALG	PADS	60
tr A0A6J3BPX4 A0A6J3BPX4_VICPA	MLGSKNMPWRRLLQGISFGMYSAEELKKLKLSVKSITNPRYLDLSLGNP	SVNGLYDLALG	PADS	60
tr A0A2Y9TC94 A0A2Y9TC94_PHYMC	MLGSKNMPWRRLLQGISFGMYSAEELKKLKLSVKSITNPRYLDLSLGNP	SVNGLYDLALG	PADS	60
tr A0A484GYD4 A0A484GYD4_SOUC	MLGSKNMPWRRLLQGISFGMYSAEELKKLKLSVKSITNPRYLDLSLGNP	SVNGLYDLALG	PADS	60
tr A0A6B0QX10 A0A6B0QX10_9CETA	MLGSKNMPWRRLLQGISFGMYSAEELKKLKLSVKSITNPRYLDLSLGNP	SVNGLYDLALG	PADS	60
tr A0A6J0XA49 A0A6J0XA49_ODOVR	MLGSKNMPWRRLLQGISFGMYSAEELKKLKLSVKSITNPRYLDLSLGNP	SVNGLYDLALG	PADS	60
tr A0A6I9KXL29 A0A6I9KXL29_CHRAS	MLGSKNMPWRRLLQGISFGMYSAEELKKLKLSVKSITNPRYLDLSLGNP	SVNGLYDLALG	PADS	60
tr A0A1U7UA15 A0A1U7UA15_CARSF	MLVSKNMPWRRLLQGISFGMYSAEELKKLKLSVKSITNPRYLDLSLGNP	SVNGLYDLALG	PADS	60
tr G1SYP7 G1SYP7_RABIT	MLGSKNMPWRRLLQGISFGMYSAEELKKLKLSVKSITNPRYLDLSLGNP	SVNGLYDLALG	PADS	60
tr H9Z7E8 H9Z7E8_MACMU	MLISKNMPWRRLLQGISFGMYSAEELKKLKLSVKSITNPRYLDLSLGNP	SVNGLYDLALG	PADS	60
tr A0A096NZX0 A0A096NZX0_PAPAN	MLISKNMPWRRLLQGISFGMYSAEELKKLKLSVKSITNPRYLDLSLGNP	SVNGLYDLALG	PADS	60
tr A0A2J8RNZ1 A0A2J8RNZ1_PONAB	MLISKNMPWRRLLQGISFGMYSAEELKKLKLSVKSITNPRYLDLSLGNP	SVNGLYDLALG	PADS	60
sp O95602 RPA1_HUMAN	MLISKNMPWRRLLQGISFGMYSAEELKKLKLSVKSITNPRYLDLSLGNP	SVNGLYDLALG	PADS	60
tr G3QHD8 G3QHD8_GORGO	MLISKNMPWRRLLQGISFGMYSAEELKKLKLSVKSITNPRYLDLSLGNP	SVNGLYDLALG	PADS	60
tr K7CHZ0 K7CHZ0_PANTR	MLISKNMPWRRLLQGISFGMYSAEELKKLKLSVKSITNPRYLDLSLGNP	SVNGLYDLALG	PADS	60
tr A0A2R9CCF8 A0A2R9CCF8_PANPA	MLISKNMPWRRLLQGISFGMYSAEELKKLKLSVKSITNPRYLDLSLGNP	SVNGLYDLALG	PADS	60
	** ** *			
tr A0A452TQ80 A0A452TQ80_URISMA	KEVQSTCVQDFNSGSGELGGLTLP	LPLTVYNPLLFDKLYLLLRGSLNCHMLTC	PRAVIHLL	120
tr S9X3I0 S9X3I0_CAMFR	KEVQSTCVQDFNNGSGELGGLTLP	LPLTVYNPLLFDKLYLLLRGSLNCHMLTC	PRAVIHLL	120
tr A0A7J8FKW0 A0A7J8FKW0_ROUAE	KEVQSTCVQDFSNACGLGGLTLP	LPLTVYNPLLFDKLYLLLRGSLNCHMLTC	PRAVIHLL	120
tr A0A3Q2I2F1 A0A3Q2I2F1_HORSE	KEVQSTCVQDFNNGSGELGGLTLP	LPLTVYNPLLFDKLYLLLRGSLNCHMLTC	PRAVIHLL	120
tr A0A3Q2HZF4 A0A3Q2HZF4_HORSE	KEVQSTCVQDFNNGSGELGGLTLP	LPLTVYNPLLFDKLYLLLRGSLNCHMLTC	PRAVIHLL	120
tr A0A673UI45 A0A673UI45_SURSU	KEVQSTCVQDFNSGPGELGGLTLP	LPLTVYNPLLFDKLYLLLRGSLNCHMLTC	PRAVIHLL	120
tr A0A6P4VUC2 A0A6P4VUC2_PANPR	KEVQSTCVQDFNSGPGELGGLTLP	LPLTVYNPLLFDKLYLLLRGSLNCHMLTC	PRAVIHLL	120
tr A0A6P6I466 A0A6P6I466_PUMCO	KEVQSTCVQDFNSGPGELGGLTLP	LPLTVYNPLLFDKLYLLLRGSLNCHMLTC	PRAVIHLL	120
tr A0A6I9ZYC2 A0A6I9ZYC2_ACIBJ	KEVQSTCVQDFNSGPGELGGLTLP	LPLTVYNPLLFDKLYLLLRGSLNCHMLTC	PRAVIHLL	120
tr M3WAJ5 M3WAJ5_FELCA	KEVQSTCVQDFNSGPGELGGLTLP	LPLTVYNPLLFDKLYLLLRGSLNCHMLTC	PRAVIHLL	120
tr J9P5G4 J9P5G4_CANLF	KEVQSTCVQDFNNGSGELGGLTLP	LPLTVYNPLLFDKLYLLLRGSLNCHMLTC	PRAVIHLL	120
tr A0A5F4C883 A0A5F4C883_CANLF	KEVQSTCVQDFNNGSGELGGLTLP	LPLTVYNPLLFDKLYLLLRGSLNCHMLTC	PRAVIHLL	120
tr A0A2U3X0D3 A0A2U3X0D3_ODORO	KEVQSTCVQDFNNGSGELGGLTLP	LPLTVYNPLLFDKLYLLLRGSLNCHMLTC	PRAVIHLL	120
tr G1LGX3 G1LGX3_AILME	KEVQSTCVQDFNNGSGELGGLTLP	LPLTVYNPLLFDKLYLLLRGSLNCHMLTC	PRAVIHLL	120
tr A0A6J3BPX4 A0A6J3BPX4_VICPA	KEVQSTCVQDFNNGSGELGGLTLP	LPLTVYNPLLFDKLYLLLRGSLNCHMLTC	PRAVIHLL	120
tr A0A2Y9TC94 A0A2Y9TC94_PHYMC	KEVQSTCVQDFNSGPGELGGLTLP	LPLTVYNPLLFEKLYLLLRGSLNCHMLTC	PRAVIHLL	120
tr A0A484GYD4 A0A484GYD4_SOUC	KEVQSTCVQDFNSGSGELGGLTLP	LPLTVYNPLLFEKLYLLLRGSLNCHMLTC	PRAVIHLL	120
tr A0A6B0QX10 A0A6B0QX10_9CETA	KEVQSTCVQDFNTNCSGELGGLTLP	LPLTVYNPLLFDKLYLLLRGSLNCHMLTC	PRAVIHLL	120
tr A0A6J0XA49 A0A6J0XA49_ODOVR	KEVQSTCVQDFNTNCSGELGGLTLP	LPLTVYNPLLFDKLYLLLRGSLNCHMLTC	PRAVIHLL	120
tr A0A6I9KXL29 A0A6I9KXL29_CHRAS	KEVQSTCVQDFNNGSGELGGLTLP	LPLTVYNPLLFDKLYLLLRGSLNCHMLTC	PRAVIHLL	120
tr A0A1U7UA15 A0A1U7UA15_CARSF	KEVQSTCAQDFNNGSGELGGLTLP	LPLMVYNPLLFDKLYLLLRGSLNCHMLTC	PRAVIHLL	120
tr G1SYP7 G1SYP7_RABIT	KEVQSTCVQDFNNGSGELGGLTLP	LPLTVYNPLLFDKLYLLLRGSLNCHMLTC	PRAVIHLL	120
tr H9Z7E8 H9Z7E8_MACMU	KEVQSTCVQDFNNGSGELGGLTLP	LPLTVYNPLLFDKLYLLLRGSLNCHMLTC	PRAVIHLL	120
tr A0A096NZX0 A0A096NZX0_PAPAN	KEVQSTCVQDFNNGSGELGGLTLP	LPLTVYNPLLFDKLYLLLRGSLNCHMLTC	PRAVIHLL	120
tr A0A2J8RNZ1 A0A2J8RNZ1_PONAB	KEVQSTCVQDFNSGSGELGGLTLP	LPLTVYNPLLFDKLYLLLRGSLNCHMLTC	PRAVIHLL	120
sp O95602 RPA1_HUMAN	KEVQSTCVQDFNSGSGELGGLTLP	LPLTVYNPLLFDKLYLLLRGSLNCHMLTC	PRAVIHLL	120
tr G3QHD8 G3QHD8_GORGO	KEVQSTCVQDFNSGSGELGGLTLP	LPLTVYNPLLFDKLYLLLRGSLNCHMLTC	PRAVIHLL	120
tr K7CHZ0 K7CHZ0_PANTR	KEVQSTCVQDFNSGSGELGGLTLP	LPLTVYNPLLFDKLYLLLRGSLNCHMLTC	PRAVIHLL	120
tr A0A2R9CCF8 A0A2R9CCF8_PANPA	KEVQSTCVQDFNSGSGELGGLTLP	LPLTVYNPLLFDKLYLLLRGSLNCHMLTC	PRAVIHLL	120
	** ** *			
tr A0A452TQ80 A0A452TQ80_URISMA	HVKNGDILLNRQPTLHRPSTQAHARILPEEKVRLRLHYANCKA	NADFDG	EMNAHFFQ	600
tr S9X3I0 S9X3I0_CAMFR	HVKNGDILLNRQPTLHRPSTQAHARILPEEKVRLRLHYANCKA	NADFDG	EMNAHFFQ	600
tr A0A7J8FKW0 A0A7J8FKW0_ROUAE	HVKNGDVLLNRQPTLHRPSTQAHARILPEEKVRLRLHYANCKA	NADFDG	EMNAHFFQ	600
tr A0A3Q2I2F1 A0A3Q2I2F1_HORSE	HVKNGDILLNRQPTLHRPSTQAHARILPEEKVRLRLHYANCKA	NADFDG	EMNAHFFQ	600
tr A0A3Q2HZF4 A0A3Q2HZF4_HORSE	HVKNGDILLNRQPTLHRPSTQAHARILPEEKVRLRLHYANCKA	NADFDG	EMNAHFFQ	600
tr A0A673UI45 A0A673UI45_SURSU	HVKNGDILLNRQPTLHRPSTQAHARILPEEKVRLRLHYANCKA	NADFDG	EMNAHFFQ	600
tr A0A6P4VUC2 A0A6P4VUC2_PANPR	HVKNGDILLNRQPTLHRPSTQAHARILPEEKVRLRLHYANCKA	NADFDG	EMNAHFFQ	600
tr A0A6P6I466 A0A6P6I466_PUMCO	HVKNGDILLNRQPTLHRPSTQAHARILPEEKVRLRLHYANCKA	NADFDG	EMNAHFFQ	600
tr A0A6I9ZYC2 A0A6I9ZYC2_ACIBJ	HVKNGDILLNRQPTLHRPSTQAHARILPEEKVRLRLHYANCKA	NADFDG	EMNAHFFQ	600
tr M3WAJ5 M3WAJ5_FELCA	HVKNGDILLNRQPTLHRPSTQAHARILPEEKVRLRLHYANCKA	NADFDG	EMNAHFFQ	600
tr J9P5G4 J9P5G4_CANLF	HVKNGDILLNRQPTLHRPSTQAHARILPEEKVRLRLHYANCKA	NADFDG	EMNAHFFQ	600
tr A0A5F4C883 A0A5F4C883_CANLF	HVKNGDILLNRQPTLHRPSTQAHARILPEEKVRLRLHYANCKA	NADFDG	EMNAHFFQ	600
tr A0A2U3X0D3 A0A2U3X0D3_ODORO	HVKNGDILLNRQPTLHRPSTQAHARILPEEKVRLRLHYANCKA	NADFDG	EMNAHFFQ	600
tr G1LGX3 G1LGX3_AILME	HVKNGDILLNRQPTLHRPSTQAHARILPEEKVRLRLHYANCKA	NADFDG	EMNAHFFQ	600
tr A0A6J3BPX4 A0A6J3BPX4_VICPA	HVKNGDILLNRQPTLHRPSTQAHARILPEEKVRLRLHYANCKA	NADFDG	EMNAHFFQ	600
tr A0A2Y9TC94 A0A2Y9TC94_PHYMC	HVKNGDILLNRQPTLHRPSTQAHARILPEEKVRLRLHYANCKA	NADFDG	EMNAHFFQ	600
tr A0A484GYD4 A0A484GYD4_SOUC	HVKNGDILLNRQPTLHRPSTQAHARILPEEKVRLRLHYANCKA	NADFDG	EMNAHFFQ	600
tr A0A6B0QX10 A0A6B0QX10_9CETA	HVKNGDILLNRQPTLHRPSTQAHARVPEEKVRLRLHYANCKA	NADFDG	EMNAHFFQ	600
tr A0A6J0XA49 A0A6J0XA49_ODOVR	HVKNGDILLNRQPTLHRPSTQAHARVPEEKVRLRLHYANCKA	NADFDG	EMNAHFFQ	600
tr A0A6I9KXL29 A0A6I9KXL29_CHRAS	HVKNGDILLNRQPTLHRPSTQAHARILPEEKVRLRLHYANCKA	NADFDG	EMNAHFFQ	600
tr A0A1U7UA15 A0A1U7UA15_CARSF	HVKNGDILLNRQPTLHRPSTQAHARILPEEKVRLRLHYANCKA	NADFDG	EMNAHFFQ	600
tr G1SYP7 G1SYP7_RABIT	HVKNGDILLNRQPTLHRPSTQAHARILPEEKVRLRLHYANCKA	NADFDG	EMNAHFFQ	600
tr H9Z7E8 H9Z7E8_MACMU	HVKNGDILLNRQPTLHRPSTQAHARILPEEKVRLRLHYANCKA	NADFDG	EMNAHFFQ	600
tr A0A096NZX0 A0A096NZX0_PAPAN	HVKNGDILLNRQPTLHRPSTQAHARILPEEKVRLRLHYANCKA	NADFDG	EMNAHFFQ	600
tr A0A2J8RNZ1 A0A2J8RNZ1_PONAB	HVKNGDILLNRQPTLHRPSTQAHARVPEEKVRLRLHYANCKA	NADFDG	EMNAHFFQ	600
sp O95602 RPA1_HUMAN	HVKNGDILLNRQPTLHRPSTQAHARILPEEKVRLRLHYANCKA	NADFDG	EMNAHFFQ	600
tr G3QHD8 G3QHD8_GORGO	HVKNGDILLNRQPTLHRPSTQAHARILPEEKVRLRLHYANCKA	NADFDG	EMNAHFFQ	600
tr K7CHZ0 K7CHZ0_PANTR	HVKNGDILLNRQPTLHRPSTQAHARILPEEKVRLRLHYANCKA	NADFDG	EMNAHFFQ	600
tr A0A2R9CCF8 A0A2R9CCF8_PANPA	HVKNGDILLNRQPTLHRPSTQAHARILPEEKVRLRLHYANCKA	NADFDG	EMNAHFFQ	600
	** ** *			

//End of the animal RNAP I A1 sequences

tr A0A452TQ80 A0A452TQ80_URSMA	MMG----	SHDELRSPSACLTVGKVVVGGTGLFELKQPLR	1629
tr S9X3I0 S9X3I0_CAMFR	MMGQSWA	SHDELRSPSACLTVGKVVVGGTGLFELKQPLR	1546
tr A0A7J8FKW0 A0A7J8FKW0_ROUAE	MMG----	SHDELRSPSACLTVGKVVVGGTGLFELKQPLR	1721
tr A0A3Q2I2F1 A0A3Q2I2F1_HORSE	MMG----	SHDELRSPSACLTVGKVVVGGTGLFELKQPLR	1637
tr A0A3Q2HZF4 A0A3Q2HZF4_HORSE	MMG----	SHDELRSPSACLTVGKVVVGGTGLFELKQPLR	1669
tr A0A673UI45 A0A673UI45_SURSU	-----	SHDELRSPSACLTVGKVVVGGTGLFELKQPLR	1663
tr A0A6P4VUC2 A0A6P4VUC2_PANPR	MMG----	SHDELRSPSACLTVGKVVVGGTGLFELKQPLR	1718
tr A0A6P6I466 A0A6P6I466_PUMCO	MMG----	SHDELRSPSACLTVGKVVVGGTGLFELKQPLR	1718
tr A0A6I9ZYC2 A0A6I9ZYC2_ACIJB	MMG----	SHDELRSPSACLTVGKVVVGGTGLFELKQPLR	1718
tr M3WAJ5 M3WAJ5_FELCA	MMG----	SHDELRSPSACLTVGKVVVGGTGLFELKQPLR	1718
tr J9P5G4 J9P5G4_CANLF	MMG----	SHDELRSPSACLTVGKVVVGGTGLFELKQPLR	1680
tr A0A5F4C883 A0A5F4C883_CANLF	MMG----	SHDELRSPSACLTVGKVVVGGTGLFELKQPLR	1664
tr A0A2U3X0D3 A0A2U3X0D3_ODORO	MLG----	SHDELRSPSACLTVGKVVVGGTGLFELKQPLR	1717
tr G1LGX3 G1LGX3_AILME	MMG----	SHDELRSPSACLTVGKVVVGGTGLFELKQPLR	1716
tr A0A6J3BPX4 A0A6J3BPX4_VICPA	MMG----	SHDELRSPSACLTVGKVVVGGTGLFELKQPLR	1650
tr A0A2Y9TC94 A0A2Y9TC94_PHYMC	MMG----	SHDELRSPSACLTVGKVVVGGTGLFELKQPLR	1715
tr A0A484GYD4 A0A484GYD4_SOUC	MMG----	SHDELRSPSACLTVGKVVVGGTGLFELKQPLR	1717
tr A0A6B0QXI0 A0A6B0QXI0_9CETA	LMG----	SHDELRSPSACLTVGKVVVGGTGLFELKQPLR	1696
tr A0A6J0XA49 A0A6J0XA49_ODOVR	LMG----	SHDELRSPSACLTVGKVVVGGTGLFELKQPLR	1663
tr A0A6I9KL29 A0A6I9KL29_CHRAS	MMG----	SHDELRSPSACLTVGKVVVGGTGLFELKQPLR	1710
tr A0A1U7UAL5 A0A1U7UAL5_CARSF	MLG----	SHDELRSPSACLTVGKVVVGGTGLFELKQPLR	1716
tr G1SYP7 G1SYP7_RABIT	MMG----	SHDELRSPSACLTVGKVVVGGTGLFELKQPLR	1618
tr H9Z7E8 H9Z7E8_MACMU	MLG----	SHDELRSPSACLTVGKVVVGGTGLFELKQPLR	1720
tr A0A096NZX0 A0A096NZX0_PAPAN	MLG----	SHDELRSPSACLTVGKVVVGGTGLFELKQPLR	1720
tr A0A2J8RNZ1 A0A2J8RNZ1_PONAB	MLG----	SHDELRSPSACLTVGKVVVGGTGLFELKQPLR	1659
sp O95602 RPA1_HUMAN	MLG----	SHDELRSPSACLTVGKVVVGGTGLFELKQPLR	1720
tr G3QHD8 G3QHD8_GORGO	MLG----	SHDELRSPSACLTVGKVVVGGTGLFELKQPLR	1720
tr K7CHZ0 K7CHZ0_PANTR	MLG----	SHDELRSPSACLTVGKVVVGGTGLFELKQPLR	1720
tr A0A2R9CCF8 A0A2R9CCF8_PANPA	MLG----	SHDELRSPSACLTVGKVVVGGTGLFELKQPLR	1708
.**.*****.*****			

Fig. 7. MSA of the elongation subunits A1 of RNAP I from animal sources

A0A452TQ80_URSMA	<i>Ursus maritimus</i>	S9X3I0_CAMFR	<i>Camelus ferus</i>
A0A7J8FKW0_ROUAE	<i>Rousettus aegyptiacus</i>	A0A3Q2I2F1_HORSE	<i>Equus caballus</i>
A0A3Q2HZF4_HORSE	<i>Equus caballus</i>	A0A673UI45_SURSU	<i>Suricata suricatta</i>
A0A6P4VUC2_PANPR	<i>Panthera pardus</i>	A0A6P6I466_PUMCO	<i>Puma concolor</i>
A0A6I9ZYC2_ACIJB	<i>Acinonyx jubatus</i>	M3WAJ5_FELCA	<i>Felis catus</i>
J9P5G4_CANLF	<i>Canis lupus familiaris</i>	A0A5F4C883_CANLF	<i>Canis lupus familiaris</i>
A0A2U3X0D3_ODORO	<i>Odobenus rosmarus divergens</i>	G1LGX3_AILME	<i>Ailuropoda melanoleuca</i>
A0A6J3BPX4_VICPA	<i>Vicugna pacos</i>	A0A2Y9TC94_PHYMC	<i>Physeter macrocephalus</i>
A0A484GYD4_SOUC	<i>Sousa chinensis</i>	A0A6B0QXI0_9CETA	<i>Bos mutus</i>
A0A6J0XA49_ODOVR	<i>Odocoileus virginianus texanus</i>	A0A6I9KL29_CHRAS	<i>Chrysochloris asiatica</i>
A0A1U7UAL5_CARSF	<i>Carlito syrichta</i>	G1SYP7_RABIT	<i>Oryctolagus cuniculus</i>
H9Z7E8_MACMU	<i>Macaca mulatta</i>	A0A096NZX0_PAPAN	<i>Papio Anubis</i>
A0A2J8RNZ1_PONAB	<i>Pongo abelii</i>	O95602 RPA1_HUMAN	<i>Homo sapiens</i>
G3QHD8_GORGO	<i>Gorilla gorilla gorilla</i>	K7CHZ0_PANTR	<i>Pan troglodytes</i>
A0A2R9CCF8_PANPA	<i>Pan paniscus</i>		

Therefore, it is clear from the analysis that all of them use a basic amino acid (K/H/R) as the catalytic amino acid, but each group use different types of template-binding pairs as -LG- in animals, -CG- in plants -TG- in higher fungi and -QG- in yeasts.

4.2 PR Function in Eukaryotic MSU RNAP II

Among the three major MSU RNAPs of eukaryotes, only the RNAP II involves in the transcription of protein-encoding genes (~25,000 genes) resulting in mRNAs. Besides, it also transcribes genes encoding most of the small nuclear RNAs (snRNAs) and microRNAs. In most organisms the RNAP II is made up of 12 subunits (with a molecular mass of ~550 kDa). However, several other proteins are required for complete activity of RNAP II holoenzyme. Therefore, in eukaryotic organisms, the complete

12-subunit RNAP II is responsible for transcription of all protein-encoding genes and thus, forms the central component of the eukaryotic transcription machinery. The RNAP II is strikingly different from other MSU RNAPs. Firstly, it is the only RNAP inhibited by the fungal toxin α -amanitin at very low concentrations, and therefore, all eukaryotic mRNA synthesis is sensitive to this inhibitor. Secondly, it possesses a unique, highly conserved heptapeptide in their carboxyl terminal domain (CTD) [1].

Figure 8 shows the MSA analysis and conserved motifs in the elongation subunits (Rpb1) of the MSU RNAPs II of yeasts and higher fungi. The *S. cerevisiae* (yeast) subunit with 1733 amino acid residues and *Neurospora crassa* (higher fungus) subunit with 1761 amino acid residues are highlighted in yellow. The N-terminal regions are not conserved among them, but the CTD

heptapeptide is highly conserved in all. However, all of them use the catalytic amino acid R. Strikingly the ‘template-binding’ pair is invariably an –FG- in all, except in few cases where they use –FA- pair. Interestingly, the elongation subunits possessed the possible built-in proposed PR active site with three completely conserved Cs within the polymerases active site region, ⁻⁵⁵DPR⁻⁶LGSIDRNLKQCQEGMNECP GHFGH⁸⁴- (numbering from *S. cerevisiae* Rpb1 subunit).

However, the Rpb2 initiation subunits of the eukaryotic RNAPs II did not show any built-in PR site; ⁻⁸⁴⁸RGLFR⁻⁵SLFFRSYMDQEKKYGM⁸⁶⁹- (numbering from *S. cerevisiae* Rpb2 subunit). Therefore, as found in the prokaryotic elongation subunits, the eukaryotic elongation subunits also

possess the PR active site which is integrated within the polymerase active site region (Fig. 8). Unlike its bacterial counterparts, the catalytic region of the elongation subunits of eukaryotes is placed very close to the N-terminal region (within ~100 amino acids) [1]. This Zn-binding site in elongation subunit β' was confirmed by X-ray crystallographic analysis of the MSU RNAP from the thermophilic bacterium, *Thermus aquaticus*, [12]. They found that the Zn²⁺ binds to the 3 invariant Cs located in the catalytic region and also suggested a possible role in the PR activity during elongation. The Zn-binding pattern in the eukaryotic elongation subunits (-CX₂CX₆C-) is different from the pattern (-CX₆CX₂C-) found in the elongation subunits of eubacteria, i.e., the pattern is just reversed in eukaryotes.

CLUSTAL O (1.2.4) MSA of elongation subunits B1 of RNAP II form yeasts and higher fungi

tr Q5KGG3 Q5KGG3_CRYNJ	DPRMGTIDRNFKCDTCEGMSRCPGHFGHIELARPVFHQGFIVKVKKILECVCYSCGKLL	114
tr A0A4Q1BT71 A0A4Q1BT71_TREME	DPRMGTIDRNFKCDTCEGMSRCPGHFGHIELARPVFHGGFMVVKKILECICFSCGKLL	114
tr A0A066VMM5 A0A066VMM5_TILAU	DPRMGTIDRNTKCDTCEGMSRCPGHFGHIELARPVFHIGFLGKVKKLEIVTCHCGKVK	116
tr A0A316YTV3 A0A316YTV3_9BASI	DPRLGTIDRNYKCDTCEGMSRCPGHFGHIELARPVFHIGFLGKVKKILECVCVTHCGKLL	116
tr E6ZML9 E6ZML9_SFORE	DPRLGTIDRNYKCDTCEGMSRCPGHFGHIELARPVFHIGFLGKVKKILECVCVTHCGKLL	118
tr A0A0D1C3I0 A0A0D1C3I0_USTMA	DPRLGTIDRNYKCDTCEGMSRCPGHFGHIELARPVFHIGFLGKVKKILECVCVTHCGKLL	118
tr G4T8R1 G4T8R1_SERID	DPRMGTIDRNFKCDTCEGMSRCPGHFGHIELARPVFHIGFLGKVKKILECICVNCGKLL	115
tr A0A2H3D1M6 A0A2H3D1M6_ARMGA	DPRMGTIDRNFKCDTCEGMSRCPGHFGHIELARPVFHIGFLGKVKKILECICVNCGKLL	116
tr A0A4S4L730 A0A4S4L730_9AGAM	DPRLGTIDRNFKCDTCEGMSRCPGHFGHIELARPVFHIGFLGKVKKILECICVNCGKLL	116
tr A0A0C9Z7X8 A0A0C9Z7X8_9AGAM	DPRMGTIDRNFKCDTCEGMSRCPGHFGHIELARPVFHIGFLGKVKKILECICVNCGKLL	116
tr A0A0C3D579 A0A0C3D579_9AGAM	DPRMGTIDRNFKCDTCEGMSRCPGHFGHIELARPVFHIGFLGKVKKILECICVNCGKLL	116
tr A0A0K3CFM9 A0A0K3CFM9_RHOTO	DPRLGTIDRNFKCDTCEGMSRCPGHFGHIELARPVFHIGFLGKVKKILECICVNCGKLL	116
tr A0A0C4EMF0 A0A0C4EMF0_PUCT1	DPRMGTIDRNFKCDTCEGMSRCPGHFGHIELARPVFHIGFLGKVKKILECICVNCGKLL	116
tr A0A180GBS5 A0A180GBS5_PUCT1	DPRMGTIDRNFKCDTCEGMSRCPGHFGHIELARPVFHIGFLGKVKKILECICVNCGKLL	116
tr A0A2U1P7X5 A0A2U1P7X5_ARTAN	DPRLGTIDRNFKCDTCEGMSRCPGHFGHIELARPVFHIGFLGKVKKILECICVNCGKLL	116
tr B5RSM9 B5RSM9_DEBHA	DPRLGSIDRNFKCDTCEGMSRCPGHFGHIELARPVFHIGFLGKVKKILECICVNCGKLL	115
tr G8BEH9 G8BEH9_CANPC	DPRLGSIDRNFKCDTCEGMSRCPGHFGHIELARPVFHIGFLGKVKKILECICVNCGKLL	115
tr A0A0H5C9X5 A0A0H5C9X5_CYBJN	DPRLGSIDRNFKCDTCEGMSRCPGHFGHIELARPVFHIGFLGKVKKILECICVNCGKLL	74
tr A0A1E4S2U3 A0A1E4S2U3_CYBJN	DPRLGSIDRNFKCDTCEGMSRCPGHFGHIELARPVFHIGFLGKVKKILECICVNCGKLL	114
tr A0A5P2U367 A0A5P2U367_KLULC	DPRLGSIDRNFKCDTCEGMSRCPGHFGHIELARPVFHIGFLGKVKKILECICVNCGKLL	114
sp Q75A34 RPB1_ASHGO	DPRLGSIDRNFKCDTCEGMSRCPGHFGHIELARPVFHIGFLGKVKKILECICVNCGKLL	114
tr A0A0X8HRG6 A0A0X8HRG6_9SACH	DPRLGSIDRNFKCDTCEGMSRCPGHFGHIELARPVFHIGFLGKVKKILECICVNCGKLL	114
tr A0A0L8RLN8 A0A0L8RLN8_SACEU	DPRLGSIDRNFKCDTCEGMSRCPGHFGHIELARPVFHIGFLGKVKKILECICVNCGKLL	114
tr A0A6CLDMV5 A0A6CLDMV5_SACPS	DPRLGSIDRNFKCDTCEGMSRCPGHFGHIELARPVFHIGFLGKVKKILECICVNCGKLL	114
sp P04050 RPB1_YEAST	DPRLGSIDRNLKCDTCEGMSRCPGHFGHIELARPVFHIGFLGKVKKILECICVNCGKLL	114
tr A0A0L8VSD2 A0A0L8VSD2_9SACH	DPRLGSIDRNLKCDTCEGMSRCPGHFGHIELARPVFHIGFLGKVKKILECICVNCGKLL	114
tr H2APV4 H2APV4_KAZAF	DPRLGSIDRNLKCDTCEGMSRCPGHFGHIELARPVFHIGFLGKVKKILECICVNCGKLL	114
tr J7S636 J7S636_KAZNA	DPRLGSIDRNLKCDTCEGMSRCPGHFGHIELARPVFHIGFLGKVKKILECICVNCGKLL	114
tr A0A177FEW1 A0A177FEW1_9EURO	DPHLGTIDRNFKCDTCEGMSRCPGHFGHIELARPVFHIGFLGKVKKILECICVNCGKLL	116
tr A0A3MOVZ74 A0A3MOVZ74_9EURO	DPHLGTIDRNFKCDTCEGMSRCPGHFGHIELARPVFHIGFLGKVKKILECICVNCGKLL	120
tr A0A2V1EE21 A0A2V1EE21_9PLEO	DTKLGTIDRNFKCDTCEGMSRCPGHFGHIELARPVFHIGFLGKVKKILECICVNCGKLL	116
tr A0A6A6W742 A0A6A6W742_9PEZI	DPKLGSIDRNFKCDTCEGMSRCPGHFGHIELARPVFHIGFLGKVKKILECICVNCGKLL	116
tr A0A0C3D813 A0A0C3D813_9PEZI	DPRLGSIDRNFKCDTCEGMSRCPGHFGHIELARPVFHIGFLGKVKKILECICVNCGKLL	116
tr A0A2J6RHJ5 A0A2J6RHJ5_9HELO	DPRLGSIDRNFKCDTCEGMSRCPGHFGHIELARPVFHIGFLGKVKKILECICVNCGKLL	116
tr A0A439CXR0 A0A439CXR0_9PEZI	DPRLGSIDRNFKCDTCEGMSRCPGHFGHIELARPVFHIGFLGKVKKILECICVNCGKLL	116
tr F7VUQ0 F7VUQ0_SORMK	DPLLGSVDRQFKCKTCEGMSRCPGHFGHIELARPVFHIGFLGKVKKILECICVNCGKLL	116
tr Q7SDN0 Q7SDN0_NEUCR	DPLLGSVDRQFKCKTCEGMSRCPGHFGHIELARPVFHIGFLGKVKKILECICVNCGKLL	116
tr S3CAX5 S3CAX5_OPHF1	DPLLGSVDRQFKCKTCEGMSRCPGHFGHIELARPVFHIGFLGKVKKILECICVNCGKLL	116
tr A0A0G4MIY4 A0A0G4MIY4_9PEZI	DPLLGSIDRQFKCKTCEGMSRCPGHFGHIELARPVFHIGFLGKVKKILECICVNCGKLL	116
tr A0A2S4L948 A0A2S4L948_9HYPO	DPLLGSIDRQFKCKTCEGMSRCPGHFGHIELARPVFHIGFLGKVKKILECICVNCGKLL	116
tr A0A1T3CTE0 A0A1T3CTE0_9HYPO	DPLLGSIDRQFKCKTCEGMSRCPGHFGHIELARPVFHIGFLGKVKKILECICVNCGKLL	116
tr A0A2T4BW54 A0A2T4BW54_TRILO	DPLLGSIDRQFKCKTCEGMSRCPGHFGHIELARPVFHIGFLGKVKKILECICVNCGKLL	116
tr A0A2T4BG85 A0A2T4BG85_9HYPO	DPLLGSIDRQFKCKTCEGMSRCPGHFGHIELARPVFHIGFLGKVKKILECICVNCGKLL	116
tr GORMT8 GORMT8_HYPJQ	DPLLGSIDRQFKCKTCEGMSRCPGHFGHIELARPVFHIGFLGKVKKILECICVNCGKLL	116
tr A0A2H3A405 A0A2H3A405_TRIPA	DPLLGSIDRQFKCKTCEGMSRCPGHFGHIELARPVFHIGFLGKVKKILECICVNCGKLL	116
tr A0A2T7A615 A0A2T7A615_TUBBO	DPHLGSIDRNFKCDTCEGMSRCPGHFGHIELARPVFHIGFLGKVKKILECICVNCGKLL	115
tr A0A0F7VID5 A0A0F7VID5_PENBI	DPRLGTIDRQWNCETCEGMSRCPGHFGHIELARPVFHIGFLGKVKKILECICVNCGKLL	116
tr A0A093V8Y5 A0A093V8Y5_TALMA	DPRLGTIDRQWNCETCEGMSRCPGHFGHIELARPVFHIGFLGKVKKILECICVNCGKLL	115
tr A0A0J6FT33 A0A0J6FT33_COCPO	DPRLGTIDRQWNCETCEGMSRCPGHFGHIELARPVFHIGFLGKVKKILECICVNCGKLL	116
tr A0A179UZA4 A0A179UZA4_BLAGS	DPRLGTIDRQWNCETCEGMSRCPGHFGHIELARPVFHIGFLGKVKKILECICVNCGKLL	116
tr C5GKA7 C5GKA7_AJEDR	DPRLGTIDRQWNCETCEGMSRCPGHFGHIELARPVFHIGFLGKVKKILECICVNCGKLL	116

//			
tr Q5KGG3 Q5KGG3_CRYNJ	RHLKDG DYVLFNRRQPSLHKMSMMSHRVKLMNYSTFRLNLSVTSPP	NADFDG	EMNLHV PQ 509
tr A0A4Q1BT71 A0A4Q1BT71_TREME	RHLKDGDFVLFNRRQPSLHKMSMMCHRVKLMNYSTFRLNLSVTSPP	NADFDG	EMNLHV PQ 510
tr A0A066VMM5 A0A066VMM5_TILAU	RHLKDGDFVLFNRRQPSLHKMSMMCHRVKLMDFSTFRLNLSVTPP	NADFDG	EMNLHV PQ 514
tr A0A316YTV3 A0A316YTV3_9BASI	RHLKDGDFVLFNRRQPSLHKMSMMCHRVKLMDFSTFRLNLSVTPP	NADFDG	EMNLHV PQ 512
tr E6ZML9 E6ZML9_SPORE	RHLKDG DYVLFNRRQPSLHKMSMMSHR I K L M D Y S T F R L N L S V T S P P	NADFDG	EMNLHV PQ 506
tr A0A0D1C3I0 A0A0D1C3I0_USTMA	RHLKDG DY I L F N R R Q P S L H K M S M M S H R I K L M D Y S T F R L N L S V T S P P	NADFDG	EMNLHV PQ 506
tr G4T8R1 G4T8R1_SERID	RHLKDG DY V L F N R R Q P S L H K M S M M S H R V K I M P Y S T F R L N L S V T S P P	NADFDG	EMNLHV PQ 505
tr A0A2H3D1M6 A0A2H3D1M6_ARMGA	RHLKDG DY V L F N R R Q P S L H K M S M M S H R V R L M P Y S T F R L N L S V T S P P	NADFDG	EMNLHV PQ 504
tr A0A4S4L730 A0A4S4L730_9AGAM	RHLKDGDFVLFNRRQPSLHKMSMMSHRVKLMDFSTFRLNLSVTPP	NADFDG	EMNLHV PQ 504
tr A0A0C9Z7X8 A0A0C9Z7X8_9AGAM	RHLKDGDFVLFNRRQPSLHKMSMMSHRVKLMDFSTFRLNLSVTPP	NADFDG	EMNLHV PQ 504
tr A0A0C3D579 A0A0C3D579_9AGAM	RHLKDGDFVLFNRRQPSLHKMSMMSHRVKLMDFSTFRLNLSVTPP	NADFDG	EMNLHV PQ 504
tr A0A0K3CFM9 A0A0K3CFM9_RHOTO	RHLKDG DY I V L F N R R Q P S L H K M S M M A H R V K L M P Y S T F R L N L S V T S P P	NADFDG	EMNLHV PQ 505
tr A0A0C4EMP0 A0A0C4EMP0_PUCT1	RHLKDG DY V L F N R R Q P S L H K M S M M S H R I K L M P Y S T F R L N L S V T S P P	NADFDG	EMNLHV PQ 512
tr A0A180GBS5 A0A180GBS5_PUCT1	RHLKDG DY V L F N R R Q P S L H K M S M M S H R I K L M P Y S T F R L N L S V T S P P	NADFDG	EMNLHV PQ 512
tr A0A2U1P7X5 A0A2U1P7X5_ARTAN	RHLKDG DY V L F N R R Q P S L H K M S M M S H R I K L M P Y S T F R L N L S V T S P P	NADFDG	EMNLHV PQ 507
tr B5RSM9 B5RSM9_DEBHA	RHLMDDDPVLFNRRQPSLHKMSMMAHVRVKMPYSTFRLNLSVTSPP	NADFDG	EMNLHV PQ 498
tr G8BEH9 G8BEH9_CANPC	RHLMDDDPVLFNRRQPSLHKMSMMAHVRVKMPYSTFRLNLSVTSPP	NADFDG	EMNLHV PQ 493
tr A0A0H5C9X5 A0A0H5C9X5_CYBJN	RHLMDDEDVLFNRRQPSLHKMSMMCHRVKLMDFSTFRLNLSVTSPP	NADFDG	EMNLHV PQ 451
tr A0A1E4S2U3 A0A1E4S2U3_CYBJN	RHLMDDEDVLFNRRQPSLHKMSMMCHRVKLMDFSTFRLNLSVTSPP	NADFDG	EMNLHV PQ 491
tr A0A5P2U367 A0A5P2U367_KLULC	RHLMDDDPVLFNRRQPSLHKMSMMAHVRVKMPYSTFRLNLSVTSPP	NADFDG	EMNLHV PQ 493
sp Q75A34 RPB1_ASHGO	RHLMDDDPVLFNRRQPSLHKMSMMAHVRVKMPYSTFRLNLSVTSPP	NADFDG	EMNLHV PQ 493
tr A0A0X8HRG6 A0A0X8HRG6_9SACH	RHLMDNDPVLFNRRQPSLHKMSMMAHVRVKMPYSTFRLNLSVTSPP	NADFDG	EMNLHV PQ 493
tr A0A0L8RLN8 A0A0L8RLN8_SACEU	RHLMDNDPVLFNRRQPSLHKMSMMAHVRVKI PYSTFRLNLSVTSPP	NADFDG	EMNLHV PQ 493
tr A0A6CLDMV5 A0A6CLDMV5_SACPS	RHLMDNDPVLFNRRQPSLHKMSMMAHVRVKI PYSTFRLNLSVTSPP	NADFDG	EMNLHV PQ 493
sp P04050 RPB1_YEAST	RHLMDNDPVLFNRRQPSLHKMSMMAHVRVKI PYSTFRLNLSVTSPP	NADFDG	EMNLHV PQ 493
tr A0A0L8VSD2 A0A0L8VSD2_9SACH	RHLMDNDPVLFNRRQPSLHKMSMMAHVRVKI PYSTFRLNLSVTSPP	NADFDG	EMNLHV PQ 493
tr H2APV4 H2APV4_KAZAF	RHLMDDDPVLFNRRQPSLHKMSMMSHRVKVPYSTFRLNLSVTSPP	NADFDG	EMNLHV PQ 493
tr J7S636 J7S636_KAZNA	RHLMDDDPVLFNRRQPSLHKMSMMSHRVKVPYSTFRLNLSVTSPP	NADFDG	EMNLHV PQ 492
tr A0A177FEW1 A0A177FEW1_9EURO	RHLMDDDPVLFNRRQPSLHKMSMMSHRVKVPYSTFRLNLSVTSPP	NADFDG	EMNLHV PQ 493
tr A0A3M0VZ74 A0A3M0VZ74_9EURO	RHLMDDDPVLFNRRQPSLHKMSMMSHRVKVPYSTFRLNLSVTSPP	NADFDG	EMNLHV PQ 502
tr A0A2V1EE21 A0A2V1EE21_9PLEO	RHLMDDDPVLFNRRQPSLHKMSMMSHRVKVPYSTFRLNLSVTSPP	NADFDG	EMNLHV PQ 505
tr A0A6A6W742 A0A6A6W742_9PEZI	RHLMDDDPVLFNRRQPSLHKMSMMSHRVKVPYSTFRLNLSVTSPP	NADFDG	EMNLHV PQ 500
tr A0A0C3D813 A0A0C3D813_9PEZI	RHLMDDDPVLFNRRQPSLHKMSMMSHRVKVPYSTFRLNLSVTSPP	NADFDG	EMNLHV PQ 498
tr A0A2J6RHJ5 A0A2J6RHJ5_9HELO	RHLMDDDPVLFNRRQPSLHKMSMMSHRVKVPYSTFRLNLSVTSPP	NADFDG	EMNLHV PQ 506
tr A0A439CXR0 A0A439CXR0_9PEZI	RHLMDDDPVLFNRRQPSLHKMSMMSHRVKVPYSTFRLNLSVTSPP	NADFDG	EMNLHV PQ 506
tr F7VUQ0 F7VUQ0_SORMK	RHLMDDDPVLFNRRQPSLHKMSMMSHRVKVPYSTFRLNLSVTSPP	NADFDG	EMNLHV PQ 504
tr I07SDN0 I07SDN0_NEUCR	RHLMDDDPVLFNRRQPSLHKMSMMSHRVKVPYSTFRLNLSVTSPP	NADFDG	EMNLHV PQ 507
tr S3CAX5 S3CAX5_OHPH1	RHLMDDDPVLFNRRQPSLHKMSMMSHRVKVPYSTFRLNLSVTSPP	NADFDG	EMNLHV PQ 507
tr A0A0G4MIY4 A0A0G4MIY4_9PEZI	RHLMDDDPVLFNRRQPSLHKMSMMSHRVKVPYSTFRLNLSVTSPP	NADFDG	EMNLHV PQ 509
tr A0A2S4L948 A0A2S4L948_9HYPO	RHLMDDDPVLFNRRQPSLHKMSMMSHRVKVPYSTFRLNLSVTSPP	NADFDG	EMNLHV PQ 494
tr A0A1T3CTE0 A0A1T3CTE0_9HYPO	RHLMDDDPVLFNRRQPSLHKMSMMSHRVKVPYSTFRLNLSVTSPP	NADFDG	EMNLHV PQ 506
tr A0A2T4BW54 A0A2T4BW54_TRILO	RHLMDDDPVLFNRRQPSLHKMSMMSHRVKVPYSTFRLNLSVTSPP	NADFDG	EMNLHV PQ 507
tr A0A2T4BG85 A0A2T4BG85_9HYPO	RHLMDDDPVLFNRRQPSLHKMSMMSHRVKVPYSTFRLNLSVTSPP	NADFDG	EMNLHV PQ 507
tr GORMT8 GORMT8_HYPJQ	RHLMDDDPVLFNRRQPSLHKMSMMSHRVKVPYSTFRLNLSVTSPP	NADFDG	EMNLHV PQ 507
tr A0A2H3A405 A0A2H3A405_TRIPA	RHLMDDDPVLFNRRQPSLHKMSMMSHRVKVPYSTFRLNLSVTSPP	NADFDG	EMNLHV PQ 507
tr A0A2T7A615 A0A2T7A615_TUBBO	RHLMDDDPVLFNRRQPSLHKMSMMSHRVKVPYSTFRLNLSVTSPP	NADFDG	EMNLHV PQ 506
tr A0A0F7VI05 A0A0F7VI05_PENBI	RHLMDDDPVLFNRRQPSLHKMSMMSHRVKVPYSTFRLNLSVTSPP	NADFDG	EMNLHV PQ 506
tr A0A093V8Y5 A0A093V8Y5_TALMA	RHLMDDDPVLFNRRQPSLHKMSMMSHRVKVPYSTFRLNLSVTSPP	NADFDG	EMNLHV PQ 505
tr A0A0J6FT33 A0A0J6FT33_COCPO	RHLMDDDPVLFNRRQPSLHKMSMMSHRVKVPYSTFRLNLSVTSPP	NADFDG	EMNLHV PQ 508
tr A0A179UZA4 A0A179UZA4_BLAGS	RHLMDDDPVLFNRRQPSLHKMSMMSHRVKVPYSTFRLNLSVTSPP	NADFDG	EMNLHV PQ 511
tr C5GKA7 C5GKA7_AJEDR	RHLMDDDPVLFNRRQPSLHKMSMMSHRVKVPYSTFRLNLSVTSPP	NADFDG	EMNLHV PQ 511

// End of B1 subunits of RNAP II from yeasts and higher fungi			
tr Q5KGG3 Q5KGG3_CRYNJ	GGYGTSPSWKS-----		1786
tr A0A4Q1BT71 A0A4Q1BT71_TREME	GGYGTSPSWKG-----		1807
tr A0A066VMM5 A0A066VMM5_TILAU	SNFTKSMYLDLRDQ-----		1796
tr A0A316YTV3 A0A316YTV3_9BASI	SRFTQSSMWANKR-----		1771
tr E6ZML9 E6ZML9_SPORE	SRMSNKPWQR-----		1785
tr A0A0D1C3I0 A0A0D1C3I0_USTMA	SRMSNKPWQR-----		1774
tr G4T8R1 G4T8R1_SERID	TQYKSSPSWE-----		1796
tr A0A2H3D1M6 A0A2H3D1M6_ARMGA	VSYFSGQRWSQSHLSSVSNPIHHVEY		1802
tr A0A4S4L730 A0A4S4L730_9AGAM	-AYSASPSYD-----		1733
tr A0A0C9Z7X8 A0A0C9Z7X8_9AGAM	-SYSTSPSWE-----		1743
tr A0A0C3D579 A0A0C3D579_9AGAM	-----		1688
tr A0A0K3CFM9 A0A0K3CFM9_RHOTO	APYSSASWKR-----		1766
tr A0A0C4EMP0 A0A0C4EMP0_PUCT1	YSYSSAPWSR-----		1794
tr A0A180GBS5 A0A180GBS5_PUCT1	YSYSSAPWSR-----		1795
tr A0A2U1P7X5 A0A2U1P7X5_ARTAN	-----		1728
tr B5RSM9 B5RSM9_DEBHA	-----		1749
tr G8BEH9 G8BEH9_CANPC	-----		1746
tr A0A0H5C9X5 A0A0H5C9X5_CYBJN	-----		1715
tr A0A1E4S2U3 A0A1E4S2U3_CYBJN	-----		1755
tr A0A5P2U367 A0A5P2U367_KLULC	-----		1713
sp Q75A34 RPB1_ASHGO	-----		1745
tr A0A0X8HRG6 A0A0X8HRG6_9SACH	-----		1725
tr A0A0L8RLN8 A0A0L8RLN8_SACEU	-----		1719
tr A0A6CLDMV5 A0A6CLDMV5_SACPS	-----		1726
sp P04050 RPB1_YEAST	-----		1733
tr A0A0L8VSD2 A0A0L8VSD2_9SACH	-----		1733

tr J7S636 J7S636_KAZNA	-----	1721
tr A0A177FEW1 A0A177FEW1_9EURO	-----	1762
tr A0A3M0VZ74 A0A3M0VZ74_9EURO	-----	1771
tr A0A2V1EE21 A0A2V1EE21_9PLEO	-----	1755
tr A0A6A6W742 A0A6A6W742_9PEZI	-----	1762
tr A0A0C3D813 A0A0C3D813_9PEZI	-----	1739
tr A0A2J6RHJ5 A0A2J6RHJ5_9HELO	-----	1737
tr A0A439CXR0 A0A439CXR0_9PEZI	-----	1737
tr F7VUQ0 F7VUQ0_SORMK	-----	1761
tr Q7SDN0 Q7SDN0_NEUCR	-----	1761
tr S3CAX5 S3CAX5_OPHP1	-----	1757
tr A0A0G4MIY4 A0A0G4MIY4_9PEZI	-----	1743
tr A0A2S4L948 A0A2S4L948_9HYPO	-----	1755
tr A0A1T3CTE0 A0A1T3CTE0_9HYPO	-----	1756
tr A0A2T4BW54 A0A2T4BW54_TRILO	-----	1561
tr A0A2T4BG85 A0A2T4BG85_9HYPO	-----	1755
tr GORMT8 GORMT8_HYPJQ	-----	1755
tr A0A2H3A405 A0A2H3A405_TRIPA	-----	1755
tr A0A2T7A615 A0A2T7A615_TUBBO	-----	1751
tr A0A0F7VID5 A0A0F7VID5_PENBI	-----	1733
tr A0A093V8Y5 A0A093V8Y5_TALMA	-----	1743
tr A0A0J6FT33 A0A0J6FT33_COCPO	-----	1750
tr A0A179UZA4 A0A179UZA4_BLAGS	-----	1746
tr C5GKA7 C5GKA7_AJEDR	-----	1746

Fig. 8. MSA of elongation subunits B1 of RNAPs II from yeasts and higher fungal sources

Q5KGG3_CRYNJ <i>Cryptococcus neoformans</i>	A0A4Q1BT71_TREME <i>Tremella mesenterica</i>
A0A066VMM5_TILAU <i>Tilletiaria anomala</i>	A0A316YTV3_9BASI <i>Acaromyces ingoldii</i>
E6ZML9_SPORE <i>Sporisorium reilianum</i>	A0A0D1C3I0_USTMA <i>Ustilago maydis</i>
G4T8R1_SERID <i>Serendipita indica</i>	A0A2H3A405_TRIPA <i>Trichoderma parareesei</i>
A0A4S4L730_9AGAM <i>Bondarzewia mesenterica</i>	A0A0C9Z7X8_9AGAM <i>Pisolithus microcarpus</i>
A0A0C3D579_9AGAM <i>Scleroderma citrinum</i>	A0A0K3CFM9_RHOTO <i>Rhodosporidium toruloides</i>
A0A0C4EMF0_PUCT1 <i>Puccinia triticina</i>	A0A180GBS5_PUCT1 <i>Puccinia triticina</i>
A0A2U1P7X5_ARTAN <i>Artemisia annua</i>	B5RSM9_DEBHA <i>Debaryomyces hansenii</i>
G8BEH9_CANPC <i>Candida parapsilosis</i>	A0A0H5C9X5_CYBJN <i>Cyberlindnera jadinii</i>
A0A1E4S2U3_CYBJN <i>Cyberlindnera jadinii</i>	A0A5P2U367_KLULC <i>Kluyveromyces lactis</i>
Q75A34 RPB1_ASHGO <i>Ashbya gossypii</i>	A0A0X8HRG6_9SACH <i>Eremothecium sincaudum</i>
A0A0L8RLN8_SACEU <i>Saccharomyces eubayanus</i>	A0A6C1DMV5_SACPS <i>Saccharomyces pastorianus</i>
P04050 RPB1_YEAST <i>Saccharomyces cerevisiae</i>	A0A0L8VSD2_9SACH <i>Saccharomyces boulardii</i>
H2APV4_KAZAF <i>Kazachstania africana</i>	J7S636_KAZNA <i>Kazachstania naganishii</i>
A0A177FEW1_9EURO <i>Fonsecaea monophora</i>	A0A3M0VZ74_9EURO <i>Chaetothyriales sp.</i>
A0A2V1EE21_9PLEO <i>Periconia macrospinosa</i>	A0A6A6W742_9PEZI <i>Pseudovirgaria hyperparasitica</i>
A0A0C3D813_9PEZI <i>Oidiodendron maius</i>	A0A2J6RHJ5_9HELO <i>Hyaloscypha variabilis</i>
A0A439CXR0_9PEZI <i>Xylaria grammica</i>	F7VUQ0_SORMK <i>Sordaria macrospora</i>
Q7SDN0_NEUCR <i>Neurospora crassa</i>	S3CAX5_OPHP1 <i>Ophiostoma piceae</i>
A0A0G4MIY4_9PEZI <i>Verticillium longisporum</i>	A0A2S4L948_9HYPO <i>Tolypocladium paradoxum</i>
A0A1T3CTE0_9HYPO <i>Trichoderma guizhouense</i>	A0A2T4BW54_TRILO <i>Trichoderma longibrachiatum</i>
A0A2T4BG85_9HYPO <i>Trichoderma citrinoviride</i>	GORMT8_HYPJQ <i>Hypocrea jecorina</i>
A0A2H3D1M6_ARMGA <i>Armillaria gallica</i>	A0A2T7A615_TUBBO <i>Tuber borchii</i>
A0A0F7VID5_PENBI <i>Penicillium brasilianum</i>	A0A093V8Y5_TALMA <i>Talaromyces marneffeii</i>
A0A0J6FT33_COCPO <i>Coccidioides posadasii</i>	A0A179UZA4_BLAGS <i>Blastomyces gilchristii</i>
C5GKA7_AJEDR <i>Ajellomyces dermatitidis</i>	

Further insights into the zinc-binding site in eukaryotes were provided by Crammer [23]. X-ray crystallographic data for the 10-subunit eukaryotic (yeast) RNAP II at 2.8 Å and 3.1 Å resolutions were reported. A 2.8 Å difference Fourier map revealed two metal ions at the active site, one persistently bound and the other possibly exchangeable during RNA synthesis, suggesting a Zn²⁺ in the exchangeable site. The Mg²⁺ (Metal A) is coordinated by amino acid residues D483 and D485 from the completely conserved block showing three invariant Ds, (D481, D483, and D485). Metal B is in the vicinity of metal A, at a distance of 5.8 Å. The

distance from metal B to the acidic residues are at 3.0 Å to 4.0 Å, and hence is too great for coordination of Zn²⁺. They also found a Zn²⁺ is bound by residues in the common motif CX₂CX_nCX₂C/H (where X is any amino acid) [23].

Donaldson and Friesen found that a highly purified yeast RNAP II bound to 7 Zn²⁺ atoms by atomic absorption spectroscopy. One of the zinc-binding motifs (⁶⁷CX₂CX₆CX₂HX₂₆CX₂C¹¹⁰) occurs in the Rpb1 elongation subunit of RNAP II and is found to be highly conserved in the largest subunits (elongation subunits) of all three RNA polymerases from a variety of eukaryotes [24].

They also proved by SDM experiments that mutations of the Zn²⁺-coordinating C residues conferred a lethal phenotype (C77→S and H80→Y were unable to support growth at 37° C). Similar results were obtained for the *E. coli* RNAP too. For example, in the double mutant where the first two Cs of the zinc-binding motif were modified to S (C→S) in the β' elongation subunit of *E. coli* RNAP, the enzyme was found to be inactive *in vivo* [25].

Figure 9 shows the MSA analysis of the elongation subunits B1 of RNAP II from various plant sources. *Triticum aestivum* (wheat) and *A. thaliana* standard sequences are highlighted in yellow, the template-binding and catalytic pairs are highlighted in yellow and the Zn-binding conserved Cs is highlighted in orange. The completely conserved Mg²⁺-binding site is highlighted in light green. No conservation is seen in the N-terminal region among them, but the CTD exhibited the highly conserved

heptapeptide. The catalytic amino acid is conserved in all and uses the basic amino acid K with one exception where it uses an R. Strikingly, the template-binding FG pair and the 3 invariant Ds in the Mg²⁺ binding site are completely conserved in all.

Figure 10 shows the MSA analysis of the elongation subunits B1 of RNAP II from various animal and insect sources. The human sequence is highlighted in yellow. The template-binding and catalytic pairs are highlighted in yellow and the Zn-binding conserved Cs is highlighted in orange. The completely conserved Mg²⁺ site is highlighted in light green. All of them use the basic amino acid R unlike in plants where they use a K. The template-binding pair -FG- is also completely conserved in all except in *Drosophila albomicans*. The Mg²⁺-binding site is completely conserved in all with the 3 invariant Ds. The CTD possess the characteristic heptapeptide repeats -YSPTSPT-, a unique feature of these enzymes.

CLUSTAL O (1.2.4) MSA of elongation subunits B1 of RNAP II from form plant sources

tr A0A1Z5RIH1 A0A1Z5RIH1_SORBI	PKAGGLSDPRMGTVDKLRKQETCMAGMAECPGHFCHLELAKPMFHIGFMKTVLSIMRCVC	106
tr C5Y387 C5Y387_SORBI	PKAGGLSDPRMGTVDKLRKQETCMAGMAECPGHFCHLELAKPMFHIGFMKTVLSIMRCVC	106
tr A0A3B6MZU3 A0A3B6MZU3_WHEAT	PKPGGLSDPRLGTIDRKMRETCMANMAECPGHFCHLELAKPMFHIGFIKTVLSIMRCVC	106
tr A0A565C923 A0A565C923_9BRAS	PKVGGLSDMRLGTIDRKYVGETCMANMAECPGHFCHLELAKPMYHVGFMTVLSIMRCVC	76
tr M4D210 M4D210_BRARP	PKVGGLSDTRLGTIDRKYVGETCMANMAECPGHFCHLELAKPMYHVGFMTVLSIMRCVC	106
tr A0A6J0KQ09 A0A6J0KQ09_RAPSA	PKVGGLSDTRLGTIDRKYVGETCMANMAECPGHFCHLELAKPMYHVGFMTVLSIMRCVC	106
tr A0A1J3F625 A0A1J3F625_NOCCA	PKVGGLSDVRLGTIDRKYVGETCMANMAECPGHFCHLELAKPMYHVGFMTVLSIMRCVC	106
tr A0A1J3JR03 A0A1J3JR03_NOCCA	PKVGGLSDVRLGTIDRKYVGETCMANMAECPGHFCHLELAKPMYHVGFMTVLSIMRCVC	106
sp P18616 NRFB1_ARATH	PKVGGLSDTRLGTIDRKYVGETCMANMAECPGHFGYLELAKPMYHVGFMTVLSIMRCVC	106
tr D7MC36 D7MC36_ARALL	PKVGGLSDIRLGTIDRKYVGETCMANMAECPGHFCHLELAKPMYHVGFMTVLSIMRCVC	106
tr V4P2F5 V4P2F5_EUTSA	PKVGGLSDIRLGTIDRKYVGETCMANMAECPGHFCHLELAKPMYHVGFMTVLSIMRCVC	106
tr ROGXL7 ROGXL7_9BRAS	PKVGGLSDIRLGTIDRKYVGETCMANMAECPGHFCHLELAKPMYHVGFMTVLSIMRCVC	106
tr A0A6J0MG42 A0A6J0MG42_RAPSA	PKVGGLSDIRLGTIDRKYVGETCMANMAECPGHFCHLELAKPMYHVGFMTVLSIMRCVC	106
tr A0A398AHR5 A0A398AHR5_BRACM	PKVGGLSDARLGTIDRKYVGETCMANMAECPGHFCHLELAKPMYHVGFMTVLSIMRCVC	106
tr A0A0D3A1P5 A0A0D3A1P5_BRAOL	PKVGGLSDARLGTIDRKYVGETCMANMAECPGHFCHLELAKPMYHVGFMTVLSIMRCVC	106
tr A0A3N6QGC8 A0A3N6QGC8_BRACR	PKVGGLSDARLGTIDRKYVGETCMANMAECPGHFCHLELAKPMYHVGFMTVLSIMRCVC	106
tr A0A0E0LRD6 A0A0E0LRD6_ORYPU	PKPGGLSDPRLGTIDRKMRETCMAGMAECPGHFCHLELAKPMFHIGFIKTVLSIMRCVC	106
tr K3YFU7 K3YFU7_SEITT	PKPGGLSDPRLGTIDRKMRETCMAGMAECPGHFCHLELAKPMFHIGFIKTVLSIMRCVC	106
tr J3MQH6 J3MQH6_ORYBR	PKPGGLSDPRLGTIDRKMRETCMAGMAECPGHFCHLELAKPMFHIGFIKTVLSIMRCVC	106
tr A0A803MAV7 A0A803MAV7_CHEQI	PKPGGLSDMRLGTIDRKLKQETCMANMAECPGHFCHLELAKPMFHIGFLKTVLSIMRCVC	106
tr A0A0K9RSK8 A0A0K9RSK8_SPIOL	PKPGGLSDMRLGTIDRKLKQETCMANMAECPGHFCHLELAKPMFHIGFLKTVLSIMRCVC	106
tr A0A6P6TFX2 A0A6P6TFX2_COFAR	PKIGGLSDPRLGTIDRKMRETCMAGMAECPGHFCHLELAKPMFHIGFIKTVLSIMRCVC	106
tr A0A6I9UDD3 A0A6I9UDD3_SESIN	PKPGGLSDPRLGTIDRKMRETCMANMAECPGHFCHLELAKPMFHIGFMKTVLSILRCVC	106
tr A0A1S3XM16 A0A1S3XM16_TOBAC	PKPGGLSDPRLGTIDRKMRETCMANMAECPGHFCHLELAKPMFHIGFMKTVLSILRCVC	106
tr A0A2G3A9T8 A0A2G3A9T8_CAPAN	PKPGGLSDPRLGTIDRKMRETCMANMAECPGHFCHLELAKPMFHIGFMKTVLSILRCVC	106
tr A0A1U8FXJ4 A0A1U8FXJ4_CAPAN	PKPGGLSDPRLGTIDRKMRETCMANMAECPGHFCHLELAKPMFHIGFMKTVLSILRCVC	106
tr M0ZVV4 M0ZVV4_SOLTU	PKPGGLSDPRLGTIDRKMRETCMANMAECPGHFCHLELAKPMFHIGFMKTVLSILRCVC	106
tr A0A6N2BNI8 A0A6N2BNI8_SOLCI	PKPGGLSDPRLGTIDRKMRETCMANMAECPGHFCHLELAKPMFHIGFMKTVLSILRCVC	106
tr A0A3Q7F7G2 A0A3Q7F7G2_SOLLC	PKPGGLSDPRLGTIDRKMRETCMANMAECPGHFCHLELAKPMFHIGFMKTVLSILRCVC	106
tr A0A6V7PIB4 A0A6V7PIB4_ANACO	AEARGLSDPRLGTIDRKMRETCMANMAECPGHFCHLELAKPMFHIGFLKTVLAIMRCVC	120
tr A0A6I9RZH4 A0A6I9RZH4_ELAVG	PKPGGLSDPRLGTIDRKMRETCMANMAECPGHFCHLELAKPMFHIGFLKTVLAIMRCVC	106
tr A0A4Y7I7U1 A0A4Y7I7U1_PAPSO	PKPGGLSDTRLGTIDRKMRETCMANMAECPGHFCHLELAKPMFHIGFMKTVLSIMRCVC	106
tr A0A6P9E4T1 A0A6P9E4T1_JUGRE	PKIAGLSDPRLGTIDRKMRETCMANMAECPGHFCHLELAKPMFHIGFMKTVLSIMRCVC	106
tr A0A7J7HU38 A0A7J7HU38_CAMSI	PKPGGLSDPRLGTIDRKMRETCMANMAECPGHFCHLELAKPMFHIGFLKTVLSIMRCVC	106
tr F6H0D9 F6H0D9_VITVI	PKPGGLSDPRLGTIDRKMRETCMANMAECPGHFCHLELAKPMFHIGFMKTVLSIMRCVC	106
tr A0A7J6EME3 A0A7J6EME3_CANSA	PKIAGLSDPRLGTIDRKMRETCMANMAECPGHFCHLELAKPMFHIGFLKTVLSIMRCVC	106
tr A0A067G7I3 A0A067G7I3_CITSI	PKPGGLSDPRLGTIDRKMRETCMANMAECPGHFCHLELAKPMFHIGFMKTVLSIMRVC	106
tr A0A5J5TP19 A0A5J5TP19_GOSBA	PKVGGLSDPRLGTIDRKMRETCMANMAECPGHFCHLELAKPMFHIGFMKTVLSIMRCVC	106
tr A0A061DGE8 A0A061DGE8_THECC	PKVGGLSDPRLGTIDRKMRETCMANMAECPGHFCHLELAKPMFHIGFMKTVLSIMRCVC	106
tr A0A6P5ZFF2 A0A6P5ZFF2_DURZI	PKPGGLSDRLGTIDRKMRETCMANMAECPGHFCHLELAKPMFHIGFLKTVLSIMRCVC	106
tr B9SXC0 B9SXC0_RICCO	PKPGGLSDRLGTIDRKMRETCMANMAECPGHFCHLELAKPMFHIGFLKTVLSIMRCVC	106
tr A0A251M2B5 A0A251M2B5_MANES	PKPGGLSDPKLGTIDRKMRETCMANMAECPGHFCHLELAKPMFHIGFMKTVLSIMRCVC	106
tr A0A314Z8L7 A0A314Z8L7_PRUYE	PKTAGLSDPRLGTIDRKMRETCMANMAECPGHFCHLELAKPMFHIGFMKTVLSVMRCVC	106
tr M5V8C7 M5V8C7_PRUPE	PKTAGLSDPRLGTIDRKMRETCMANMAECPGHFCHLELAKPMFHIGFMKTVLSIMRCVC	106
tr A0A6J5XYF9 A0A6J5XYF9_PRUAR	PKTAGLSDPRLGTIDRKMRETCMANMAECPGHFCHLELAKPMFHIGFMKTVLSVMRCVC	106
tr A0A6JLL0Z7 A0A6JLL0Z7_CUCMA	PKVAGLSDPRLGTIDRKLKQETCMANMAECPGHFCHLELAKPMFHIGFMKTVLIMRVC	106
tr A0A0A0L655 A0A0A0L655_CUCSA	PKVAGLSDPRLGTIDRKLKQETCMANMAECPGHFCHLELAKPMFHIGFMKTVLIMRVC	106

tr A0A4Y7I7U1 A0A4Y7I7U1_PAPSO	SPQFSPSAGYSPTAPGYSPTSSTQFTPETS NKDDGSTR-----	1845
tr A0A6P9E4T1 A0A6P9E4T1_JUGRE	SPPYSPSAGYSPSPGYSPTSSTQYTPQMSNKDDRS DKDDRSTR-----	1847
tr A0A7J7HU38 A0A7J7HU38_CAMSI	SPQYSPSVGYSPSAPGYSPTSSTQYTPQMSNKDNGSKR-----	1859
tr F6H0D9 F6H0D9_VITVI	SPQYSPSAGYSPSAPGYSPTSSTQYTPQMSNKDNGSPQ-----	1852
tr A0A7J6EME3 A0A7J6EME3_CANSA	SPQYSPSAGYSPSQPGYSPTSSTQYTPQTS DKDDNDKSTR-----	1806
tr A0A067G7I3 A0A067G7I3_CITSI	SPQYSPSAGYSPSAPGYSPTSSTQYTPQTNRDDSTTKDDKNTKGDKSSR---	1815
tr A0A5J5TPI9 A0A5J5TPI9_GOSBA	SPQYSPSAGYSPSAPGYSPTSSTQYTPSN--KDGSRNKD-----DRSKR---	1853
tr A0A061DGE8 A0A061DGE8_THECC	SPQYSPSAGYSPSAPGYSPTSSTQYTPQTS NKDDRATKDDRSKDDRSKR---	1861
tr A0A6P5ZFF2 A0A6P5ZFF2_DURZI	SPQYSPSAGYSPSAPGYSPTSSTQYTPS--NKDDHATKDDRSKDDRSKH---	1859
tr B9SXC0 B9SXC0_RICCO	SPQYSPSAGYSPSAPGYSPTSSTQYTPQ--TSTKDDRTDKGDRNGRDNKDEKSSR	1855
tr A0A251M2B5 A0A251M2B5_MANES	SPQYSPSAGYSPSAPGYSPTSSTQYTPQTS AKDDRRNKGDRNGRDNKG----	1858
tr A0A314Z8L7 A0A314Z8L7_PRUYE	SPQYSPSAGYSPSQPGYSPTSSTQYTPQTS EKDKDDRSTR-----	1837
tr M5VSC7 M5VSC7_PRUPE	SPQYSPSAGYSPSQPGYSPTSSTQYTPQTS EKDKDDRSTR-----	1844
tr A0A6J5XYF9 A0A6J5XYF9_PRUAR	SPQYSPSAGYSPSQPGYSPTSSTQYTPQTS EKDKDDRSTR-----	1844
tr A0A6J1L0Z7 A0A6J1L0Z7_CUCMA	SPQYSPSAGYSPTAPGYSPTSSTQYTPQTS DKDDRSNR-----	1848
tr A0A0A0L655 A0A0A0L655_CUCSA	SPQYSPSAGYSPTAPGYSPTSSTQYTPQTS DKDDRSRKKDDRRN-----	1867

Fig. 9. MSA of the elongation subunits B1 of RNAP II from plant sources

A0A1Z5RIH1_SORBI, <i>Sorghum bicolor</i>	C5Y387_SORBI, <i>Sorghum bicolor</i>
A0A3B6MZU3_WHEAT, <i>Triticum aestivum</i>	A0A565C923_9BRAS, <i>Arabidopsis nemorensis</i>
M4D210_BRARP, <i>Brassica rapa</i>	A0A6J0KQ09_RAPSA, <i>Raphanus sativus</i>
A0A1J3F625_NOCCA, <i>Noccaea caerulescens</i>	A0A1J3JR03_NOCCA, <i>Noccaea caerulescens</i>
P18616 NRPB1_ARATH, <i>Arabidopsis thaliana</i>	D7MC36_ARALL, <i>Arabidopsis lyrata</i>
V4P2F5_EUTSA, <i>Eutrema salsugineum</i>	ROGLX7_9BRAS, <i>Capsella rubella</i>
A0A6J0MG42_RAPSA, <i>Raphanus sativus</i>	A0A398AHR5_BRACM, <i>Brassica campestris</i>
A0A0D3A1P5_BRAOL, <i>Brassica oleracea</i>	A0A3N6QGC8_BRACR, <i>Brassica cretica</i>
A0A0E0LRD6_ORYPU, <i>Oryza punctata</i>	K3YFU7_SETIT, <i>Setaria italic</i>
J3MQH6_ORYBR, <i>Oryza brachyantha</i>	A0A803MAV7_CHEQI, <i>Chenopodium quinoa</i>
A0A0K9RSK8_SPIOL, <i>Spinacia oleracea</i>	A0A6P6TFX2_COFAR, <i>Coffea Arabica</i>
A0A6I9UDD3_SESIN, <i>Sesamum indicum</i>	A0A1S3XM16_TOBAC, <i>Nicotiana tabacum</i>
A0A2G3A9T8_CAPAN, <i>Capsicum annum</i>	A0A1U8FXJ4_CAPAN, <i>Capsicum annum</i>
M0ZVV4_SOLTUSolanum tuberosum	A0A6N2BN18_SOLCI, <i>Solanum chilense</i>
A0A3Q7F7G2_SOLLC, <i>Solanum lycopersicum</i>	A0A6V7PIB4_ANACO, <i>Ananas comosus</i>
A0A6I9RZH4_ELAVG, <i>Elaeis guineensis</i>	A0A4Y7I7U1_PAPSO, <i>Papaver somniferum</i>
A0A6P9E4T1_JUGRE, <i>Juglans regia</i>	A0A7J7HU38_CAMSI, <i>Camellia sinensis</i>
F6H0D9_VITVI, <i>Vitis vinifera</i>	A0A7J6EME3_CANSA, <i>Cannabis sativa</i>
A0A067G7I3_CITSI, <i>Citrus sinensis</i>	A0A5J5TPI9_GOSBA, <i>Gossypium barbadense</i>
A0A061DGE8_THECC, <i>Theobroma cacao</i>	A0A6P5ZFF2_DURZI, <i>Durio zibethinus</i>
B9SXC0_RICCO, <i>Ricinus communis</i>	A0A251M2B5_MANES, <i>Manihot esculenta</i>
A0A314Z8L7_PRUYE, <i>Prunus yedoensis</i>	M5VSC7_PRUPE, <i>Prunus persica</i>
A0A6J5XYF9_PRUAR, <i>Prunus armeniaca</i>	A0A6J1L0Z7_CUCMA, <i>Cucurbita maxima</i>
A0A0A0L655_CUCSA, <i>Cucumis sativus</i>	

4.3 PR Function in the MSU RNAP III

The RNAP III is the largest and most complex of these multisubunit enzymes and involves in the transcription of genes encoding small, nontranslated RNAs such as tRNAs, 5S rRNA, and U6 snRNA. It is composed of 17 subunits and with a molecular mass of ~ 700 kDa (Table 1). Out of the 17 subunits, 10 are unique to RNAP III and the others are common to two or all three of the RNAPs. The yeast RNAP III binds 1 Mg²⁺ and 5 Zn²⁺ atoms [26]. The second-largest subunit of the RNAP III (C1) is responsible for the transcription of tRNA, 5S RNA and other low molecular weight RNA genes (Table 1). Although the promoters for RNAP I and RNAP II lie upstream of the transcription start site (as in prokaryotes), RNAP III uses 3 types of promoters where two are internal to the gene (Type 1 for 5S rRNA and Type 2 for tRNAs promoters lie downstream of the transcription start site) and

one is external to the gene (Type 3 promoters for U6 SnRNA).

Figure 11 shows the MSA analysis of the elongation subunits C1 of RNAP III from different types of yeasts. The template-binding and catalytic pairs are highlighted in yellow and the zinc-binding conserved Cs is highlighted in orange. The completely conserved Mg²⁺-binding site is highlighted in light green. The catalytic pair is slightly different from others as having an invariant M as -R/KM-. The template-binding pair -FG- and the Mg²⁺-binding site with the 3 invariant Ds is conserved in all.

In contrast to RNAP I and RNAP II, three to four S residues are seen immediately followed by the catalytic pair in all and a big 9 amino acid gap is seen between the catalytic amino acid and the first C of the Zn²⁺-binding site.

The PR exonuclease reaction of RNAP III from *S. cerevisiae* was studied by Whitehall et al. [27].

They found that the ribonuclease activity was totally dependent on the presence of a divalent cation and was stimulated by the addition of non-cognate ribonucleotides. Zn²⁺ or Co²⁺ at 7 mM yielded transcripts predominantly shortened by two nucleotides, but not significantly more. Remarkably, the deletion mutant RNAP III Δ, deprived of C11 subunit, lacked the intrinsic RNA cleavage activity of complete RNAP III.

Therefore, Chédin et al. [28] have concluded that the C11 subunit is essential for the PR functions and proposed that C11 (= to RpB9 of RNAP II and A12.2 of RNAP I) allows the enzyme to switch between RNA elongation and RNA cleavage modes and plays an essential role of the RNAP III RNA intrinsic cleavage activity.

CLUSTAL O (1.2.4) MSA of the elongation subunits B1 of RNAP II from animal and insect sources

tr W2TT11 W2TT11_NECAM	GLMDFR	QGVIER	PGHFC	AGNLAD	PGHFC	LELARPVFHIGFLTKILKVLRCVFCYCSKLLL	114									
tr A0A6P8Y2M5 A0A6P8Y2M5_DROAB	GLMDFR	QGVLDL	RNTK	CD	CSGNMTE	CPGHFC	HELTKPVFHIGFIAKTIKILRCVFCYCSKLLV									
tr A0A1X7VVZ9 A0A1X7VVZ9_AMPQE	GLMDFR	QGVIDR	ASHCD	CD	CAGNMNT	CPGHFC	HISLTKPVFHVCFMTKIVKIMRCVFCYCSRLLI									
tr V5HBP6 V5HBP6_IXORI	GLMDFR	QGVIDR	TSRCD	CD	CAGSMTE	CPGHFC	HIEELAKPVFHCGFLTKTKILRCVFCYCSKLLV									
tr A0A7J5XJ09 A0A7J5XJ09_DISMA	GLMDFR	QGVIDR	SGRCD	CD	CAGNMTE	CPGHFC	HIEELAKPVFHVGFVTKIMKILRCVFCYCSKLLV									
tr A0A671PGW1 A0A671PGW1_9TELE	GLMDFR	QGVIDR	SGRCD	CD	CAGNMTE	CPGHFC	HIEELAKPVFHVGFVTKIMKILRCVFCYCSKLLV									
tr A0A3P9D2C8 A0A3P9D2C8_9CICH	GLMDFR	QGVIER	TGRCD	CD	CAGNMTE	CPGHFC	HIEELAKPVFHVGFVTKIMKILRCVFCYCSKLLV									
tr A0A1S3SD38 A0A1S3SD38_SALSA	GLMDFR	QGVIER	SGRCD	CD	CAGNMTE	CPGHFC	HIEELAKPVFHVGFVTKIMKILRCVFCYCSKLLV									
tr A0A060XGJ1 A0A060XGJ1_ONCMY	GLMDFR	QGVIER	SGRCD	CD	CAGNMTE	CPGHFC	HIEELAKPVFHVGFVTKIMKILRCVFCYCSKLLV									
tr A0A1S3N6M0 A0A1S3N6M0_SALSA	GLMDFR	QGVIER	SGRCD	CD	CAGNMTE	CPGHFC	HIEELAKPVFHVGFVTKIMKILRCVFCYCSKLLV									
tr A0A3B1J9R7 A0A3B1J9R7_ASTMX	GLMDFR	QGVIER	SGRCD	CD	CAGNMTE	CPGHFC	HIEELAKPVFHVGFVTKIMKILRCVFCYCSKLLV									
tr A0A4W4GG80 A0A4W4GG80_ELEEL	GLMDFR	QGVIER	TGRCD	CD	CAGNMTE	CPGHFC	HIEELAKPVFHVGFVTKIMKILRCVFCYCSKLLV									
tr A0A484CCJ1 A0A484CCJ1_PERFV	GLMDFR	QGVIER	TGRCD	CD	CAGNMTE	CPGHFC	HIEELAKPVFHVGFVTKIMKILRCVFCYCSKLLV									
tr A0A1A8DQ60 A0A1A8DQ60_9TELE	GLMDFR	QGVIER	TGRCD	CD	CAGNMTE	CPGHFC	HIEELAKPVFHVGFVTKIMKILRCVFCYCSKLLV									
tr A0A1A8ER05 A0A1A8ER05_9TELE	GLMDFR	QGVIER	TGRCD	CD	CAGNMTE	CPGHFC	HIEELAKPVFHVGFVTKIMKILRCVFCYCSKLLV									
tr A0A3P9D2C4 A0A3P9D2C4_9CICH	GLMDFR	QGVIER	TGRCD	CD	CAGNMTE	CPGHFC	HIEELAKPVFHVGFVTKIMKILRCVFCYCSKLLV									
tr A0A3B5KXA5 A0A3B5KXA5_9TELE	GLMDFR	QGVIER	SGRCD	CD	CAGNMTE	CPGHFC	HIEELAKPVFHVGFVTKIMKILRCVFCYCSKLLV									
tr H2LPT8 H2LPT8_ORYLA	G---	FR	QGVIER	SGRCD	CD	CAGNMTE	CPGHFC	HIEELAKPVFHVGFVTKIMKILRCVFCYCSKLLV								
tr A0A4W6CUU1 A0A4W6CUU1_LATCA	GLMDFR	QGVIER	TGRCD	CD	CAGNMTE	CPGHFC	HIEELAKPVFHVGFVTKIMKILRCVFCYCSKLLV									
tr A0A3L7GMG1 A0A3L7GMG1_CRIGR	GLMDFR	QGVIER	TGRCD	CD	CAGNMTE	CPGHFC	HIEELAKPVFHVGFVTKIMKILRCVFCYCSKLLV									
tr A0A6P3HSN8 A0A6P3HSN8_BISBI	GLMDFR	QGVIER	TGRCD	CD	CAGNMTE	CPGHFC	HIEELAKPVFHVGFVTKIMKILRCVFCYCSKLLV									
tr A0A5N3WI13 A0A5N3WI13_MUNMU	GLMDFR	QGVIER	TGRCD	CD	CAGNMTE	CPGHFC	HIEELAKPVFHVGFVTKIMKILRCVFCYCSKLLV									
tr A0A5N4D616 A0A5N4D616_CAMDR	GLMDFR	QGVIER	TGRCD	CD	CAGNMTE	CPGHFC	HIEELAKPVFHVGFVTKIMKILRCVFCYCSKLLV									
tr A0A452RK12 A0A452RK12_URSAM	GLMDFR	QGVIER	TGRCD	CD	CAGNMTE	CPGHFC	HIEELAKPVFHVGFVTKIMKILRCVFCYCSKLLV									
tr A0A670ZA05 A0A670ZA05_PSETE	GLMDFR	QGVIER	TGRCD	CD	CAGNMTE	CPGHFC	HIEELAKPVFHVGFVTKIMKILRCVFCYCSKLLV									
tr G3RTC9 G3RTC9_GORGO	GLMDFR	QGVIER	TGRCD	CD	CAGNMTE	CPGHFC	HIEELAKPVFHVGFVTKIMKILRCVFCYCSKLLV									
tr A0A7M4DUC2 A0A7M4DUC2_PIG	GLMDFR	QGVIER	TGRCD	CD	CAGNMTE	CPGHFC	HIEELAKPVFHVGFVTKIMKILRCVFCYCSKLLV									
tr A0A2K6DF42 A0A2K6DF42_MACNE	GLMDFR	QGVIER	TGRCD	CD	CAGNMTE	CPGHFC	HIEELAKPVFHVGFVTKIMKILRCVFCYCSKLLV									
tr A0A1S2ZNJ1 A0A1S2ZNJ1_ERIEU	GLMDFR	QGVIER	TGRCD	CD	CAGNMTE	CPGHFC	HIEELAKPVFHVGFVTKIMKILRCVFCYCSKLLV									
tr O08847 O08847_MOUSE	GLMDFR	QGVIER	TGRCD	CD	CAGNMTE	CPGHFC	HIEELAKPVFHVGFVTKIMKILRCVFCYCSKLLV									
tr A0A1D5RJ13 A0A1D5RJ13_MACMU	GLMDFR	QGVIER	TGRCD	CD	CAGNMTE	CPGHFC	HIEELAKPVFHVGFVTKIMKILRCVFCYCSKLLV									
tr G3MZY8 G3MZY8_BOVIN	GLMDFR	QGVIER	TGRCD	CD	CAGNMTE	CPGHFC	HIEELAKPVFHVGFVTKIMKILRCVFCYCSKLLV									
tr A0A6P3E8E8 A0A6P3E8E8_SHEEP	GLMDFR	QGVIER	TGRCD	CD	CAGNMTE	CPGHFC	HIEELAKPVFHVGFVTKIMKILRCVFCYCSKLLV									
tr A0A667HCS4 A0A667HCS4_LYNCA	GLMDFR	QGVIER	TGRCD	CD	CAGNMTE	CPGHFC	HIEELAKPVFHVGFVTKIMKILRCVFCYCSKLLV									
sp P24928 RPB1_HUMAN	GLMDP	QGVIER	TGRCD	CD	CAGNMTE	CPGHFC	HIEELAKPVFHVGFVTKIMKILRCVFCYCSKLLV									
tr G3TV69 G3TV69_LOXAF	GLMDFR	QGVIER	TGRCD	CD	CAGNMTE	CPGHFC	HIEELAKPVFHVGFVTKIMKILRCVFCYCSKLLV									
tr F627Q4 F627Q4_HORSE	GLMDFR	QGVIER	TGRCD	CD	CAGNMTE	CPGHFC	HIEELAKPVFHVGFVTKIMKILRCVFCYCSKLLV									
sp P11414 RPB1_CRIGR	GGLMDP	QGVIER	TGRCD	CD	CAGNMTE	CPGHFC	HIEELAKPVFHVGFVTKIMKILRCVFCYCSKLLV									
tr A0A6I9L929 A0A6I9L929_PERMB	GLMDFR	QGVIER	TGRCD	CD	CAGNMTE	CPGHFC	HIEELAKPVFHVGFVTKIMKILRCVFCYCSKLLV									
tr I3LYD0 I3LYD0 ICTTR	GLMDFR	QGVIER	TGRCD	CD	CAGNMTE	CPGHFC	HIEELAKPVFHVGFVTKIMKILRCVFCYCSKLLV									
tr A0A2K6RYV7 A0A2K6RYV7_SAIBB	GLMDFR	QGVIER	TGRCD	CD	CAGNMTE	CPGHFC	HIEELAKPVFHVGFVTKIMKILRCVFCYCSKLLV									
tr F7I1JW5 F7I1JW5_CALJA	GLMDFR	QGVIER	TGRCD	CD	CAGNMTE	CPGHFC	HIEELAKPVFHVGFVTKIMKILRCVFCYCSKLLV									
tr A0A671F2F4 A0A671F2F4_RHIFE	GLMDFR	QGVIER	TGRCD	CD	CAGNMTE	CPGHFC	HIEELAKPVFHVGFVTKIMKILRCVFCYCSKLLV									
tr A0A6J0ZAW1 A0A6J0ZAW1_ODOVR	GLMDFR	QGVIER	TGRCD	CD	CAGNMTE	CPGHFC	HIEELAKPVFHVGFVTKIMKILRCVFCYCSKLLV									
tr A0A6J3I271 A0A6J3I271_SAPAP	GLMDFR	QGVIER	TGRCD	CD	CAGNMTE	CPGHFC	HIEELAKPVFHVGFVTKIMKILRCVFCYCSKLLV									
tr A0A091CJT9 A0A091CJT9_FUKDA	GLMDFR	QGVIER	TGRCD	CD	CAGNMTE	CPGHFC	HIEELAKPVFHVGFVTKIMKILRCVFCYCSKLLV									
tr K9J413 K9J413_DESRO	GLMDFR	QGVIER	TGRCD	CD	CAGNMTE	CPGHFC	HIEELAKPVFHVGFVTKIMKILRCVFCYCSKLLV									
tr A0A6J2NJ44 A0A6J2NJ44_9CHIR	GLMDFR	QGVIER	TGRCD	CD	CAGNMTE	CPGHFC	HIEELAKPVFHVGFVTKIMKILRCVFCYCSKLLV									
tr G1MCZ1 G1MCZ1_AILME	GLMDFR	QGVIER	TGRCD	CD	CAGNMTE	CPGHFC	HIEELAKPVFHVGFVTKIMKILRCVFCYCSKLLV									
tr A0A3Q7XG12 A0A3Q7XG12_URSAR	GLMDFR	QGVIER	TGRCD	CD	CAGNMTE	CPGHFC	HIEELAKPVFHVGFVTKIMKILRCVFCYCSKLLV									
tr A0A2U3Y5R9 A0A2U3Y5R9_LEPWE	GLMDFR	QGVIER	TGRCD	CD	CAGNMTE	CPGHFC	HIEELAKPVFHVGFVTKIMKILRCVFCYCSKLLV									
tr A0A6J2AXC2 A0A6J2AXC2_ZALCA	GLMDFR	QGVIER	TGRCD	CD	CAGNMTE	CPGHFC	HIEELAKPVFHVGFVTKIMKILRCVFCYCSKLLV									
tr D4A5A6 D4A5A6_RAT	GLMDFR	QGVIER	TGRCD	CD	CAGNMTE	CPGHFC	HIEELAKPVFHVGFVTKIMKILRCVFCYCSKLLV									
tr A0A2I3M9H2 A0A2I3M9H2_PAPAN	GLMDFR	QGVIER	TGRCD	CD	CAGNMTE	CPGHFC	HIEELAKPVFHVGFVTKIMKILRCVFCYCSKLLV									
tr A0A2I3RTL5 A0A2I3RTL5_PANTR	GLMDFR	QGVIER	TGRCD	CD	CAGNMTE	CPGHFC	HIEELAKPVFHVGFVTKIMKILRCVFCYCSKLLV									
tr A0A0R4J0V5 A0A0R4J0V5_MOUSE	GLMDFR	QGVIER	TGRCD	CD	CAGNMTE	CPGHFC	HIEELAKPVFHVGFVTKIMKILRCVFCYCSKLLV									
tr A0A6J1YFT5 A0A6J1YFT5_ACIJB	GLMDFR	QGVIER	TGRCD	CD	CAGNMTE	CPGHFC	HIEELAKPVFHVGFVTKIMKILRCVFCYCSKLLV									
tr G3T277 G3T277_LOXAF	GLMDFR	QGVIER	TGRCD	CD	CAGNMTE	CPGHFC	HIEELAKPVFHVGFVTKIMKILRCVFCYCSKLLV									
tr H0VRW6 H0VRW6_CAVFO	GLMDFR	QGVIER	TGRCD	CD	CAGNMTE	CPGHFC	HIEELAKPVFHVGFVTKIMKILRCVFCYCSKLLV									
tr A0A480L5T3 A0A480L5T3_PIG	GLMDFR	QGVIER	TGRCD	CD	CAGNMTE	CPGHFC	HIEELAKPVFHVGFVTKIMKILRCVFCYCSKLLV									
sp P08775 RPB1_MOUSE	GLMDFR	QGVIER	TGRCD	CD	CAGNMTE	CPGHFC	HIEELAKPVFHVGFVTKIMKILRCVFCYCSKLLV									
tr A0A340X8C7 A0A340X8C7_LIPVE	GLMDFR	QGVIER	TGRCD	CD	CAGNMTE	CPGHFC	HIEELAKPVFHVGFVTKIMKILRCVFCYCSKLLV									
*****	***	::	*	*	::	***	::	*****	*	*	::	*****	::	***	::	*****

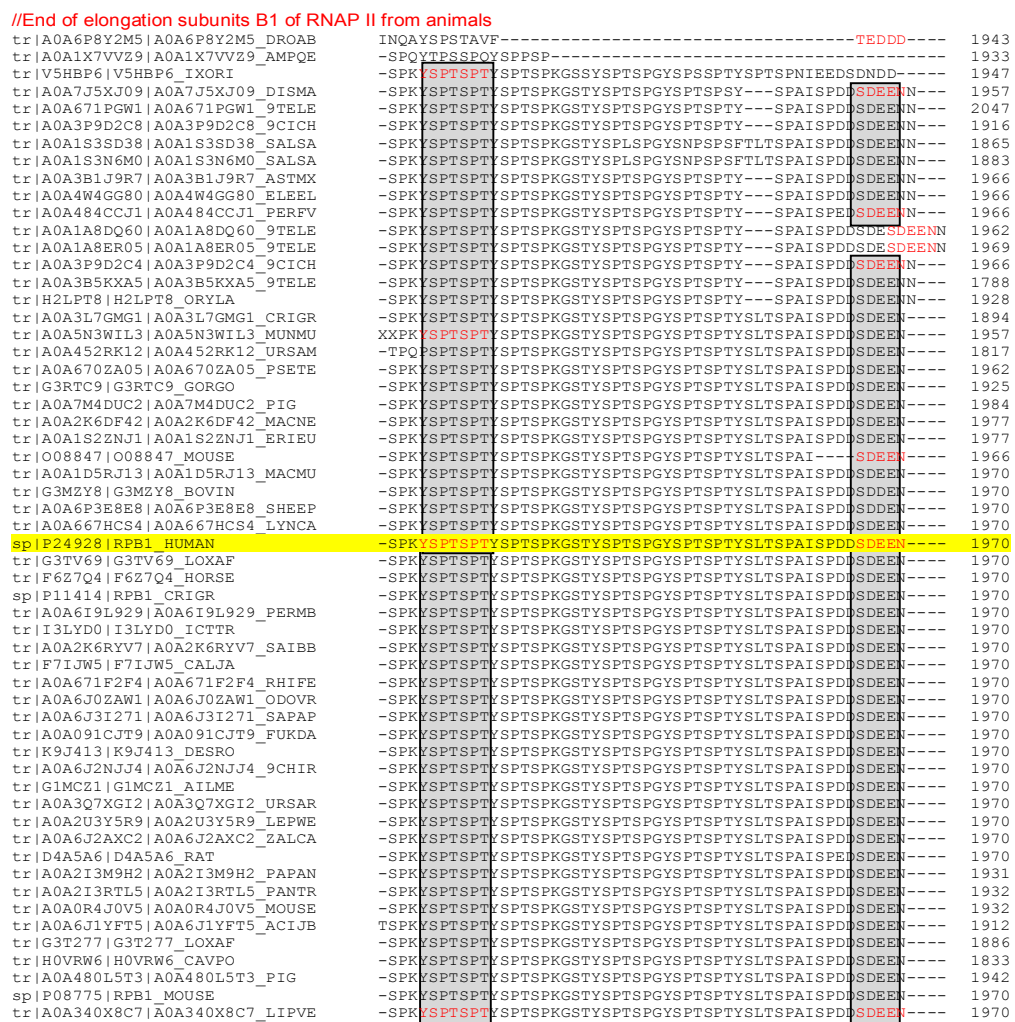


Fig. 10. MSA of the elongation subunits B1 of RNAP II from animal and insect sources

A0A6P8Y2M5_DROAB <i>Drosophila albomicans</i>	A0A1X7VVZ9_AMPQE <i>Amphimedon queenslandica</i>
V5HBP6_IXORI <i>Ixodes ricinus</i>	A0A7J5XJ09_DISMA <i>Dissostichus mawsoni</i>
A0A671F2F4_RHIFE <i>Rhinolophus ferrumequinum</i>	A0A3P9D2C8_9CICH <i>Maylandia zebra</i>
A0A1S3N6M0_SALSA <i>Salmo salar</i>	A0A060XGJ1_ONCMY <i>Oncorhynchus mykiss</i>
A0A1S3SD38_SALSA <i>Salmo salar</i>	A0A3B1J9R7_ASTMX <i>Astyanax mexicanus</i>
A0A4W4GG80_ELEEL <i>Electrophorus electricus</i>	A0A484CCJ1_PERFV <i>Perca flavescens</i>
A0A1A8DQ60_9TELE <i>Nothobranchius kadleci</i>	A0A1A8ER05_9TELE <i>Nothobranchius korthausae</i>
A0A3P9D2C4_9CICH <i>Maylandia zebra</i>	A0A3B5KXA5_9TELE <i>Xiphophorus couchianus</i>
H2LPT8_ORYLA <i>Oryzias latipes</i>	A0A4W6CUU1_LATCA <i>Lates calcarifer</i>
A0A3L7GMG1_CRIGR <i>Cricetulus griseus</i>	A0A6P3HSN8_BISBI <i>Bison bison bison</i>
A0A5N3WIL3_Muntiac <i>muntjak</i>	A0A5N4D616_CAMDR <i>Camelus dromedaries</i>
A0A452RK12_URSAM <i>Ursus americanus</i>	A0A670ZA05_PSETE <i>Pseudonaja textilis</i>
G3RTC9_GORGO <i>Gorilla gorilla gorilla</i>	H0VRW6_CAVPO <i>Cavia porcellus</i>
A0A7M4DUC2_PIG <i>Sus scrofa</i>	A0A2K6RYV7_SAIBB <i>Saimiri boliviensis boliviensis</i>
F7IJW5_CALJA <i>Callithrix jacchus</i>	A0A1S2ZJ1_ERIEU <i>Erinaceus europaeus</i>
O08847_MOUSE <i>Mus musculus</i>	A0A1D5RJ13_MACMU <i>Macaca mulatta</i>
G3MZY8_BOVIN <i>Bos Taurus</i>	A0A6P3E8E8_SHEEP <i>Ovis aries</i>
A0A667HCS4_LYNCA <i>Lynx Canadensis</i>	P24928 RPB1_HUMAN <i>Homo sapiens</i>
G3TV69_LOXAF <i>Loxodonta Africana</i>	F6Z7Q4_HORSE <i>Equus caballus</i>
P11414 RPB1_CRIGR <i>Cricetulus griseus</i>	A0A6I9L929_PERMB <i>Peromyscus maniculatus bairdii</i>
I3LYD0 ICTTR <i>Ictidomys tridecemlineatus</i>	A0A2K6DF42_MACNE <i>Macaca nemestrina</i>
A0A671PGW1_9TELE <i>Sinocyclocheilus anshuiensis</i>	A0A6J0ZAW1_ODOVR, <i>Odocoileus vir. texanus</i>

A0A6J3I271_SAPAP, *Sapajus paella*
 K9J413_DESRO *Desmodus rotundus*
 G1MCZ1_AILME *Ailuropoda melanoleuca*
 A0A2U3Y5R9_LEPWE *Leptonychotes weddellii*
 D4A5A6_RAT *Rattus norvegicus*
 A0A2I3RTL5_PANTR *Pan troglodytes*
 A0A6J1YFT5_ACJOB *Acinonyx jubatus*
 A0A480L5T3_PIG *Sus scrofa*
 A0A340X8C7_LIPVE *Lipotes vexillifer*

A0A091CJT9_FUKDA, *Fukomys damarensis*
 A0A6J2NJJ4_9CHIR, *Phyllostomus discolor*
 A0A3Q7XGI2_URSAR *Ursus arctos horribilis*
 A0A6J2AXC2_ZALCA *Zalophus californianus*
 A0A2I3M9H2_PAPAN *Papio anub*
 A0A0R4J0V5_MOUSE *Mus musculus*
 G3T277_LOXAF *Loxodonta africana*
 P08775|RPB1_MOUSE *Mus musculus*

CLUSTAL O (1.2.4) MSA of elongation subunits C1 of RNAP III from different yeasts

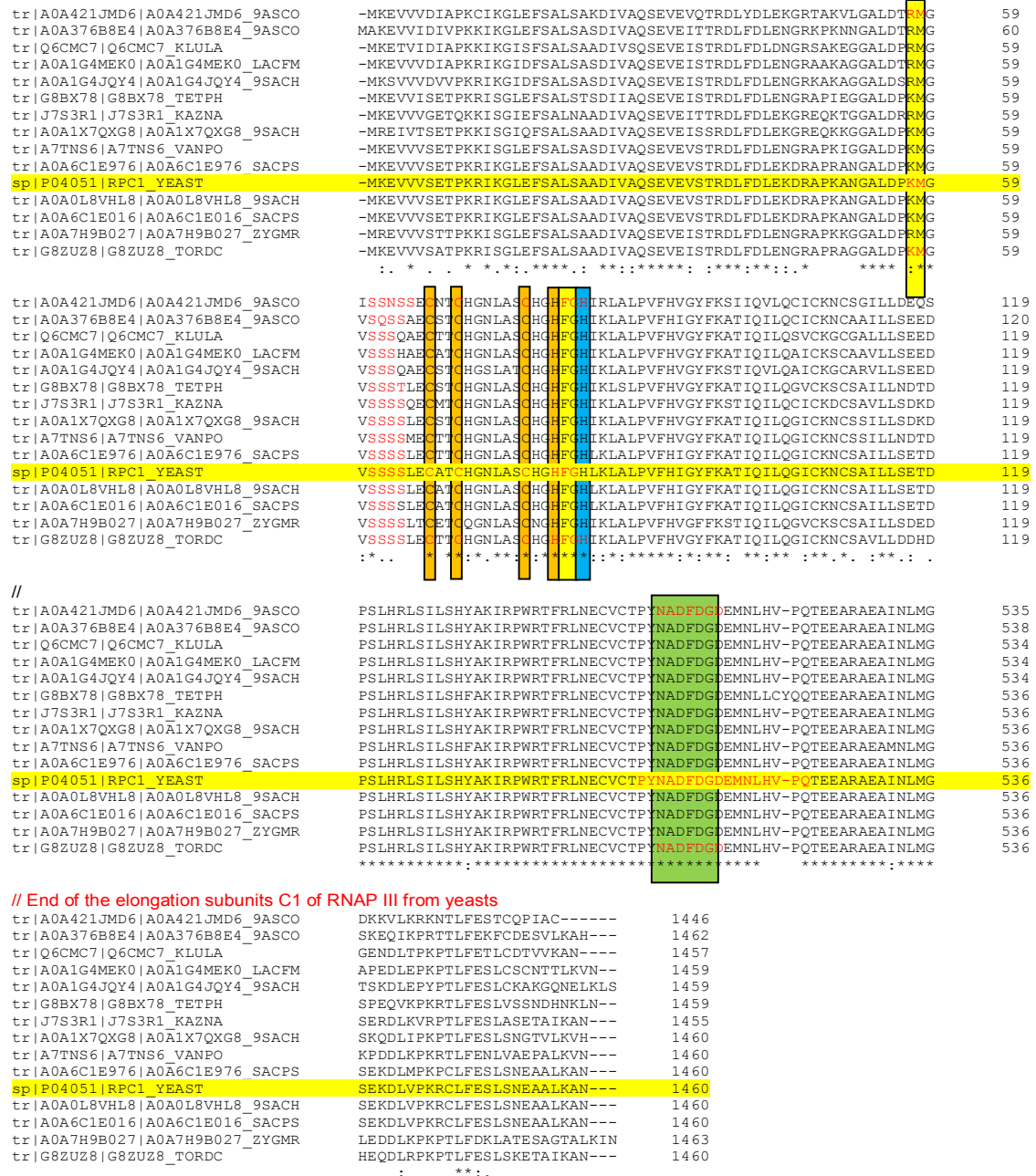


Fig. 11. MSA of elongation subunits C1 of RNAP III from different yeasts

A0A421JMD6_9ASCO *Spathaspora* sp.
 Q6CMC7_KLULA *Kluyveromyces lactis*
 A0A1G4JQY4_9SACH *Lachancea mirantina*
 A0A1X7QXG8_9SACH *Kazachstania saulgeensis*
 A7TNS6_VANPO *Vanderwaltozyma polyspora*
P04051|RPC1_YEAST *Saccharomyces cerevisiae*
 A0A6C1E016_SACPS *Saccharomyces pastorianus*
 G8ZUZ8_TORDC *Torulasporea delbrueckii*

A0A376B8E4_9ASCO *Saccharomycodes ludwigii*
 A0A1G4MEK0_LACFM *Lachancea fermentati*
 J7S3R1_KAZNA *Kazachstania naganishii*
 G8BX78_TETPH *Tetrapisispora phaffii*
 A0A6C1E976_SACPS *Saccharomyces pastorianus*
 A0A0L8VHL8_9SACH *Saccharomyces boulardii*
 A0A7H9B027_ZYGMR *Zygorulasporea mrakii*

Figure 12 shows the MSA analysis of the elongation subunits C1 of RNAP III from higher fungi. The template-binding and catalytic pairs are highlighted in yellow and the Zn-binding conserved Cs is highlighted in orange. The completely conserved Mg²⁺-binding site is highlighted in light green. The catalytic amino acid -K/H- is conserved in all whereas the template-binding pair is varied as -FG/YG/YA- and the Mg²⁺-binding site with the 3 invariant Ds are conserved in all. A 9 amino acid-gap is seen between the catalytic amino acid and the first C of the Zn²⁺-binding site as in yeasts. The Mg²⁺-binding invariant Ds are completely conserved in all (Fig. 12). The invasive fungal pathogens (highlighted in light blue) use either a V or an I (highlighted in red) immediately after the template-binding pair, -FG-. *Powellomyces hirtus*, *Batrachochytrium salamandrivorans*, *Batrachochytrium dendrobatidis*, *Spizellomyces punctatus*, *Spizellomyces palustris* are zoosporic (i.e., reproduce with zoospores) invasive fungal pathogens and belong to Chytridiomycota.

site is highlighted in light green. The catalytic amino acid -K- is conserved in all, whereas the template-binding pair is varied as -Y/FG- and the Mg²⁺-binding site with the 3 invariant Ds are conserved in all. The distance conservation between the catalytic amino acid and the first C of the Zn²⁺-binding site is maintained in plant sources also as in yeasts and higher fungi.

Figure 13 shows the MSA analysis of the elongation subunits C1 of RNAP III from various plant sources. The template-binding and catalytic pairs are highlighted in yellow and the Zn-binding conserved Cs is highlighted in orange. The completely conserved Mg²⁺ binding

Figure 14 shows the MSA analysis of the elongation subunits C1 of RNAP III from animals and animal parasites. The template-binding and catalytic pairs are highlighted in yellow and the Zn-binding conserved Cs is highlighted in orange. The completely conserved Mg²⁺-binding site is highlighted in light green. The catalytic amino acid -R- is conserved in all except in the malarial parasite, where an equivalent amino acid -K- is used. Similarly, the template-binding pair is found to be different in the sequences from the animal pathogen/parasites where they mainly use -FG/WG- instead of an -YG- used by others (the parasite sequence are highlighted in light blue). It is not clear whether these changes in the template-binding pairs have any advantage for the parasites to bind and transcribe differentially from their host machinery. However, the Mg²⁺-binding site with the 3 invariant Ds is conserved in all.

CLUSTAL O (1.2.4) MSA of elongation subunits C1 of RNAP III from higher fungi
 (Only the polymerase/PR active site and the Mg²⁺-binding regions are shown)

tr J3P867 J3P867_GAET3	N-N-RTPSRHGPLDRL	GTSSKTAET	QTR	QAQPLQNS	SGHFC	YVRLPLPAFHIGYLRVQ	112					
tr A0A0F8B363 A0A0F8B363_CERFI	K-N-RTPYLHGPLDRL	GTSSKMSK	STCNELLQ	TCM	GHFC	YVRLPLPAFHIGYLRVQ	109					
tr A0A2C5X0T2 A0A2C5X0T2_9PEZI	K-N-RTPYLHGPLDRL	GTSSKMSK	STCNELLQ	TCM	GHFC	YVRLPLPAFHIGYLRVQ	109					
tr A0A2C5YCW5 A0A2C5YCW5_9HYPO	K-N-RAPYRHGPLDRL	GTSSKIGR	CATC	QDALKI	CI	GHFC	YVRLPLPAFHIGYLRVMS	107				
tr A0A179GT68 A0A179GT68_PURLI	N-N-RAPYRHGPLDRL	GTSSKIGK	CATC	QDLSLQ	TC	GHFC	YVRLPLPAFHIGYLRVMS	109				
tr M1WGG0 M1WGG0_CLAP2	N-N-RSPYRHGPLDRL	GTSSKIGK	CE	QDLSLT	NC	GHFC	YVRLPLPAFHIGYLRVMS	109				
tr A0A0D9PC02 A0A0D9PC02_METAN	N-N-RAPYRHGPLDRL	GTSSKSGK	CDT	CHDSLQ	NC	GHFC	YVRLPLPAFHIGYLRVMS	109				
tr A0A179FJW8 A0A179FJW8_METCM	N-N-RAPYRHGPLDRL	GTSSKGGK	CDT	QDLSLQ	NC	GHFC	YVRLPLPAFHIGYLRVMS	109				
tr A0A4Q7JYL8 A0A4Q7JYL8_METCM	N-N-RAPYRHGPLDRL	GTSSKGGK	CDT	QDLSLQ	NC	GHFC	YVRLPLPAFHIGYLRVMS	109				
tr A0A177WGH3 A0A177WGH3_BATDL	K-NRPPAKFGALDRL	GTADKSI	IF	CE	TC	GE	ATK	CVGH	FC	YVRLVLPVPHIGYFKLMIT	102	
tr A0A1S8VVR9 A0A1S8VVR9_9FUNG	K-TTRPPAKFGALDRL	GTADKSI	IF	CD	TG	ENI	Q	CVGH	FC	YVRLVLPVPHIGYFKLMIT	102	
tr A0A507E4D4 A0A507E4D4_9FUNG	Q-SHRPSVKFGVLDRL	LG	VADK	VK	CE	TC	GE	GLQ	CI	GHFC	YVRLVLPVPHIGYFKLMIQ	108
tr A0A0LOHMV1 A0A0LOHMV1_SPIP	Q-PNRPSVKFGVLDRL	GTADKMGK	CE	TC	GLGLQ	CI	GHFC	YVRLVLPVPHIGYFKLMLS	112			
tr A0A507F1C9 A0A507F1C9_9FUNG	Q-PNRPSVKFGVLDRL	GTADKMGK	CE	TC	GLGLQ	CI	GHFC	YVRLVLPVPHIGYFKLMLS	102			
tr A0A1Y1UMB3 A0A1Y1UMB3_9TREE	EDGTRTAKDGPLDRL	GPNDK	KT	HT	CE	EE	AT	K	CVGH	FC	YVRLKLVLPVPHIGYFRPTIN	110
tr A0A427XWW1 A0A427XWW1_9TREE	EDGSRRTA	PHGPLDRL	GPNEKGGI	CT	CH	ED	HT	CVGH	FC	YVRLKLVLPVPHIGYFRPTIN	113	
tr A0A1E3JS41 A0A1E3JS41_9TREE	EDGSRRTVA	SHGPLDRL	GPNEKGGK	CA	TC	EE	NA	CVGH	FC	YVRLKLVLPVPHIGYFRPTIN	113	
tr A0A397TI21 A0A397TI21_9GLOM	---NRKPMENGLDRL	GTSDHDTL	Q	TC	GE	KMA	CI	GHFC	YVRLVLPVPHIGYFKRAVIN	99		
tr A0A397TXX1 A0A397TXX1_9GLOM	---NRAPMENGLDRL	GTSDHDTL	ET	GERMA	CI	GHFC	YVRLVLPVPHIGYFKRAVIN	99				

```

tr |A0A397HR92|A0A397HR92_9GLOM ---NRAPMENGVLDRRIGTSDHDI...ETG...GKMA...V...IKLILPVFHI...GYFKAVIN 99
tr |A0A4T0Q4W3|A0A4T0Q4W3_9BASI T-PDRAPQRNGVLD...RRTGSDKSGS...DTG...GSM...V...IKLALPVFHI...GYFKDIIA 101
tr |A0A5C3R213|A0A5C3R213_9AGAR --VERLPAKNGVLD...RRTGTEKGA...G...G...MTAVE...V...IKLVVPVPH...GPKHVVG 100
tr |A0A165Y5Y1|A0A165Y5Y1_9AGAM --TDRLPVKNGVLD...RRTGSDKSAB...G...G...L...G...V...IKLVVPVPH...GYFKHAI...G 100
tr |A0A4R5XE50|A0A4R5XE50_9AGAM --TERVPAKGGVLD...RRTGTEKNA...G...G...L...S...A...D...V...IKLALPVFHI...GYFKHTI...A 100
tr |W4KH03|W4KH03_HETIT --TDROPVKDGVLD...RRTGTSEKN...R...G...G...L...K...S...V...D...V...IKLVVPVPH...GYFKHTI...G 100
tr |A0A5C3NIH7|A0A5C3NIH7_9AGAM --PDRVPVKNVLD...RRTGSDKTT...R...G...G...L...N...S...A...E...V...IKLVVPVPH...GYFKHTI...G 100
tr |A0A066WN95|A0A066WN95_TILAU T-TERKPMVGGPND...QRIGIWDK...S...A...T...G...G...H...M...S...E...I...G...E...V...IKLVVPVH...GVGFKHIVQ 102
tr |A0A317XL4|A0A317XL4_9BASI E-AERFPVANGTLD...RRTGVS...D...K...N...S...I...G...E...T...C...H...L...K...M...A...D...V...G...Y...IKLVLPV...FHV...G...F...K...H...T...V...A 102
tr |I2FP81|I2FP81_USTH4 E-AERKFPVANGTLD...RRTGVS...D...K...N...S...I...G...E...T...C...H...L...K...M...A...D...V...G...Y...IKLVLPV...FHV...G...F...K...H...T...V...A 102
tr |A0A0D1DT74|A0A0D1DT74_USTMA E-SERKFPVANGTLD...RRTGVS...D...K...N...S...I...G...E...T...C...H...L...K...M...A...D...V...G...Y...IKLVLPV...FHV...G...F...K...H...T...V...A 102
tr |E6ZW18|E6ZW18_SPORE E-AERKFPVANGTLD...RRTGVS...D...K...N...S...I...G...E...T...C...H...L...K...M...A...D...V...G...Y...IKLVLPV...FHV...G...F...K...H...T...V...A 102
tr |A0A4U7KRJ3|A0A4U7KRJ3_9BASI E-AERKFPVANGTLD...RRTGVS...D...K...N...S...I...G...E...T...C...H...L...K...M...A...D...V...G...Y...IKLVLPV...FHV...G...F...K...H...T...V...A 102

```

```

//
tr |J3P867|J3P867_GAET3 VANLRFRGDDVVERHIEDGDIVL...FNRQPSLH...KLSIMSHLVKVRP...WRTFR...LNECVCTP...Y...N...A...L 513
tr |A0A0FB8363|A0A0FB8363_CERFI TAEQLRFGDDVVERHLEDGDIVL...FNRQPSLH...KLSIMSHLAKIRP...WRTFR...LNECVCG...Y...N...A...D 510
tr |A0A2C5X0T2|A0A2C5X0T2_9PEZI TAEQLRFGDDVVERHLEDGDIVL...FNRQPSLH...KLSIMSHLAKIRP...WRTFR...LNECVCG...Y...N...A...D 510
tr |A0A2C5YCW5|A0A2C5YCW5_9HYPO IARDLRIGDIVERHLEDGDIVL...FNRQPSLH...KLSIMSHLVKVRP...WRTFR...LNECVCTP...Y...N...A...D 508
tr |A0A179GT68|A0A179GT68_PURLI LARQLKAGDIVERHLEDGDIVL...FNRQPSLH...KLSIMSHLVKVRP...WRTFR...LNECVCTP...Y...N...A...D 510
tr |M1WGG0|M1WGG0_CLAP2 ASRQLRIGDDVVERHLEDGDIVL...FNRQPSLH...KLSIMSHRAKIRP...WRTFR...LNECVCTP...Y...N...A...D 510
tr |A0A0D9PC02|A0A0D9PC02_METAN AAKQLSYGDIVERHLEDGDIVL...FNRQPSLH...KLSIMSHLAKIRP...WRTFR...LNECVCTP...Y...N...A...D 509
tr |A0A179FJW8|A0A179FJW8_METCM AAKQLSYGDIVERHLEDGDIVL...FNRQPSLH...KLSIMSHVAKIRP...WRTFR...LNECVCTP...Y...N...A...D 510
tr |A0A4Q7JYL8|A0A4Q7JYL8_METCM AAKQLSYGDIVERHLEDGDIVL...FNRQPSLH...KLSIMSHVAKIRP...WRTFR...LNECVCTP...Y...N...A...D 510
tr |A0A177WGH3|A0A177WGH3_BATDL TADELQVGDVVERHLQDDVV...L...FNRQPSLH...KLSIMSHFVKVRP...WRTFR...LNECVCTP...Y...N...A...D 496
tr |A0A1S8VVK9|A0A1S8VVK9_9FUNG TAEDLQVGDVVERHLQDDVV...L...FNRQPSLH...KLSIMSHFVKVRP...WRTFR...LNECVCTP...Y...N...A...D 496
tr |A0A507E4D4|A0A507E4D4_9FUNG VAE...D...S...I...G...D...V...D...R...H...L...D...G...D...I...V...L...F...N...R...Q...P...S...L...H...K...L...S...I...S...H...Y...V...K...V...R...P...W...R...T...F...R...L...N...E...C...V...C...T...P...Y...N...A...D 501
tr |A0A0L0HMV1|A0A0L0HMV1_SPIPD TAAQLNIGDDVDRHLQDGDVV...L...FNRQPSLH...KLSIMSHFVKVRP...WRTFR...LNECVCTP...Y...N...A...D 505
tr |A0A507F1C0|A0A507F1C0_9FUNG TAAQLNIGDDVDRHLQDGDVV...L...FNRQPSLH...KLSIMSHFVKVRP...WRTFR...LNECVCTP...Y...N...A...D 495
tr |A0A1Y1UMB3|A0A1Y1UMB3_9TREE IAQLRLIGDVIHRHVRDGDIVL...FNRQPSLH...KLSIMCHRVKVRP...WRTFR...LNECVCTP...Y...N...A...D 503
tr |A0A427XWV1|A0A427XWV1_9TREE MARNLRIGDVIHRHVRDGDIVL...FNRQPSLH...KLSIMCHRVKVRP...WRTFR...LNECVCTP...Y...N...A...D 508
tr |A0A1E3JS41|A0A1E3JS41_9TREE WARDLMVGDIVHRHVRDGDIVL...FNRQPSLH...KLSIMCHRVKVRP...WRTFR...LNECVCTP...Y...N...A...D 510
tr |A0A397TI21|A0A397TI21_9GLOM CAEELQIGDIVERHLRDE...D...V...L...F...N...R...Q...P...S...L...H...K...L...S...I...M...A...H...Y...R...V...K...P...W...R...T...F...R...L...N...E...C...V...C...S...P...Y...N...A...D 491
tr |A0A397TXX1|A0A397TXX1_9GLOM CASELQIGDDVVERHLR...D...G...D...V...L...F...N...R...Q...P...S...L...H...K...L...S...I...M...A...H...Y...R...V...K...P...W...R...T...F...R...L...N...E...C...V...C...Y...N...A...D 491
tr |A0A397HR92|A0A397HR92_9GLOM CAEELQIGDIVERHLR...D...G...D...V...L...F...N...R...Q...P...S...L...H...K...L...S...I...M...A...H...Y...R...V...K...P...G...R...T...F...R...L...N...E...C...V...C...T...Y...N...A...D 491
tr |A0A4T0Q4W3|A0A4T0Q4W3_9BASI IANRLRIGDIVERHLR...D...L...I...L...F...N...R...Q...P...S...L...H...R...L...S...I...M...C...H...R...V...K...V...R...P...W...R...T...L...R...L...N...E...C...A...C...N...Y...N...A...D 494
tr |A0A5C3R213|A0A5C3R213_9AGAR VAESLSIGDIVERH...I...D...G...V...L...F...N...R...Q...P...S...L...H...K...L...S...I...M...C...H...R...A...K...I...R...P...W...R...T...F...R...L...N...E...C...A...C...G...P...Y...N...A...D 492
tr |A0A165Y5Y1|A0A165Y5Y1_9AGAM VADGLRYGDDVVERH...I...D...G...V...L...F...N...R...Q...P...S...L...H...K...L...S...I...M...C...H...R...V...K...V...R...P...W...R...S...F...R...L...N...E...C...V...C...N...Y...N...A...D 492
tr |A0A4R5XE50|A0A4R5XE50_9AGAM IADGLRIGDDVVERH...I...D...G...D...V...L...F...N...R...Q...P...S...L...H...K...L...S...I...M...C...H...R...V...K...V...R...P...W...R...S...F...R...L...N...E...C...V...C...G...Y...N...A...D 492
tr |W4KH03|W4KH03_HETIT IADGLRFGDDVVERH...I...D...G...D...V...L...F...N...R...Q...P...S...L...H...K...L...S...I...M...C...H...R...V...K...V...R...P...W...R...S...F...R...L...N...E...C...V...C...G...Y...N...A...D 492
tr |A0A5C3NIH7|A0A5C3NIH7_9AGAM MADGLRVGDDVVERH...I...D...G...D...V...L...F...N...R...Q...P...S...L...H...R...L...S...I...M...S...H...R...V...K...V...R...P...W...R...S...F...R...L...N...E...C...V...C...T...Y...N...A...D 492
tr |A0A066WN95|A0A066WN95_TILAU AAKNLKYGDIVERH...I...R...D...G...D...I...V...L...F...N...R...Q...P...S...L...H...K...L...S...I...M...S...H...R...V...K...V...R...P...W...R...T...F...R...L...N...E...C...A...C...N...Y...N...A...D 502
tr |A0A317XL4|A0A317XL4_9BASI LASKLRVGDIVERH...I...R...D...G...D...I...V...L...F...N...R...Q...P...S...L...H...K...L...S...I...M...S...H...R...A...K...I...R...P...W...R...T...F...R...L...N...E...C...A...C...N...Y...N...A...D 498
tr |I2FP81|I2FP81_USTH4 LAQKLRVGDIVERH...I...R...D...G...D...I...V...L...F...N...R...Q...P...S...L...H...K...L...S...I...M...S...H...R...A...K...I...R...P...W...R...T...F...R...L...N...E...C...A...C...N...Y...N...A...D 498
tr |A0A0D1DT74|A0A0D1DT74_USTMA LAEKL...R...V...G...D...V...E...R...H...I...R...D...G...D...I...V...L...F...N...R...Q...P...S...L...H...K...L...S...I...M...S...H...R...A...K...I...R...P...W...R...T...F...R...L...N...E...C...A...C...N...Y...N...A...D 498
tr |E6ZW18|E6ZW18_SPORE LAQKLRVGDIVERH...I...R...D...G...D...I...V...L...F...N...R...Q...P...S...L...H...K...L...S...I...M...S...H...R...A...K...I...R...P...W...R...T...F...R...L...N...E...C...A...C...N...Y...N...A...D 498
tr |A0A4U7KRJ3|A0A4U7KRJ3_9BASI LASKLRVGDIVERH...I...R...D...G...D...I...V...L...F...N...R...Q...P...S...L...H...K...L...S...I...M...S...H...R...A...K...I...R...P...W...R...T...F...R...L...N...E...C...A...C...N...Y...N...A...D 498

```

```

tr |J3P867|J3P867_GAET3 FDGDEMNL-----HVPQTEEARAEA...I...N...L...M...G...V...K...N...L...A...T...P...K...N...G...E...P...I...A...A...T...Q...D...F...I...T...A...A...Y...L...L...S 567
tr |A0A0FB8363|A0A0FB8363_CERFI FDGDEMNL-----HVPQTEEARAEA...I...T...L...M...G...V...K...N...L...A...T...P...K...N...G...E...P...I...A...A...T...Q...D...F...I...T...A...A...Y...V...F...S 564
tr |A0A2C5X0T2|A0A2C5X0T2_9PEZI FDGDEMNL-----HVPQTEEARAEA...I...T...L...M...G...V...K...N...L...A...T...P...K...N...G...E...P...I...A...A...T...Q...D...F...I...T...A...A...Y...V...F...S 564
tr |A0A2C5YCW5|A0A2C5YCW5_9HYPO FDGDEMNL-----HVPQTEEARAEA...I...N...L...M...G...V...K...Y...N...L...A...T...P...K...N...G...E...P...I...A...A...T...Q...D...F...I...T...A...A...F...L...S 562
tr |A0A179GT68|A0A179GT68_PURLI FDGDEMNL-----HVPQTEEARAEA...I...N...L...M...G...V...K...Y...N...L...A...T...P...K...N...G...E...P...I...A...A...T...Q...D...F...I...T...A...A...F...L...S 564
tr |M1WGG0|M1WGG0_CLAP2 FDGDEMNL-----HVPQTEEARAEA...I...S...L...M...G...V...K...Y...N...L...A...T...P...K...N...G...E...P...I...A...A...T...Q...D...F...I...T...A...A...F...L...S 564
tr |A0A0D9PC02|A0A0D9PC02_METAN FDGDEMNL-----HVPQTEEARAEA...I...N...L...M...G...V...K...Y...N...L...A...T...P...K...N...G...E...P...I...A...A...T...Q...D...F...I...T...A...A...F...L...S 563
tr |A0A179FJW8|A0A179FJW8_METCM FDGDEMNL-----HVPQTEEARAEA...I...N...L...M...G...V...K...Y...N...L...A...T...P...K...N...G...E...P...I...A...A...T...Q...D...F...I...T...A...A...F...L...S 564
tr |A0A4Q7JYL8|A0A4Q7JYL8_METCM FDGDEMNL-----HVPQTEEARAEA...I...N...L...M...G...V...K...Y...N...L...A...T...P...K...N...G...E...P...I...A...A...T...Q...D...F...I...T...A...A...F...L...S 564
tr |A0A177WGH3|A0A177WGH3_BATDL FDGDEMNL-----HVPQTEEARAE...A...E...L...M...G...T...K...N...N...L...V...T...P...R...N...G...E...P...I...A...A...T...Q...D...F...I...T...A...S...Y...L...L...S 550
tr |A0A1S8VVK9|A0A1S8VVK9_9FUNG FDGDEMNL-----HVLQTEEARAEA...I...E...L...M...G...V...K...N...L...V...T...P...R...N...G...E...P...I...A...A...T...Q...D...F...I...T...A...S...Y...L...L...S 550
tr |A0A507E4D4|A0A507E4D4_9FUNG FDGDEMNL-----HVPQTEEARTE...A...I...Q...L...M...G...V...K...N...L...V...T...P...R...N...G...E...P...I...A...A...T...Q...D...F...I...T...A...S...Y...L...L...S 555
tr |A0A0L0HMV1|A0A0L0HMV1_SPIPD FDGDEMNL-----HVPQTEEARAE...A...M...L...M...G...T...K...N...L...V...T...P...R...N...G...E...P...I...A...A...T...Q...D...F...I...T...A...S...Y...L...L...S 559
tr |A0A507F1C0|A0A507F1C0_9FUNG FDGDEMNL-----HVPQTEEARAE...A...M...L...M...G...T...K...N...L...V...T...P...R...N...G...E...P...I...A...A...T...Q...D...F...I...T...A...S...Y...L...L...S 549
tr |A0A1Y1UMB3|A0A1Y1UMB3_9TREE FDGDEMNL-----HVPQTEEARTE...A...L...E...L...M...S...V...K...N...L...V...T...P...R...N...G...E...P...I...A...A...T...Q...D...F...I...T...A...A...F...L...S 557
tr |A0A427XWV1|A0A427XWV1_9TREE FDGDEMNL-----HVPQTEEARTE...A...L...I...M...S...V...K...N...L...V...T...P...R...N...G...E...P...I...A...A...T...Q...D...F...I...T...A...S...Y...L...L...S 562
tr |A0A1E3JS41|A0A1E3JS41_9TREE FDGDEMNL...R...K...Y...L...P...F...H...V...P...Q...T...E...A...R...E...A...L...E...L...M...S...V...K...N...L...V...T...P...R...N...G...E...P...I...A...A...T...Q...D...F...I...T...A...S...Y...L...L...S 570
tr |A0A397TI21|A0A397TI21_9GLOM FDGDEMNL-----HVPQTEEAR...I...E...A...I...E...L...M...G...V...K...N...L...V...T...P...R...N...G...D...P...I...A...A...T...Q...D...F...I...T...S...S...Y...L...I...T 545
tr |A0A397TXX1|A0A397TXX1_9GLOM FDGDEMNL-----HVPQTEEAR...V...E...A...I...E...L...M...G...V...K...N...L...V...T...P...R...N...G...D...P...I...A...A...T...Q...D...F...I...T...S...S...Y...L...I...T 545
tr |A0A397HR92|A0A397HR92_9GLOM FDGDEMNL-----HVPQTEEAR...V...E...A...I...E...L...M...G...V...K...N...L...V...T...P...R...N...G...D...P...I...A...A...T...Q...D...F...I...T...S...S...Y...L...I...T 545
tr |A0A4T0Q4W3|A0A4T0Q4W3_9BASI FDGDEMNM-----HVPQTEEAR...E...A...Q...E...L...M...G...V...K...N...M...V...T...P...R...N...G...E...P...I...A...A...T...Q...D...F...I...T...A...A...Y...L...L...S 548
tr |A0A5C3R213|A0A5C3R213_9AGAR FDGDEMNL-----HVPQTEEARTE...A...L...Q...L...M...N...V...K...N...L...V...T...P...R...N...G...E...P...I...A...A...T...Q...D...F...I...T...A...S...F...L...L...S 546
tr |A0A165Y5Y1|A0A165Y5Y1_9AGAM FDGDEMNL-----H...I...P...Q...T...E...A...R...E...A...L...Q...L...M...D...V...K...N...I...V...T...P...R...N...G...E...P...I...A...A...T...Q...D...F...I...T...A...A...F...L...L...T 546
tr |A0A4R5XE50|A0A4R5XE50_9AGAM FDGDEMNM-----HVPQTEEARTE...A...L...E...L...M...N...V...K...N...L...V...T...P...R...N...G...E...P...I...A...A...T...Q...D...F...I...T...A...S...Y...L...L...S 546
tr |W4KH03|W4KH03_HETIT FDGDEMNL-----HVPQTEEARTE...A...L...E...L...M...S...V...K...N...M...V...T...P...R...N...G...E...P...I...A...A...T...Q...D...F...I...T...A...A...W...L...L...S 546
tr |A0A5C3NIH7|A0A5C3NIH7_9AGAM FDGDEMNL-----HVPQTEEARTE...A...L...E...L...M...N...V...K...N...I...V...S...P...R...N...G...E...P...I...A...A...T...Q...D...F...I...T...A...S...Y...L...L...S 546
tr |A0A066WN95|A0A066WN95_TILAU FDGDEMNM-----HVPQTEEARTE...A...T...I...L...M...G...V...K...N...L...V...T...P...R...N...G...E...P...I...A...A...T...Q...D...F...I...T...A...S...F...L...I...S 556
tr |A0A317XL4|A0A317XL4_9BASI FDGDEMNM-----HVPQTEEARTE...A...T...I...L...M...G...V...K...N...L...V...T...P...R...N...G...E...P...I...A...A...T...Q...D...F...I...T...A...S...Y...L...I...T 552
tr |I2FP81|I2FP81_USTH4 FDGDEMNM-----HVPQTEEARTE...A...T...I...L...M...G...V...K...N...L...V...T...P...R...N...G...E...P...I...A...A...T...Q...D...F...I...T...A...S...Y...L...I...S 552
tr |A0A0D1DT74|A0A0D1DT74_USTMA FDGDEMNM-----HVPQTEEARTE...A...T...I...L...M...G...V...K...N...L...V...T...P...R...N...G...E...P...I...A...A...T...Q...D...F...I...T...A...S...Y...L...I...S 552
tr |E6ZW18|E6ZW18_SPORE FDGDEMNM-----HVPQTEEARTE...A...T...I...L...M...G...V...K...N...L...V...T...P...R...N...G...E...P...I...A...A...T...Q...D...F...I...T...A...S...Y...L...I...S 552
tr |A0A4U7KRJ3|A0A4U7KRJ3_9BASI FDGDEMNM-----HVPQTEEARTE...A...T...I...L...M...G...V...K...N...L...V...T...P...R...N...G...E...P...I...A...A...T...Q...D...F...I...T...A...S...Y...L...I...S 552

```


// End of the elongation subunits C1 of RNAP III from animals and animal parasites

tr Q8SRM3 Q8SRM3_ENCCU	-----	1316
tr L2GLN2 L2GLN2_VITCO	-----	1442
sp P27625 RPC1_PLAFA	E--RETAMNY--	2339
tr A0A4W3H8T6 A0A4W3H8T6_CALMI	--NSEFHIPLVT-	1383
tr A0A672YVR8 A0A672YVR8_9TELE	--HADFHPLIT-	1380
tr A0A6I8R0Q8 A0A6I8R0Q8_XENTR	--HEDFHHPFLNM	1381
tr A0A7J7FM28 A0A7J7FM28_DICBM	--TNEFHIPLVT-	1380
sp O14802 RPC1_HUMAN	--TNEFHIPLVT-	1390
tr A0A4X1SK18 A0A4X1SK18_PIG	--TDEFHIPLVT-	1291
tr A0A452DL11 A0A452DL11_CAPHI	--TNEFHIPLVT-	1449
tr A0A3Q1MCV3 A0A3Q1MCV3_BOVIN	--TNEFHIPLVT-	1390
tr W5PIV0 W5PIV0_SHEEP	--TNEFHIPLVT-	1392
tr A0A6P3TAA7 A0A6P3TAA7_SHEEP	--TNEFHIPLVT-	1402
sp A4IF62 RPC1_BOVIN	--TNEFHIPLVT-	1390
tr A0A6P3H018 A0A6P3H018_BISBI	--TNEFHIPLVT-	1402
tr A0A6P8QR08 A0A6P8QR08_GEOSA	--NNEFHIPIT-	1390
tr A0A452HFN6 A0A452HFN6_9SAUR	-----	1354
tr A0A1U7RT71 A0A1U7RT71_ALLSI	--SNEFHIPIT-	1393
tr A0A7M4ES18 A0A7M4ES18_CROPO	--SNEFHIPIT-	1390
tr A0A091FXB7 A0A091FXB7_CORBR	--HNEFHIPIVT-	1373
tr A0A7K5TMQ4 A0A7K5TMQ4_9PASS	--HNEFHIPIVT-	1397
tr A0A7L1RK83 A0A7L1RK83_9PASS	--HNEFHIPIVT-	1375
tr A0A7L2EGD4 A0A7L2EGD4_ANTMN	--HNEFHIPIVT-	1390
tr A0A7K8B9L6 A0A7K8B9L6_9CORV	--HNEFHIPIVT-	1390
tr A0A7K7MJ33 A0A7K7MJ33_9PASS	--HNEFHIPIVT-	1375
tr A0A7LOWJ47 A0A7LOWJ47_ALELA	--NNEFHIPIVT-	1376
tr A0A0Q3TVG4 A0A0Q3TVG4_AMAAE	--NSDFHPIVIT-	1390
tr A0A091HHL6 A0A091HHL6_BUCRH	--NNEFHIPIVT-	1383
tr A0A7K9Y006 A0A7K9Y006_9GALL	-----	1327
tr A0A663MLL4 A0A663MLL4_ATHCN	--NNEFHIPIVT-	1402
tr A0A7L4DPP2 A0A7L4DPP2_9AVES	--NNEFHIPIVT-	1375
tr A0A7LOBEM6 A0A7LOBEM6_9AVES	--NNEFHIPIVT-	1375
tr A0A091NWW0 A0A091NWW0_HALAL	--NNEFHIPIVT-	1375
tr A0A091UL65 A0A091UL65_NIPNI	--NNEFHIPIVT-	1375
sp Q5ZL98 RPC1_CHICK	--NNEFHIPIVT-	1390
tr A0A3Q2TTP3 A0A3Q2TTP3_CHICK	--NNEFHIPIVT-	1402
tr F0VB53 F0VB53_NEOCL	FGLQEKHAV----	1769
tr A0A125YX49 A0A125YX49_TOXGM	YGLPEKHTV----	1746
tr A0A7J6KCU7 A0A7J6KCU7_TOXGO	YGLPEKHTV----	1747

Fig. 14. MSA of C1 elongation subunits of RNAP III from animal and animal parasites

Q8SRM3_ENCCU	<i>Encephalitozoon cuniculi</i>	L2GLN2_VITCO	<i>Vittaforma corneae</i>
P27625 RPC1_PLAFA	<i>Plasmodium falciparum</i>	A0A4W3H8T6_CALMI	<i>Callorhynchus milii</i>
A0A672YVR8_9TELE	<i>Sphaeramia orbicularis</i>	A0A6I8R0Q8_XENTR	<i>Xenopus tropicalis</i>
A0A6P9CJ55_PANGU	<i>Pantherophis guttatus</i>	A0A7J7FM28_DICBM	<i>Diceros bicornis minor</i>
O14802 RPC1_HUMAN	<i>Homo sapiens</i>	A0A4X1SK18_PIG	<i>Sus scrofa</i>
A0A3Q1MCV3_BOVIN	<i>Bos Taurus</i>	W5PIV0_SHEEP	<i>Ovis aries</i>
A0A6P3H018_BISBI	<i>Bison bison</i>	A4IF62 RPC1_BOVIN	<i>Bos taurus</i>
A0A6P3TAA7_SHEEP	<i>Ovis aries</i>	A0A6P8QR08_GEOSA	<i>Geotrypetes seraphini</i>
A0A452HFN6_9SAUR	<i>Gopherus agassizii</i>	A0A1U7RT71_ALLSI	<i>Alligator sinensis</i>
A0A7M4ES18_CROPO	<i>Crocodylus porosus</i>	A0A091HHL6_BUCRH	<i>Buceros rhinoceros silvestris</i>
A0A7K5TMQ4_9PASS	<i>Cephalopterus ornatus</i>	A0A7L1RK83_9PASS	<i>Locustella ochotensis</i>
A0A7L2EGD4_ANTMN	<i>Anthoscopus minutes</i>	A0A7K8B9L6_9CORV	<i>Cnemophilus lorae</i>
A0A7K7MJ33_9PASS	<i>Brachypodium atriceps</i>	A0A7LOWJ47_ALELA	<i>Alectura lathamii</i>
A0A0Q3TVG4_AMAAE	<i>Amazona aestiva</i>	A0A091HHL6_BUCRH	<i>Buceros rhinoceros silvestris</i>
A0A7K9Y006_9GALL	<i>Odontophorus gujanensis</i>	A0A663MLL4_ATHCN	<i>Athene cunicularia</i>
A0A7L4DPP2_9AVES	<i>Eurystomus gularis</i>	A0A7LOBEM6_9AVES	<i>Spizaetus tyrannus</i>
A0A091NWW0_HALAL	<i>Haliaeetus albicilla</i>	A0A091UL65_NIPNI	<i>Nipponia nippon</i>
Q5ZL98 RPC1_CHICK	<i>Gallus gallus</i>	A0A3Q2TTP3_CHICK	<i>Gallus gallus</i>
F0VB53_NEOCL	<i>Neospora caninum</i>	A0A125YX49_TOXGM	<i>Toxoplasma gondii</i>
A0A7J6KCU7_TOXGO	<i>Toxoplasma gondii</i>		

4.4 PR Functions in the Plant-Specific RNAPs IV and V

In addition to the three canonical MSU RNAPs, viz. RNAP I, II and III found in all eukaryotes, two non-redundant plant-specific RNA polymerases, viz. RNAP IV and RNAP V have also been reported from many plant species [29]. Plants

have evolved these two specialized RNAPs that mainly involve in transcriptional gene silencing (TGS) in plants. Whereas the RNAP IV is required for small interfering RNA (siRNA) biogenesis, the RNAP V transcripts are required for siRNA methylations of RNA-directed DNA methylation (RdDM) loci. Both are localized in the nucleus, composed of 12 subunits each and

are structurally and functionally distinct from other canonical eukaryotic polymerases discussed above. For example, 4 subunits of RNAP IV and 6 subunits of RNAP V are distinct from RNAP II. The largest catalytic subunit 1 and subunit 7 are unique for RNAP II, IV and V and the subunits 2 and 4 are common for IV and V but different from RNAP II. RNAP IV precursor RNAs are only ~30–40 nucleotides (nts) in length, just long enough to encode single 24-nt siRNAs, whereas the RNAP V makes longer transcripts than RNAP IV (i.e.), ~200 nts or longer [30 and references therein]. Furthermore, RNAP IV and V use the same initiation subunit, but differ only in their elongation subunits. However, they are found to be non-essential for viability but required for RNA-mediated TGS and heterochromatin formation in plants [31].

RNAP IV is known to mainly involve in the formation of heterochromatin (the silenced regions of DNA in the chromatin and are stained intensively by the DNA-binding dyes) by the RdDM pathway. In the first step of heterochromatin formation, RNAP IV couples with an RNA-dependent RNA polymerase (RDR2) to synthesize double-stranded RNA precursors from the single-stranded RNA transcripts of RNAP IV at all repeated loci. In the next step, a dicer-like protein (DLP3), an enzyme belonging to RNase III family, slices the double-stranded RNA precursors into 24 nts long siRNAs. These siRNAs are then methylated at their 3'-ends by a protein known as HUA-Enhancer 1 (HEN1) and finally, these methylated siRNAs complex with a protein known as Argonaute (AGO4) to form the silencing complex. Now the silencing complex performs methylation of the target regions on the chromosomes resulting in the formation of heterochromatin [17,31,32].

The gene silencing pathway involves in switching off genes. In the first step, they generate noncoding RNAs. The noncoding RNAs accomplish gene-silencing at transcriptional level (TGS) via the RdDM pathway. Thus, the RdDM pathway essentially requires two types of noncoding RNAs, (i.e.), one from the RNAP IV-dependent 24-nt siRNAs and the second one from the RNAP V-dependent intergenic noncoding (IGN) RNAs. They mediate cytosine methylation of complementary DNA sequences in all sequence contexts (CG, CHG and CHH, where H=A, C or T) by a *de novo* methyltransferase. Thus, the RdDM pathway involves in silencing of thousands of

transposons, endogenous repeats, invading RNA viruses, transgenes and also some protein-coding genes [17 and references therein]. Therefore, analysis of these two different plant-specific RNAPs offers insight into their unique active sites and PR functions in gene silencing pathways in plants.

Figure 15 shows the MSA analysis of the elongation subunit of MSU RNAP IV. The template-binding and catalytic pairs are highlighted in yellow and the Zn-binding conserved Cs is highlighted in orange. The completely conserved Mg²⁺-binding site is highlighted in light green. The polymerase region and the Mg²⁺-binding site are highly conserved among them. The MSA analysis data shows that the catalytic and template-binding pairs in the polymerase/PR active sites are similar in the elongation subunits of RNAP III (-PRM¹GPPNKKSI¹⁰TT¹³EGNFQNC²⁰PGHY²⁴GYLKL- *A. thaliana*) and RNAP IV (-SRL¹GLPNPDSVC¹⁰RTC¹³GSKDRKVC²¹EGHF²⁵GVINF - *A. thaliana*).

The distance conservations between the catalytic amino acid and first C of the Zn²⁺-binding are also maintained in RNAP IV suggesting its possible origin from RNAP III rather than from RNAP II (Table 2). Furthermore, the invasive fungal pathogens use either a V or an I immediately after the template-binding pairs in their C1 elongation subunits of RNAP III (Fig. 12) as in RNAP IV (highlighted in red) further supporting their possible origin from PNAP III. The three invariant Ds in Mg²⁺-binding regions, viz. -DxDxD- are completely conserved in all (Table 2).

Figure 16 shows the MSA analysis of the elongation subunits of the MSU RNAP V from various plant sources. The template-binding and catalytic pairs are highlighted in yellow and the Zn-binding conserved Cs is highlighted in orange. The completely conserved Mg²⁺-binding site is highlighted in light green. The polymerase region and the Mg²⁺-binding site are highly conserved in all. Unlike RNAP IV, some of them possess a conserved repeat in their CTD, a characteristic feature that is found only in the elongation subunits of RNAP II, but the sequence motifs are different. The distance conservations of the template binding pairs and the conserved Cs of the Zn²⁺-binding sites are different in both the elongation subunits of RNAP II and RNAP V, e.g., ⁶²RKV¹KC³ETC⁶MANMAEC¹³PGHF¹⁷GYLELAK-

in RNAP II from *A. thaliana* and -⁴¹SQL¹TNAFLGLPLEFGK¹⁵ESC¹⁸GATEPDKC²⁶EGHF³⁰GYIQLPVP- in RNAP V from *A. thaliana*, showing conservation only in the template-binding pairs (-FG-), but differ in their possible catalytic amino acids (-KV- in RNAP II and -QL- in RNAP V-) Furthermore, the distance between the template binding pair and the catalytic pair is markedly different between RNAP II and RNAP V (Fig. 16 and Table 2). However, the Zn²⁺ binding Cs are completely

CLUSTAL O (1.2.4) MSA of the elongation subunits of RNAP IV from various plant sources (Only polymerization/ PR sites and Mg²⁺-binding sites are shown)

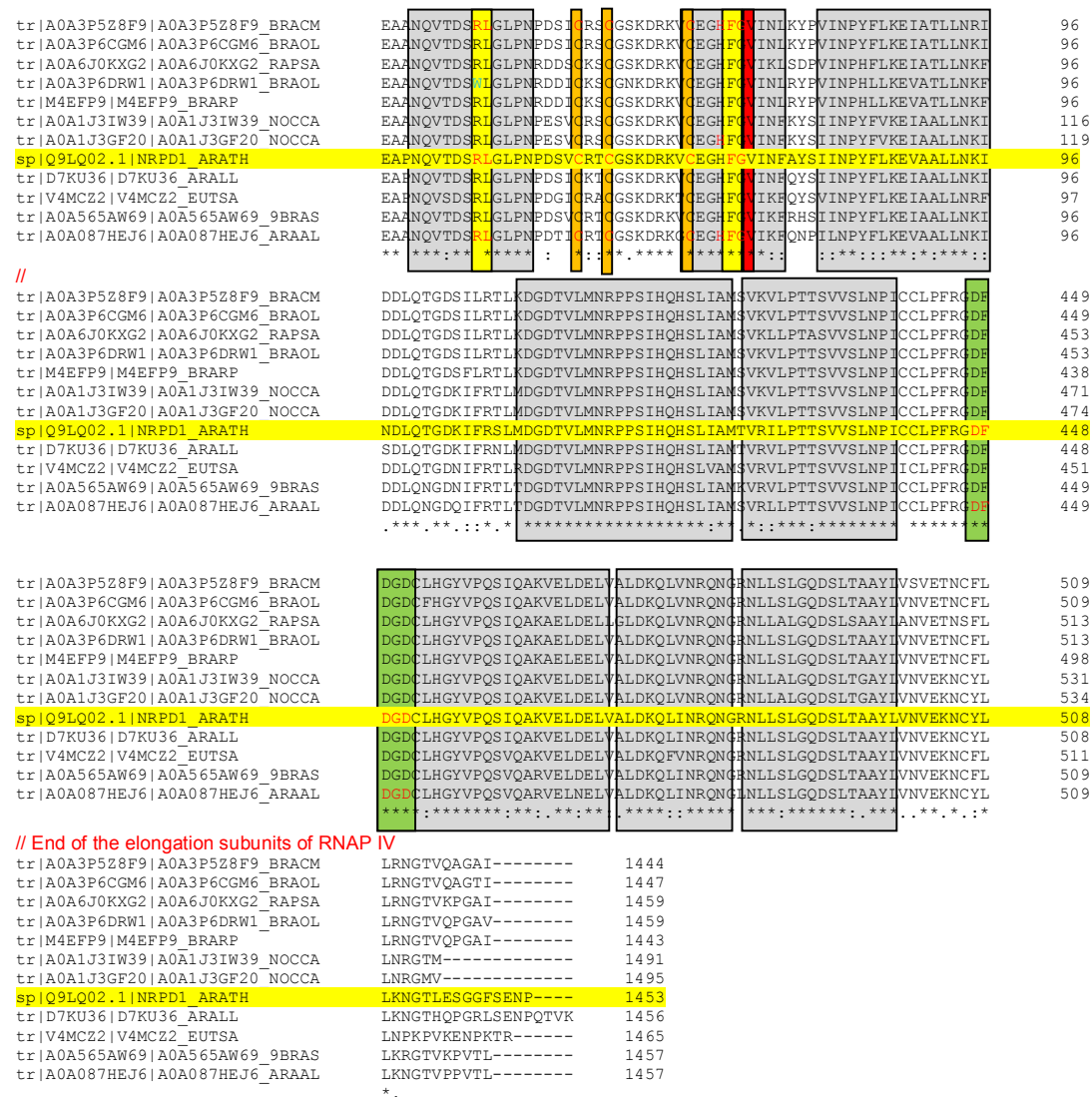


Fig. 15. MSA of the elongation subunits of the RNAP IV from various plant sources

- | | |
|--|--|
| A0A3P5Z8F9_BRACM <i>Brassica campestris</i> | A0A3P6CGM6_BRAOL <i>Brassica oleracea</i> |
| A0A6J0KXG2_RAPSA <i>Raphanus sativus</i> | A0A3P6DRW1_BRAOL <i>Brassica oleracea</i> |
| M4EFP9_BRARP <i>Brassica rapa subsp. Pekinensis</i> | A0A1J3GF20_NOCCA <i>Nocca caerulea</i> |
| A0A1J3IW39_NOCCA <i>Nocca caerulea</i> | Q9LQ02 NRPD1_ARATH <i>Arabidopsis thaliana</i> |
| D7KU36_ARALL <i>Arabidopsis lyrata subsp. Lyrata</i> | V4MCZ2_EUTSA <i>Eutrema salsugineum</i> |
| A0A565AW69_9BRAS <i>Arabis nemorensis</i> | A0A087HEJ6_ARAAL <i>Arabis alpina</i> |

conserved in the organisms, viz. from yeasts, higher fungi, plants and animals. The plant-specific RNAPs IV and V exhibit similarities to RNAP III, i.e., having a similar polymerase active site with the integrated Zn²⁺-binding site and with more or less similar distance conservation between the catalytic amino acid and the first C in the zinc-binding site. These similarities suggest that the plant-specific RNAPs IV and V might have evolved from RNAP III, as all three RNAPs are localized in the nucleus and involve in transcription of low molecular weight RNAs. RNAP IV transcription is found to be the most error-prone [30] and it also uses unusually a Val

Table 2. Summary of the proposed polymerase/PR active sites and MBS[^] in MSU RNAPs*

<u>TYPE and SOURCE</u>	<u>POLYMERASE/PR ACTIVE SITES*</u>	<u>Mg²⁺-BINDING SITE</u>
<u>PROKARYOTES</u>		
a. <u>MSU RNAP from Bacteria</u>		
Eubacteria (<i>E. coli</i>)	- ⁸⁸³ V ^R S ¹ VVSC ⁵ DTDFGVC ¹² AHC ¹⁵ YGRDLARG-(β')	-AYNADFDGDMQMAVHVPL ⁴⁷² - (β')
b. <u>MSU RNAP from Plant Chloroplasts (Prokaryotic-type)</u>		
Chloroplasts (<i>A. thaliana</i>)	- ²⁸⁷ I ^R T ¹ PFTC ⁵ RSTSWIC ¹² R ^L C ¹⁵ YGRSPTHG-(β'')	-GFNADFDGDMQMAVHVPL ⁵⁰¹ - (β')
Chloroplasts (<i>Z. mays</i>)	- ²⁹⁰ I ^R T ¹ PFTC ⁵ RSTSWIC ¹² Q ^L C ¹⁵ YGRSPTHG-(β'')	-GFNADFDGDMQMAVHLPL ⁵⁰¹ - (β')
<u>EUKARYOTES</u>		
A. <u>RNAP I (A1) from Fungal, Plant and Animal Sources</u>		
Yeast (<i>Sc</i>) A1	- ⁵⁸ L ^R N ¹ LC ³ STCGLDEKFC ¹³ PGH ^Q GHIELPV-	-AYNADFDGDEMNMHFPQ ⁶³⁹ -
Higher fungi (<i>Pc</i>) A1	- ⁶⁰ D ^H V ¹ C ² TTCRQNSFTC ¹² TGHP ^G HIELPV-	-TYNADFDGDEMNMHFPQ ⁶³³ -
Plants (<i>At</i>) A1	- ⁷⁵ D ^K Q ¹ AC ³ NSCGQLKLAC ¹³ PGH ^C GHIELVFPI-	-TYNADFDGDEINVHFPQ ¹⁴⁶ -
Plants (<i>Ah</i>) A1	- ⁶⁰ E ^K L ¹ PC ³ KTCGQLYHLC ¹³ PGH ^F GRIELVSPV-	-TYNADFDGDEINVHFPQ ¹²⁰ -
Animals (Human)	- ⁶⁰ S ^K E ¹ VC ³ STCVQDFSNC ¹³ SGH ^L GHIELPL-	-AYNADFDGDEMNAHFPQ ⁶⁰⁰ -
B. <u>RNAP II (B1) from Fungal, Plant and Animal Sources</u>		
Yeast (<i>Sc</i>) B1	- ⁶² D ^R N ¹ LKC ⁴ QTCQEGMNEC ¹⁴ PGH ^F GHIIDLAK-	-PYNADFDGDEMNLHVPQ ⁴⁹³ -
Higher fungi (<i>Nc</i>) B1	- ⁶⁴ D ^R Q ¹ FKC ⁴ KTCGENMSEC ¹⁴ PGH ^F GHIELAR-	-PYNADFDGDEMNLHVPQ ⁵⁰⁷ -
Plants (<i>At</i>) B1	- ⁶² R ^K V ¹ KC ³ ETCMANMAEC ¹³ PGH ^F GYLELAK-	-PYNADFDGDEMNMHVPQ ⁵⁰⁶ -
Plants (Wheat) B1	- ⁶² R ^R T ¹ KC ³ ETCMAGMAEC ¹³ PGH ^F GHIELAK-	-PYNADFDGDEMNMHVPQ ⁵⁰⁷ -
Animals (Human) B1	- ⁶⁶ E ^R T ¹ GRC ⁴ QTCAGNMTEC ¹⁴ PGH ^F GHIELAK-	-PYNADFDGDEMNLHLPQ ⁵⁰⁷ -
C. <u>RNAP III (C1) from Fungal, Plant and Animal Sources</u>		
Yeast (<i>Sc</i>) C1	- ⁵⁵ DP ^K M ¹ GVSSSSLEC ¹⁰ ATCHGNLASC ²⁰ HGH ^F GHLKLAL-	-PYNADFDGDEMNLHVPQ ⁵²³ -
Higher fungi (<i>Um</i>) C1	- ⁵⁶ DR ^R L ¹ GVSDKNSLC ¹⁰ ETCHLMADC ²⁰ VGH ^Y GYIKLVL-	-PYNADFDGDEMNMHVPQ ⁵¹⁰ -
Plants (<i>At</i>) C1	- ⁶³ DP ^R M ¹ GPPNKKSIC ¹⁰ TTCEGNFQNC ²⁰ PGH ^Y GYLKLDL-	-PYNADFDGDEMNMHVPQ ⁵¹¹ -
Plants (Rice) C1	- ⁶⁴ DT ^R M ¹ GAANKLGEC ¹⁰ STCHGSFAEC ²⁰ PGH ^F GYLKLAL-	-PYNADFDGDEMNLHVPQ ⁴⁹⁹ -
Animals (Human) C1	- ⁵⁷ DH ^R M ¹ GTSEKDRPC ¹⁰ ETCGKNLADC ²⁰ LGH ^Y GYIDLEL-	-PYNADFDGDEMNLHLPQ ⁵¹⁰ -
D. <u>RNAPs IV AND V - Plant-specific</u>		
<i>A. thaliana</i> IV	- ⁴⁵ S ^R L ¹ GLPNPDSVC ¹⁰ RTCGSKDRKVC ²¹ EGHF ²⁵ GVINFAV-	-PFRGDFDGDCLHGYVPQ ⁴⁵⁹ -
<i>A. thaliana</i> V	- ³⁰ S ^Q L ¹ TNAFLGLPLEFGKC ¹⁵ ESCGATEPDKC ²⁶ EGHF ³⁰ GYIQLPV-	-PLSADFDGDVHLFYVPQ ⁴⁶¹ -

*Proposed, ^MBS, Metal-binding site; unusual type of template binding amino acids is highlighted in light green. *Sc*, *Saccharomyces cerevisiae*; *Pc*, *Penicillium chrysogenum*; *At*, *Arabidopsis thaliana*; *Ah*, *A. hypogaea*; *Um*, *Ustilago maydis*. *Nc*, *Neurospora crassa*
The Mg²⁺ ions which positions the NTP at the polymerization active site is completely conserved

residue immediately after the template-binding pair (Table 2). When compared to RNAPs III and V, RNAP IV transcripts are ~ 30 to 40 nts in length, long enough for formation of 24-nt siRNAs. Whereas all the 6 RNAPs have a proton acceptor amino acid (R/H/Y) immediately downstream of the template-binding pairs, only the RNAP IV uses a different amino acid (Val) at that position, possibly explaining its error-prone nature [30] (Table 2). It is interesting to note, that the RNAP III from invasive fungal pathogens also use either a Val or an Ile, immediately after the template-binding pair (Fig. 12), similar to RNAP IV. Kostyuk et al. [33] shown that in T7 RNA polymerase, a single amino acid substitution at the template binding triad -YGS- (S⁶⁴¹→A) lost its ability to discriminate NTPs/dNTPs and was able to synthesize DNA, suggesting that the downstream amino acid at the template-binding pair plays an important role in nucleotide selection, and hence suggesting the possible error-prone nature of RNAP IV.

It is interesting to note that the invariant Asn (N) in the Mg²⁺-binding site -NADFFD-, which is shown to involve in nucleotide selection, is completely conserved in all MSU RNAPs except in the plant-specific RNAPs IV and V, where an -R and -S are used, respectively (Table 2).

Table 3 shows the proposed PR sites and their distance conservations between the C residues

in Zn-binding motif of the elongation subunits of prokaryotes (β'), eukaryotes (A1, B1 and C1), plant chloroplasts (β'') and plant-specific MSU RNAPs. It is clear from Table 3 that the distance between the first and the last C is always maintained at 11/12, suggesting a Zn-binding site in all the MSU RNAPs and therefore, a Zn-mediated excision of the mismatched nucleotide during transcription is proposed. In all the cases, the PR site is embedded within the active site of the respective MSU RNAPs. Furthermore, the template binding pair is immediately followed by a basic amino acid R/H except in the plant-specific RNAPs IV and V.

Table 4 shows the uncommon template-binding pairs like -SG-, -PG-, -MG-, -AG- that are observed in the elongation subunits of RNAP I and RNAP III. Uncommon template-binding pairs are seen in the RNAP I of yeasts and higher fungi, where they are found to be either human pathogens or could not ferment sugars. Uncommon template-binding pairs and its immediate downstream amino acid are also observed in the RNAP III of animal and human pathogens. These results suggest that pathogens, parasites and organisms which could not ferment sugars are adapted to different types of template-binding pairs. It is not clear whether such differences offer any advantages to these organisms for transcription in their hosts.

Table 3. Distance conservations of Cs in ZBS* in the elongation subunits of MSU RNAPs

<u>Organism</u>	<u>Proposed Polymerase/PR Active Sites</u>	<u>Distance Conservations of Cs</u>
1. Prok-MSU RNAP (<i>Ec</i>)	⁻⁸⁸³ VRS ¹ VVSC ⁵ DTDFGVC ¹² AHC ¹⁵ Y ¹⁶ GR- (β')	(C5+C12+C15 = C1 to C3 = 11)
2a. Chloroplasts (<i>At</i>)	⁻²⁸⁷ IRT ¹ PFTC ⁵ RSTSWIC ¹² RLC ¹⁵ YGR- (β'')	(C5+C12+C15 = C1 to C3 = 11)
2b. Chloroplast (<i>Zm</i>)	⁻²⁹² IRT ¹ PFTC ⁵ RSTSWIC ¹² QLC ¹⁵ Y ¹⁶ GR- (β'')	(C5+C12+C15 = C1 to C3 = 11)
3. Euk- Pol I-A1 (<i>Sc</i>)	⁻⁵⁸ LRN ¹ LC ³ STC ⁶ GLDEKFC ¹³ PGHQ ¹⁷ GH-	(C3+C6+C13 = C1 to C3 = 11)
4. Euk- Pol II-B1 (<i>Sc</i>)	⁻⁶² DRN ¹ LKC ⁴ QTC ⁷ QEGMNEC ¹⁴ PGHF ¹⁸ GH-	(C4+C7+C14 = C1 to C3 = 11)
5. Euk- Pol III-C1 (<i>Sc</i>)	⁻⁵⁶ PKM ¹ GVSSSSLEC ¹⁰ ATC ¹³ HGNLASC ²⁰ HGHF ²⁴ GH-	(C10+C13+C20 = C1 to C3 = 11)
6. Euk- Pol IV (<i>At</i>)	⁻⁴⁵ SL ¹ GLPNPDSVC ¹⁰ RTC ¹³ GSKDRKVC ²¹ EGHF ²⁵ GV-	(C10+C13+C21 = C1 to C3 = 12)
7. Euk- Pol V (<i>At</i>)	⁻³⁰ SQ ¹ TNAFLGLPLEFGKC ¹⁵ ESC ¹⁸ GATEPDKC ²⁶ EGHF ³⁰ GY-	(C15+C18+C26 = C1 to C3 = 12)

Ec, *E. coli*; *Zm*, *Z. mays*; *Sc*, *Saccharomyces cerevisiae*; *At*, *Arabidopsis thaliana*

*ZBS, Zinc-binding site in the proposed PR site within the polymerization active site is shown

Table 4. Uncommon template-binding pairs in the MSU RNAPs I and III

<u>RNAP/Organism</u>	<u>Nature of the Organism</u>	<u>Catalytic and Template-Binding Pairs*</u>	<u>MBS[^]</u>
<u>RNAP I (Elongation subunit, A1)</u>			
a. <u>From Yeasts</u>			
<i>Tortispora caseinolytica</i>	Unable to ferment sugars	- ⁵⁹ L ^R H ^P C ³ ATCRLDERFC ¹³ PGH ^S G ^H IEL-	Identical
<i>Yarrowia lipolytica</i>	Unable to ferment sugars	- ⁵⁹ L ^R NN ^C ATCNLDNRFC ¹³ QGH ^P G ^H IEL-	Identical
<i>Candida lipolytica</i>	Human pathogen	- ⁵⁹ L ^R NN ^C ATCNLDNRFC ¹³ QGH ^P G ^H IEL-	Identical
<i>Spathaspora passalidarum</i>	Unable to ferment sugars	- ⁵⁹ L ^R N ^V C ³ TT ^C GLDEKFC ¹³ PGH ^M G ^H IEL-	Identical
<i>Candida albicans</i>	Human pathogen	- ⁵⁹ L ^R N ^L C ³ TT ^C GLDEKFC ¹³ PGH ^M G ^H IEL-	Identical
b. <u>From Higher Fungi</u>			
<i>Talaromyces marneffeii</i>	Human pathogen	- ⁶⁰ D ^H V ^C TT ^C RASSWSC ¹² PGH ^P G ^H IEL-	Identical
<i>Talaromyces cellulolyticus</i>	Cellulolytic fungus	- ⁶⁰ D ^H V ^C TT ^C RASSWSC ¹² PGH ^P G ^H IEL-	Identical
<i>Ajellomyces capsulatus</i> #	Human pathogen	- ⁶⁰ D ^H I ^C TT ^C R ^L NSWSC ¹² NGH ^A G ^H IEL-	Identical
<i>Blastomyces dermatitidis</i>	Human pathogen	- ⁶⁰ D ^H V ^C TT ^C RQNSFTC ¹² TGH ^P G ^H IEL-	Identical
<u>RNAP III (Elongation subunit, C1)</u>			
a. <u>From Human and Animal Parasites</u>			
<i>Encephalitozoon cuniculi</i>	Animal parasite	- ⁵⁵ DL ^R L ¹ GVGNKKDK ¹⁰ ATC ¹³ GEGLATC ²⁰ IGH ^F G ^E VR-	Identical
<i>Vittaforma corneae</i>	Animal parasite	- ⁵⁵ DL ^R L ¹ GVSTKSGIC ¹⁰ STCKENIQNC ²⁰ AGH ^F G ^Q IQL-	Identical
<i>Plasmodium falciparum</i>	Human parasite	- ⁷⁶ DL ^K L ¹ GAHKSNSVC ¹⁰ ETCNKLLINC ²⁰ SGH ^F G ^Y IEL-	Identical
<i>Neospora caninum</i>	Animal parasite	- ¹⁸⁰ DL ^R L ¹ GPNKSDSRC ¹⁰ QTCGHTLLQC ²⁰ TGH ^W G ^Y MDL-	Identical
<i>Toxoplasma gondii</i> (M)	Animal & Human parasite	- ¹⁵³ DL ^R L ¹ GPNKSDSRC ¹⁰ QTCGHTLLQC ²⁰ TGH ^W G ^Y MDL-	Identical
<i>Toxoplasma gondii</i> (O)	Animal & Human parasite	- ¹⁵⁴ DL ^R L ¹ GPNKSDSRC ¹⁰ QTCGHTLLQC ²⁰ TGH ^W G ^Y MDL-	Identical

*Proposed; [^]MBS, Mg²⁺-binding site with 3 invariant Ds as -DxDxD-

Uncommon template-binding pairs in:

RNAP I, A1 subunits– From Yeasts

Tortispora caseinolytica occurs in the rotting tissues of opuntias cactus in the Sonoran desert. It does not ferment any sugar, but could assimilate only a limited number of carbon compounds. *Yarrowia lipolytica* is characterized by its inability to ferment sugars but possesses unique physiological capabilities to utilize polyalcohols, organic acids, and long-chain hydrocarbons, crude oils, *n*-paraffins and hydrocarbons. *Yarrowia lipolytica lyrata* also known as *Candida lipolytica* is a human pathogen but rarely infect humans. *Spathaspora passalidarum* (Debaryomycetaceae) is a wood-boring beetle associated fungus and one of a few yeasts known to efficiently ferment and metabolise xylose, a major component of plant cell walls. This rare ability enables this for the production of biofuel from plant materials.

Candida albicans is the most prevalent cause of fungal infections in humans including urinary tract infections.

RNAP I, A1 subunits– From Higher Fungi

Talaromyces (Penicillium) marneffeii is a human pathogen. Patients are presented with fever, altered mental status, headaches, facial nerve palsy, seizures, vision loss and mainly affects immuno-compromised patients like HIV/AIDS. *Talaromyces cellulolyticus* is a cellulolytic fungus which could utilize the complex carbohydrate. *Ajellomyces capsulatus*, also known as *Histoplasma capsulatum* a thermal dimorphic fungus that causes histoplasmosis, a potentially fatal disease of the lungs. *Blastomyces dermatitidis* is the causal agent of blastomycosis, an invasive and often serious fungal infection.

RNAP III, C1 subunits- From Animal and Human Parasites

Encephalitozoon cuniculi is a microsporidial parasite (intracellular animal pathogen) that causes renal and central nervous system diseases in farmed rabbits.

Vittaforma corneae is a microsporidial pathogen cause keratitis and keratoconjunctivitis, an obligate intracellular parasite adapted to parasitic life in a wide range of eukaryotic organisms. *Plasmodium falciparum* is a unicellular protozoan parasite of humans, and the deadliest species of Plasmodium that causes malaria in humans. *Neospora caninum* is a coccidian parasite of animals. It is a major pathogen of cattle and dogs. *Toxoplasma gondii* is one of the world's most common parasites and is considered to be a leading cause of death attributed to food-borne illness. It is a protozoan, single celled, obligate intracellular parasite that infects most species of warm-blooded animals, including humans, and causes the disease toxoplasmosis.

5. A UNIFIED MECHANISM OF ACTION FOR THE PR EXONUCLEASES OF MSU RNAPS

Unlike the PR functions in DNA polymerases, the PR function in MSU RNAPs is not very well understood. In an attempt to explain the PR exonuclease activity of MSU RNAPs, a unified mechanism of action is proposed in this communication, based on the completely conserved Zn²⁺-binding site embedded within the polymerase active site region in all the 7 known MSU RNAPs from prokaryotes and eukaryotes. It has been well established that zinc acts as the cofactor for >450 enzymes and proteins, where it plays both structural and catalytic roles. It is interesting to note that zinc is also an integral component of both prokaryotic and eukaryotic DNA and RNA polymerases and is found to be essential for their function [34,35]. As the Zn-mediated reactions are exceedingly faster and efficient, many enzymes use Zn²⁺ as the catalytic metal ion. For example, the mechanisms of several zinc metalloenzymes have been proposed to be facilitated by the formation of the highly reactive zinc-hydroxide. Palanivelu [1,7] has shown that Zn²⁺ excise mismatched bases/nucleotides in DNA and RNA polymerases as well as in RNA modifying enzymes. For example, PR functions in prokaryotic DNAPs like DNAP I, II, III and DNAP X and RdRps of SARS-CoV-2 are proposed to be mediated by Zn-mediated hydrolysis [36].

Involvement of Zn²⁺ is in the PR function of the MSU RNAPs is arrived at based on two important findings. For example, the X-ray crystallographic analysis [12] and MSA data have shown that the MSU RNAPs harbour a Zn-binding site within the polymerase region itself. Therefore, Sydow and Cramer [11] suggested that the MSU RNAPS could use the same

catalytic region for PR function too. In fact, Zenkin et al [16] studies on a prokaryotic MSU RNAP from the thermophilic bacterium, *Thermus thermophilus*, strongly supports their views. They have shown that when a wrong nucleotide is incorporated, the *T. thermophilus* RNAP stalls and moved one step backwards and made a cleavage at the penultimate base, resulting in the removal of a dimer which includes the wrongly added nucleotide. Subsequently, the polymerase resumed polymerization with the correct nucleotide inserted into the polymerization site. They further suggested that the terminal RNA nucleotide mismatch itself could play an active role in RNA PR activity. Furthermore, the first X-ray crystallographic analysis of a eukaryotic RNAP II complex from *S. cerevisiae* with its transcription factor and the elongation factor TFIIIS, supported the idea that the polymerase has a 'tunable' active site that switches between mRNA synthesis and repair [10]. These results further strengthen the model of a bifunctional active site in MSU RNAPs [37]. Moreover, a 2.8 Å difference Fourier map revealed the presence of two metal ions at the active site of the yeast RNAP II, a persistently bound metal ion (metal A) and a mobile metal ion (metal B) suggesting that the metal ion A possibly participating in regular polymerization reactions and the mobile metal ion B in the PR function, only when a wrong nucleotide is inserted [38]. In addition to, the SDM experiments from both prokaryotic and eukaryotic MSU RNAPs have proved that the conserved Cs are not only essential for the enzyme activity but also lethal to the organism [13,25] suggesting also a structural role for the Zn²⁺ in maintaining the polymerase and PR functions tightly coordinated. In support of these findings, all the 7 MSU RNAPs from prokaryotes and eukaryotes possess a completely conserved 3 Cys residues (the Zn²⁺-binding site) and an invariant H (as proton acceptor) within the polymerase active site region itself. Only in chloroplast MSU RNAP, a Q or an R could possibly do the job as there was no invariant H at the expected position as in others. Based on these findings, a unified PR mechanism is proposed for these MSU RNAPs (Fig. 17). A schematic diagramme (Fig. 2A) shows the mechanism of action of the polymerase and PR exonuclease activities in prokaryotes (*E. coli*). Proposed steps for the mechanism of action PR exonuclease activity of eukaryotic (*S. cerevisiae*) MSU RNAP II is shown in Fig. 17.

Some amino acid(s) participate in sugar selection and some involve in base selection, and are

mostly non-overlapping. The N residue in the completely conserved ⁴⁷⁹NADFDGD of the Mg²⁺-binding site in all major RNAPs plays a crucial role in nucleotide discriminations. Functional *in vitro* analysis demonstrated that the substitutions of the corresponding N⁴⁵⁸ residue in the prokaryotic (*E. coli*) elongation subunit β' not only led to the loss of discrimination between NTP and dNTP substrates but also led to defects in RNA chain extension [19,39]. It is interesting to note that substitution of the corresponding amino acid in yeast elongation subunit, Rpb1 (N⁴⁷⁹→Y) is lethal in the same sequence motif ⁴⁷⁹NADFDGD found in eukaryotes [40]. They suggested that the absolutely conserved N in both the cases could discriminate the NTP from dNTP by recognizing the 2'-OH of the ribose and suggested that the crucial N could interact with both the 2'-OH as well 3'-OH [40,41]. A similar mechanism should be operating in all other 6 MSU RNAPs as the PR site is integrated into the polymerase active site itself in all (Table 2). All of them use a basic amino acid R/K/H as the proton acceptor except the plant-specific RNAP V where a Q is found (the -QL- diad is found in the MSP RNAPs of chloroplasts and RNAP V).

5.1 Involvement of Additional Proteins for PR Functions

It was proposed that the PR activity in prokaryotes may use additional protein like GreA for excising the mismatches during transcription [36]. However, further insights into the participation of any extraneous protein factors for PR activity were provided by Zenkin et al [16]. They have shown that the RNAP efficiently cleaved the penultimate (P2) phosphodiester bond, but not the P1 (ultimate phosphodiester bond), suggesting that MSU RNAP backtracked (sliding backwards) by 1 base pair relative to the pre-translocated state and cleaved the penultimate phosphodiester bond. Furthermore, they have found that the selective removal of mismatched residues during transcription did not require GreA in *T. aquaticus* RNAP, proving that the PR activity is independent of other factors. They found that the cleavage factors are not also essential *in vivo*. In other words, their findings show that the mRNA itself could correct error(s) that might occur during its own synthesis. Similar findings were also reported for the eukaryotic RNAPs. For example, Khun et al [18] found that the conserved polymerase active site of RNAP I was capable of RNA cleavage in the absence of

cleavage stimulatory factors. Similar observations were made for RNAP II and RNAP III also, (i.e.), that the hydrolytic activity is intrinsic to RNAPs II and III and factor-independent [27,42]. The intrinsic cleavage activity was stimulated greatly by mildly basic pHs and divalent metal ions. After the stalled, nascent transcript was cleaved by the intrinsic PR activity, they resume elongation as usual [27,42]. Therefore, during transcription elongation, a hydrolytic reaction stimulated by misincorporated nucleotides proofreads the misincorporation events and thus, serves as an intrinsic mechanism of transcription fidelity. The terminal mismatch nucleotide itself plays an active role by stimulating the repair reaction. Thus, the MSU RNAPs carryout both these functions using the same active site region. However, the transcription elongation factor TFIIs of RNAP II and its equivalent factors in RNAP I and RNAP III play a crucial role not only in the elongation process but also switching between polymerization and cleavage modes when mismatch occurs [11,16,28,43].

The release of dinucleotides, and larger oligonucleotides during PR activity has been detected by different workers [44,45]. When the RNAP II progress is blocked by mismatch(s), it is resolved by temporary backtracking of the RNAP and deleting of the mismatch in a transcription elongation factor S-II (TFIIS)-dependent or independent manner. Dinucleotides tend to originate from SII-independent mechanism, whereas 7–14 base products were observed from SII-dependent mechanism [44]. By the backtracking mechanism the enzyme retreats on the template resulting in the extruding of the 3'-end of the RNA and reaching the penultimate nucleotide for excision [45].

Steps 1 and 2: The mismatch induces the PR reaction. The PR exonuclease frays the mismatched nucleotide from the DNA template and backtracks to the penultimate nucleotide. The PR exonuclease active site initiates proton transfer from the water-bound Zn²⁺ with the simultaneous nucleophilic attack on the susceptible phosphodiester bond by the highly reactive Zn-hydroxide.

Step 3 and 4: The wrongly added nucleotide is excised along with the penultimate nucleotide as a dimer and the polymerase resume synthesis from penultimate nucleotide with the correct nucleotide.

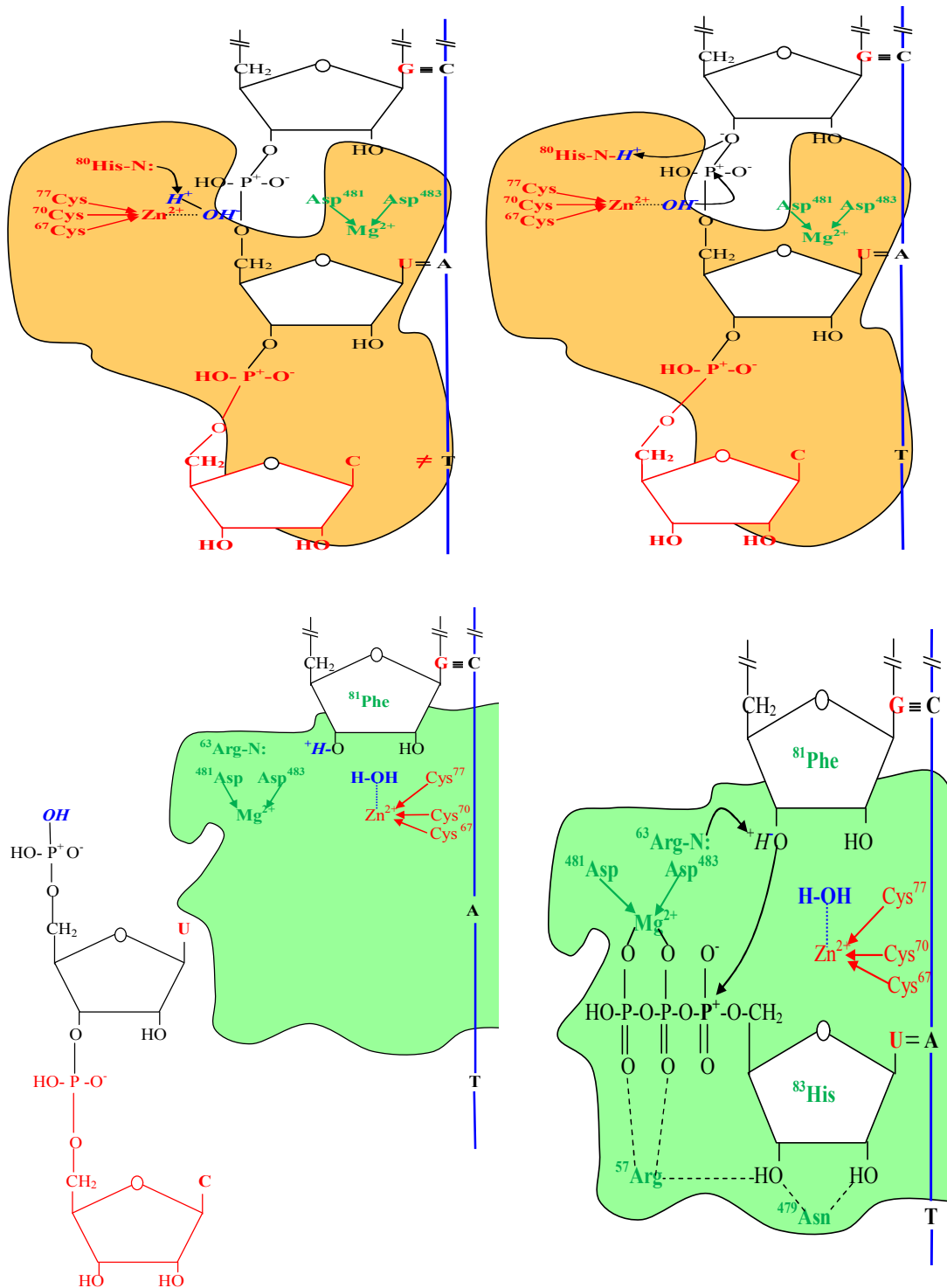


Fig. 17. Steps (1-4) Involved in the Proposed Mechanism of Action of PR Function in MSU RNAPs II (*S. cerevisiae*)

6. CONCLUSION

RNAPs play a crucial role in gene expression, where the genetic blueprint on DNA is copied into RNA. Some of these RNAPs are SSU types (e.g., viral, nuclear-encoded mitochondrial and chloroplast RNAPs) and others are MSU types. Prokaryotic, prokaryotic-type (chloroplast) and all the eukaryotic RNAPs are MSU types. These RNAPs rarely make mistakes ($\sim 10^{-5}$) during the transcription process. As some of these mistakes could drastically affect the growth and very survival of the organisms, the RNAPs correct these mistakes by an intrinsic PR mechanism. Unlike in DNA polymerases, in the MSU RNAPs the PR mechanism is found to be integrated into the polymerase active site itself. This PR activity is proposed to be accomplished by a Zn^{2+} -mediated excision by the integrated Zn^{2+} -binding site in these MSU RNAPS. Thus, the discovery of an intrinsic mechanism in self-correcting RNA transcripts fulfils a missing link in molecular evolution.

ACKNOWLEDGEMENTS

The author wishes to thank Dr. N. Srinivasan, Former Professor, Department of Endocrinology, Post Graduate Institute of Basic Medical Sciences, University of Madras, Chennai, for his useful suggestions on the manuscript.

COMPETING INTERESTS

Author has declared that no competing interests exist.

REFERENCES

1. Palanivelu P. Eukaryotic Multi-subunit DNA dependent RNA Polymerases: An Insight into their Active Sites and Catalytic Mechanism. In: *Advances and Trends in Biotechnology and Genetics*. Sciencedomain International Book Publishers, UK. 2020;1:1-38. DOI: 10.9734/bpi/atbg/v1
2. Anikin M, Molodtsov V, Temiakov D, McAllister WT. Transcript slippage and recoding. In: Atkins JF, Gesteland RF, Bujnicki JM. editors. *Recoding: Expansion of decoding rules enriches gene expression*. 24th ed. Springer, New York; 2010.
3. Sahin U, Kariko K, Türeci Ö. mRNA-based therapeutics- Developing a new class of drugs. *Nat Rev Drug Discov*. 2014;13:759–780.
4. Damase TR, Sukhovshin R, Boada C, Taraballi F, Pettigrew RI, John P, Cooke JP. The Limitless Future of RNA Therapeutics. *Front. Bioeng. Biotechnol*. 2021; 9: 1-24.
5. Conry RM, LoBuglio AF, Wright M, Sumerel L, Pike MJ. Characterization of a messenger RNA polynucleotide vaccine vector. *Cancer Res*. 1995;55:1397–1400.
6. Pardi N, Hogan MJ, Porter FW, Weissman D. mRNA vaccines-a new era in vaccinology. *Nat Rev Drug Discov*. 2018;17:261–279.
7. Palanivelu P. DNA polymerases – An insight into their active sites and mechanism of action. In: *Recent Advances in Biological Research*, SCIENCEDOMAIN International Book Publishers, UK. 2019;1:1-39. DOI: 10.9734/bpi/rabr/v1
8. Palanivelu P. Multisubunit RNA Polymerases of Bacteria - An insight into their active sites and catalytic mechanism. *Indian J Sci Technol*. 2018;11:1-37.
9. Palanivelu P. Active Sites of the Multi-subunit RNA Polymerases of Eubacteria and Chloroplasts are Similar in Structure and Function: Recent Perspectives. In: *Current Research Trends in Biological Science*, SCIENCEDOMAIN International Book Publishers, UK. 2020;2:26-61. DOI: 10.9734/bpi/crtbs/v2
10. Cramer P. RNA polymerase II structure: from core to functional complexes. *Curr Opin Genet Dev*. 2004;14:218-226.
11. Sydow JF, Cramer P. RNA polymerase fidelity and transcriptional proofreading. *Curr Opin Struct Biol*. 2009;19:732–739.
12. Zhang G, Campbell EA, Minakhin L, Richter C, Severinov K, Darst SA. Crystal structure of *Thermus aquaticus* core RNA polymerase at 3.3 Å resolution. *Cell*. 1999;98:811-824.
13. Zaychikov E, Martin E, Denissova L, Kozlov M, Markovtsov V, Kashlev M, Heumann H, Nikiforov V, Goldfarb A, Mustaev A. Mapping of catalytic residues in the RNA polymerase active center. *Science*. 1996;273:107–109.
14. Carpousis AJ, Gralla JD. Interaction of RNA polymerase with lacUV5 promoter DNA during mRNA initiation and elongation. Foot-printing, methylation, and rifampicin-sensitivity changes

- accompanying transcription initiation. *J Mol Biol.* 1985;183:165-77.
15. Sydow JF, Brueckner F, Cheung AC, Damsma GE, Dengl S, Lehmann E, Vassilyev D, Cramer P: Structural basis of transcription: mismatch-specific fidelity mechanisms and paused RNA polymerase II with frayed RNA. *Mol Cell.* 2009;34:710-721.
 16. Zenkin N, Yuzenkova Y, Severinov K. Transcript-Assisted Transcriptional Proofreading. *Science.* 2006;313:518-520.
 17. Zhou M, Law JA, RNA Pol IV and V in Gene Silencing: Rebel Polymerases Evolving Away From Pol II's Rules. *Curr Opin Plant Biol.* 2015;27:154–164. DOI: 10.1016/j.pbi.2015.07.005
 18. Kuhn CD, Geiger SR, Baumli S, Gartmann M, Gerber J, Jennebach S, Mielke T, schochner HT, Beckmann R, Cramer P. Functional Architecture of RNA Polymerase I. *Cell.* 2007;131:1260–1272.
 19. Gnatt AL, Cramer P, Fu J, Bushnell DA, Kornberg RD. Structural Basis of Transcription: An RNA polymerase II Elongation Complex at 3.3 Å Resolution; 2001. Available:www.scienceexpress.org 10.1126/science.1059495
 20. Engel C, Sainsbury S, Cheung AC, Kostrewa D, Cramer P. RNA polymerase I structure and transcription regulation *Nature.* 2013;502:650-656.
 21. Russell J, Zomerdijk JCBM. The RNA polymerase I transcription machinery. *Biochem Soc Symp.* 2006;73:203–216.
 22. Vanittanakom N, Cooper CR, Fisher MC, Sirisanthana T. *Penicillium marneffe* infection and recent advances in the epidemiology and molecular biology aspects. *Clinical Microbiol Rev.* 2006; 19:95–110.
 23. Cramer P. Multisubunit RNA polymerases. *Curr Opin Struct Biol.* 2002;12:89-97.
 24. Donaldson IM, Friese JD. Zinc Stoichiometry of Yeast RNA Polymerase II and Characterization of Mutations in the Zinc-binding Domain of the Largest Subunit. *J Biol Chem.* 2000;275:13780–13788.
 25. Nudler, E., Avetisova, E., Markovtsov, V., and Goldfarb, A. Transcription processivity: protein-DNA interactions holding together the elongation complex. *Science.* 1996;273:211–217.
 26. Geiduschek EP, Kassavetis GA. The RNA polymerase III transcription apparatus. *J. Mol. Biol.* 2001;310:1-26.
 27. Whitehall SK, Bardeleben C, Kassavetis GA. Hydrolytic cleavage of nascent RNA in RNA polymerase III ternary transcription complexes. *J Biol Chem.* 1994;269:2299-306.
 28. Chédin S, Riva M, Schultz P, Sentenac A, Carles C. The RNA cleavage activity of RNA polymerase III is mediated by an essential TFIIS-like subunit and is important for transcription termination. *Genes Dev.* 1998;12:3857–3871.
 29. Pontier D, Yahubyan G, Vega D, Bulski A, Saez-Vasquez J, Hakimi MA, Lerbs-Mache S, Colot V, Lagrange T. Reinforcement of silencing at transposons and highly repeated sequences requires the concerted action of two distinct RNA polymerases IV in Arabidopsis. *Genes Dev.* 2005;19:2030–2040.
 30. Marasco M, Li W, Lynch M, Pikaard CS. Catalytic properties of RNA polymerases IV and V: accuracy, nucleotide incorporation and rNTP/dNTP discrimination. *Nuc Acids Res.* 2017;45:11315–11326.
 31. Haag JR, Pikaard CS. Multisubunit RNA polymerases IV and V: purveyors of non-coding RNA for plant gene silencing. *Nature Rev. Mol Cell Biol.* 2011;12:483-492.
 32. Xie M, Yu B. siRNA-directed DNA Methylation in Plants. *Curr Genomics.* 2015;16:23-31.
 33. Kostyuk SM, Dragan DL, Lyakhov VO, Rechinsky VL, Tunitskaya BK, Chernov SN, Kochetkov E. Mutants of T7 RNA polymerase that are able to synthesize both RNA and DNA. *FEBS Lett.* 1995;369:165–168.
 34. Palanivelu P. RNA-Dependent RNA Polymerases of Severe Acute Respiratory Syndrome-Related Coronaviruses- An Insight into their Active Sites and Mechanism of Action. *Int J Biochem Res Rev.* 2020;29:29-52.
 35. Coleman JE. in *Zinc Enzymes* (Spiro TG., editor). John Wiley and Sons. Toronto; 1983.
 36. Palanivelu P. An overview of the proofreading functions in bacteria and SARS-Coronaviruses. *Int J Biochem Res Rev.* 2021;30:33-62.
 37. Sosunov V, Sosunova E, Mustaev A, Bass I, Nikiforov V, Goldfarb A. Unified two-metal mechanism of RNA synthesis and

- degradation by RNA polymerase. EMBO Journal. 2003;22:2234-2244.
38. Cramer P, Bushnell DA, Kornberg RD. Structural Basis of Transcription: RNA Polymerase II at 2.8 Angstrom Resolution. Science. 2001;292:1863-1876.
39. Svetlov V, Vassylyev DG, Artsimovitch I. Discrimination against deoxyribonucleotide substrates by bacterial RNA polymerase. J Biol Chem. 2004;279:38087-38090.
40. Trinh V, Langelier MF, Archambault J, Coulombe B. Structural Perspective on Mutations Affecting the Function of Multisubunit RNA Polymerases. Microbiol Mol Biol Rev. 2006;70:12-36.
41. Thomas MJ, Platas AA, Hawley DK: Transcriptional fidelity and proofreading by RNA polymerase II. Cell. 1998;93:627-637.
42. Weilbaecher RG, Awrey DE, Edwards AM, Kane CM. Intrinsic Transcript Cleavage in Yeast RNA Polymerase II Elongation Complexes. J Biol Chem. 2003;278: 24189-24199.
43. Jeon C and Agarwal K: Fidelity of RNA polymerase II transcription controlled by elongation factor TFIIIS. Proc Nat Acad Sci. (USA). 1996;93:13677-13682.
44. Gu W and Reines D. Variation in the Size of Nascent RNA Cleavage Products as a Function of Transcript Length and Elongation Competence. J Biol Chem. 1995;270:30441-30447.
45. Wang D, Bushnell DA, Huang X, Westover KD, Levitt M, and Kornberg RD. Structural basis of transcription: Backtracked RNA polymerase II at 3.4 Å resolution. Science. 2009;29(324):1203-1206.

© 2021 Palanivelu; This is an Open Access article distributed under the terms of the Creative Commons Attribution License (<http://creativecommons.org/licenses/by/4.0>), which permits unrestricted use, distribution, and reproduction in any medium, provided the original work is properly cited.

Peer-review history:
The peer review history for this paper can be accessed here:
<http://www.sdiarticle4.com/review-history/75573>